MASS SPECTROMETRY OF SUBSTITUTED BENZILS

by

Joseph Herbert O'Toole

Dissertation submitted to the Graduate Faculty of the

Virginia Polytechnic Institute and State University

in partial fulfillment of the requirements for the degree of

DOCTOR OF PHILOSOPHY

in

Chemistry

APPROVED:

Chairman: Michael A. Ogliaruso, Ph.D.

Alan F. Clifford, Ph.D.

John G. Mason, Ph.D.

James F. Wolfe, Ph.D.

Larry T. Taylor, Ph.D.

John G. Dillard, Ph.D.

May, 1975

Blacksburg, Virginia

DEDICATION

This work is dedicated to the memory of J. Edward Nohe and to the other Americans whose lives were lost or ruined in the insanity of the Southeast Asian War. May the knowledge their blood bought us be used to insure that such a tragedy never occurs again.

"Perhaps they are like the rest of us and are afraid to die."

— Henry Cabot Lodge
Saigon, August, 1963

TABLE OF CONTENTS

LIST OF FIGURES

LIST OF TABLES

SECTION I

INTRODUCTION

Mass spectrometry as a technique for characterizing chemical compounds was first demonstrated by J. J. Thomson in the first decade of this century,[1] and F. W. Aston was able to demonstrate the existence of Xe-124 with a natural abundance of 0.1% as early as 1923.[2] It comes as a surprise, therefore, to read in the preface to the reference work Interpretation of Mass Spectra of Organic Compounds, by Budzikiewicz, Djerassi, and Williams,[3] written in 1963:

> "The use of mass spectrometry in organic chemistry is becoming increasingly widespread, and mass spectrometers are now being installed in many laboratories. Three years ago one had to search far and wide in the organic chemical literature to find examples of its use in structural problems."

Eleven years hence, mass spectrometers threaten to attain the ubiquity of infrared spectrometers and are being used in combination with other instruments in routine drug analyses. In the interval, theoretical[4] and empirical[5] rules to explain the formation of fragmentation of ions have been postulated and demonstrated, and mass spectrometry has been established both as an analytical method and as a vehicle for the study of fundamental chemical processes. It was the purpose of this study to analyze the positive and negative ion mass spectra of an homologous series of organic compounds, the benzils, so as to determine from the ions produced and their relative appearance potentials whether the substitution of groups of different electronegativity and polarizability alters the configuration of the molecular ions or the stability of the daughter ions. Calculated and experimental appearance

potentials have been compared, and mechanisms for the formation and decomposition of the observed ions have been proposed. The results so obtained have been compared with data obtained in solution, and conclusions have been drawn concerning the effects of solvation and the changes in fragmentation processes accompanying changes in substituent and electron energy.

SECTION II

HISTORICAL

Attempts to correlate the mass spectral behavior of organic molecules with their structures have been made using two basic approaches, one theoretical and one empirical. The theoretical approach, known as the quasi-equilibrium theory (QET), was initially postulated by Eyring's group at Utah in the early 1950's.[6,7] Proceeding from the generally accepted assumption that the ionization process by electron impact is a vertical transition, and in accordance with the Franck-Condon principle, they postulated that the excited parent-molecule ion does not immediately decompose into various fragments but that the parent-molecule ion may undergo several vibrations prior to decomposition. During these vibrations, there is a high probability of radiationless transitions which result in a distribution of the excitational energy in a completely random fashion. The parent-molecule ion decomposes only when it reaches a certain "activated complex" configuration with sufficient energy in particular degrees of freedom. The result is a "quasi-equilibrium" between parent-molecule ion, activated complex, and fragment ions and molecules. Predictions can then be made of the relative populations of the parent-molecule ions and the principle fragments based on an analysis of the rate constants for each fragmentation in terms of a system of harmonic oscillators. Subsequent researchers[9,10] have placed the theory on a sound theoretical base and demonstrated its applicability to a large number of systems. No attempt has been made herein to calculate relative populations of ions based on the QET, but the basic postulates

are encountered in every attempt to analyze the processes occurring within the spectrometer.

The empirical approach uses general concepts of physical organic chemistry - inductive and resonance effects and stereochemistry - to make qualitative predictions concerning the likely fragmentation patterns of organic molecules.[5,11] Quantitative correlations of fragmentation patterns with the Hammett substituent constants (σ)[12] obtained in solution indicated that both ionic abundances and appearance potentials might be predictable.[13,14,15] The correlations have been demonstrated to be valid both theoretically[16,17] and in practice.[18,19]

The substituent may alter the population of a particular ion as a result of one or more of the following effects:[20,21]

a) change in internal energy distribution of the parent-molecule ion or a precursor fragment,

b) change in the rate of formation of a specific fragment, and

c) change in the rate of fragmentation into smaller or different ions via rearrangement.

Chin and Harrison[16] have used the above, in conjunction with several of the postulates of the QET, to derive an expression correlating the rates of decomposition with ionic concentration. The parent-molecule ion, $[M^+]$, formed by electron impact, will decompose if it has sufficient internal energy (excitation), and the product distribution will depend upon the factors listed supra. In Equation 1, the concentration of the particular fragment of interest, $[A^+]$, will be determined by Equation 2, where k_t is the sum of all rate constants resulting in decomposition of the molecular ion.

$$[M^+] \begin{cases} \xrightarrow{k_1} [A^+] \xrightarrow{k_d} [C^+] \\ \xrightarrow{k_2} [D^+] \end{cases} \qquad (1)$$

$$[A_0^+] = \frac{k_1}{k_t} \left[[M_0]^+ - [M]^+ \right] \qquad (2)$$

and $[M]^+ = f[M_0]^+$ where $[M_0]^+$ is the total number of parent-molecule ions formed by the initial electron impact process, and $[M]^+$ is the concentration observed at any one time. The quantity f represents the fraction of the total ionization appearing as $[M]^+$. If the observed concentration $[A]^+$ is determined from Equation 3

$$[A]^+ = f'[A_0]^+ \qquad (3)$$

where f' is the fraction of $[A_0]^+$ ions incapable of further fragmentation, then the ratio of daughter to parent-molecule ion is determined by Equation 4, which can be greatly simplified when $f' \longrightarrow 1$ and $k_t \longrightarrow k_1$.

$$\frac{[A]^+}{[M]^+} = \frac{f'[A_0]^+}{f\,[M_0]^+} = .f' \frac{k_1}{k_t} \left[(1/f) - 1 \right] \qquad (4)$$

As can be seen from the assumptions, this treatment is valid only when decomposition of the daughter ion is negligible and when the stabilities of the parent-molecule ion and daughter ion are approximately equal, i.e. when the ratio observed at the detector is not significantly different from the ratio at the source.

Bursey and McLafferty[13] demonstrated that for substituted benzophenone systems, linear free energy relationships based on the Hammett Equation[12] (Equation 5) were observed

$$\log \frac{Z}{Z_0} = p \qquad (5)$$

where

$Z = [A]^+ / [M]^+$ for the substituted benzophenone,

$Z_0 = [A]^+ / [M]^+$ for benzophenone,

p = Hammett Reaction parameter,

σ = Hammett Substituent parameter, and

$[A]^+ = [C_6H_5]^+$.

Bursey and Twine[18] extended the study to include disubstituted benzophenones, and Einolf and Munson[19] investigated the ratios of rate constants (k_1 vs k_2) for the benzophenone system by plotting $[A]^+ / [D]^+$ vs σ. Their results indicate that the correlation exists, but the slope is of different sign than that of the $[A]^+ / [M]^+$ vs σ plot. Einolf and Munson extended their investigation to benzils and found a similar correlation.[22] The abundance of a fragment is related to the appearance potential (A.P.) since the fragment with the lowest A.P. is most likely to be formed when the parent-molecule ion is formed with limited excess energy. At higher energies, the possibility of successive fragmentation increases, resulting in different ratios of fragment abundances at 15 eV and 50 eV.[22] Plots of A.P. versus the Hammett substituent, therefore, may be more informative than McLafferty and Chin-Harrison type plots because the problem of choosing the correct electron energy is obviated. The validity of such plots has been demonstrated by Chin and Harrison[16] for the acetophenone system.

Knaggs and Lonsdale[23] reported in 1939 that benzil has a skew conformation, the conjugation between adjacent carbonyls being greatly reduced in favor of cross-conjugation between a carbonyl and the geminal phenyl group. Infrared[24,25] and electronic spectra[26,27,28] and nuclear magnetic resonance spectroscopy[29] have established that benzil, at least in solution, exists in a twisted structure in which the benzoyl groups are approximately perpendicular, with a dihedral angle of approximately 97°. Bauld[30] examined the configuration of the benzil anion and dianion (formed with potassium in tetrahydrofuran) and found both to be predominantly cis. Bauld verified this conclusion with HMO calculations which showed the planar cis form to be the minimum energy conformation for an anion radical and dianion of benzil. Evans and Leermakers[31] postulated, as the result of the shift between the absorption maximum and the phosphorescence maximum, that the carbonyls were coplanar in the lowest neutral excited state and suggested that this would likewise be true for unsymmetrical benzils also. Ogata, Takagi and Fujii[32] compared the absorption maximum and phosphorescence maximum for 4-dimethylaminobenzil, 4-methoxybenzil, 4-methylbenzil, 4-chlorobenzil, and 4-nitrobenzil, among others, and concluded from the shifts in maxima (from 5800 to 7700 cm^{-1}) that they are planar (probably trans) in the lowest triplet state. Ogata, et al.[32] also examined the products from the photoreduction (>300 nm, 2-propanol) of the unsymmetrical benzils and found that the yield of photoproduct (a benzoin or pinacol in most cases) increases with increasing electron-withdrawing ability of the substituent and that the carbonyl reduction is exclusively at the carbonyl with the more electronegative substituent. The result is ascribed to greater

reactivity at the carbonyl on the electronegative side, and not to a skew conformation. It appears, then, from these studies that the conformation of the benzils is a function of the number of electrons present and the energy levels in which they are distributed. If the ion formed in the gas phase is formed in an excited state, similar to that observed in solution, then the substituted ring will be part of the excited system. Natalis and Franklin,[33] and Bursey and McLafferty[13] have observed in acetophenone and benzophenone systems that the substituted phenyl ion should be formed directly from the excited state molecular ion, but that the benzoyl ion should be formed first, and the phenyl ion from it if the fragmentation occurs from the ground state (skew).

The initial mass spectrometric study on benzil was done by Natalis and Franklin.[33] They found the predominant ion at 70 eV to be m/e 105, which corresponds to the benzoyl ion. The second most abundant ion (76%), at m/e 77, was the phenyl ion. The parent-molecule ion appeared in only 2% abundance. The spectrum of benzil was compared to that of benzophenone, with the only significant difference found in the abundance of the parent-molecule ion (25%).

Einolf and Munson[22] plotted log $[Y\text{-}C_6H_4CO^+/C_6H_5CO^+]$ at 15 eV and at 70 eV versus σ and σ^+ for <u>para</u>-substituted benzils and benzophenones, noting that the major difference between the two systems is that only one bond need be broken in the <u>para</u>-substituted benzils to give either set of products (i.e. either <u>para</u>-substituted or unsubstituted benzoyl ion), whereas different carbon-carbon bonds are broken to get analogous ions from <u>para</u>-substituted benzophenones. They found that the benzils' spectra correlate better with σ, while the benzophenones' spectra correlate

better with σ^+. In both cases, the magnitude of the substituent effect (as measured by p, the slope of the correlation line) increased as predicted with decreasing electron energy, i.e. as $k_t \longrightarrow k_1$ in Equation 4. The only para-substituted benzils which deviated from the correlation line were the 4-fluoro- and 4-methyl benzils. Einolf and Munson also measured charge-exchange spectra using carbon monoxide as the reactant gas and found a satisfactory correlation with σ. They concluded that the $C_6H_5^+$ and $Y\text{-}C_6H_4^+$ ions found in the spectra of the substituted benzils are formed primarily by decomposition of $C_6H_5CO^+$ and $Y\text{-}C_6H_4CO^+$ respectively, and not directly from the parent-molecule ion, but they published no metastable data in support of this conclusion.

Scheppele, et al.[34] investigated the fragmentation pattern of 4-methylbenzil, evaluating appearance potentials by the second derivative of the ionization efficiency technique (SDIE). Based on their comparison of calculated and measured appearance potentials, and on the metastable data at 70 eV, they concluded that initial fragmentation of the parent-molecule ion produced a substituted and an unsubstituted benzoyl ion and a benzoyl radical corresponding to cleavage between carbonyls. Loss of carbon monoxide from the benzoyl ions produced the phenyl ions found in the spectrum and loss of acetylene from the phenyl ions produced the only other significant ions in the spectrum, $C_5H_5^+$ and $C_4H_3^+$. A more complete discussion of their appearance potential data is found in Section VI, of their metastable data in Section V, and a generalized scheme corresponding to their proposed fragmentation pattern is presented in Figure 16.

While most studies of organic compounds in the mass spectrometer

have focused on positive ion spectra, negative ions are also formed in many instances,[35,36] although usually at much lower abundances. Although specially designed sources are sometimes preferred,[37,38] negative ion spectra can be obtained with conventional commercial equipment normally used for positive ion spectra. Kiser[39] ascribes the formation of negative ions to two processes: a) resonance electron capture, (Equations 6 and 6a) and b) ion pair production (Equation 7). These two processes may be written as shown in the following equations:

$$AB + e^- \longrightarrow AB^- \qquad \text{(resonance capture)} \qquad (6a)$$

$$AB + e^- \longrightarrow A^- + B \qquad \text{(dissociative attachment)} \qquad (6b)$$

$$AB + e^- \longrightarrow A^+ + B^- + e^- \qquad \text{(ion pair production)} \qquad (7)$$

The characteristic distinction between these two processes lies in the fate of the incident electron. When the incident electron is not captured, but merely serves to excite the molecule to an electronic level that leads to the production of a positive and a negative ion, ion pair production (7) occurs. No parent-molecule ion can be formed by this process. Electron capture involves initial attachment of the incident electron to form an excited state, followed by one of three processes.[40] The excited ion may dissociate to form a negative daughter ion and a neutral fragment (dissociative attachment, 6b), it may be accelerated as the excited parent-molecule ion before subsequent decomposition or collision (temporary non-dissociative attachment), or it may emit energy in the form of a photon and be detected as the parent-molecule ion (resonant capture, 6a).

Clearly, the process which predominates should depend upon the

energy of the incident electron, with attachment processes predominating at lower energies and ion pair production predominating at higher energies (>10 eV). Experimentally, however, molecular ions often are abundant or even predominant in 70 eV spectra.[36] Such "inexplicable phenomena," when combined with low ion currents, relatively few peaks, and poor correlation of spectra with the functional group patterns found in positive ion spectra, led Djerassi[41] to conclude, in 1965, that there was little utility in an investigation of the negative ion mass spectra of organic compounds.

Bowie and his coworkers[42-48] have developed several methods to obviate most of the difficulties cited supra. To bring some order to their studies, they chose to investigate a series of compounds built around a common unit which has four properties they deemed desirable:[42] a) augmentation of production of an abundant parent-molecule ion at high energies, i.e. 70 eV, b) stability of the unit, c) augmentation of the unimolecular decomposition of the attached functional group, and d) high cross-section for electron capture. Suitable units used by Bowie have included dicarbonyl,[42] anthraquinone,[42] nitro groups,[43-46] and carbalkoxys.[47,48] Anthraquinones with carbalkoxys in the 2-position do not undergo fragmentation to a significant degree under normal conditions, indicating probable formation of the parent-molecule ion via electron capture, most likely of a secondary electron. Anthraquinones with carbalkoxys in the 1-position, however, readily fragment to form ions indicating loss of RO• which is explained as a dissociative attachment process made possible by the proximity of the substituent carbalkoxy group to the carbonyl of the anthraquinone.

Proximity effects are also demonstrable in the o-nitrobenzanilide system (I), and a McLafferty-type plot of log Z/Z_0, where Z is the ratio of the intensities of fragment ion and parent-molecule ion, and $Z = Z_0$ when the substituent is hydrogen, versus σ, for loss of HO• was found to correlate quite well.[44]

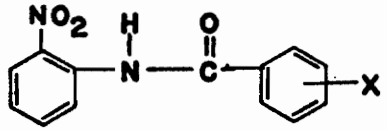

X = H, p-$N(CH_3)_2$, p-CH_3O, p-Cl, p-Br, m-Cl, p-NO_2

Aryl nitro compounds are unique because they involve the only skeletal rearrangement which has been shown to occur in both positive and negative parent-molecule ions. The rearrangement involves the formal loss of NO• from the parent-molecule ion, with the remaining oxygen atom being bound to the carbon atom to which the nitrogen was originally bound.[46,49] The intensity of the [M-NO•] species has been found to increase with increasing electron withdrawing character of the substituents for negative ion spectra, and with increasing electron donating character for positive ion spectra of p-nitrobenzoate ions. The loss of NO• from the o-nitrobenzanilides and m- and p-nitrobenzoates, however, appears to be independent of substituent, and Bowie[44] suggests a radical mechanism to explain the rearrangement:

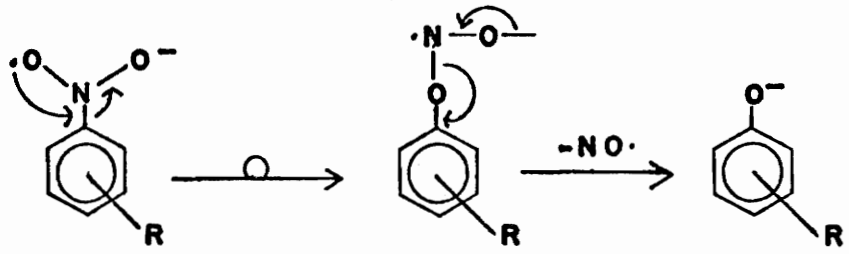

Bowie[48] examined the spectra of substituted phenyl p-cyanobenzoates and substituted phenyl-(p-nitrophenyl)acetates and benzoates to determine which Hammett-type plots provide the best fit for the data. In all three cases, the McLafferty type plot (log Z/Z_0 vs σ) and a plot of relative appearance potentials (A.P. Z - A.P. Z_0) gave an acceptable correlation, but a Chin-Harrison type plot (log $[A]/[M]$ vs σ) failed to show any correlation. Since most positive ion spectra correlate with both McLafferty and Chin-Harrison type plots, the difference in this case must be ascribed to one or more of the following: a) the difference in electron energy in the initial ionization step, i.e. 70 eV versus secondary electron capture, b) difference in the stabilities of the fragment ions produced, i.e. differences in f and f' greater than those assumed in the Chin-Harrison approximations, and c) the possibility of ion formation by two different processes, since at a nominal 70 eV, fragmentation by ion pair production and dissociative attachment is possible.

Todd et al.[36] have proposed some rules to explain negative ion fragmentation patterns in terms of the processes which may lead to stabilization of the excited parent-molecule ions. Their conclusions are as follows:

> "The primary fragmentation modes of organic molecular ions may be predicted qualitatively on the basis of a set of simple axioms: (1) If a molecule contains an electronegative substituent it is likely to give relatively intense yields of negative ions. (2) For dipolar molecules slow electrons will attack preferentially at the positive centre (c f. nucleophilic attack). (3) If the electron enters an anti-bonding orbital the energetic prime molecular anion formed will stabilize by electron coupling consequent upon homolysis of a π- or σ-bond at the site of attachment. This leads to the

formation of stable molecular anions or rapid fragmentation, respectively; competition will be determined by relative bond strengths and product stabilities. (4) The net result is a reduction in oxidation number at the site of attachment."

Subsequent to the commencement of this investigation, Christophorou et al.[50] published data on the negative lifetime and negative ion current as a function of electron energy for benzil. Their data are presented in Figure 1.

A frequently encountered pitfall in attempts to relate data accumulated via a number of techniques is the question of solvation and the effect of solvation on the observed geometries and energy levels. Since the Hammett substituent parameters, the pmr and phosphorescence studies, and all of Bauld's[30] experiments and calculations were in or about solutions, it was felt necessary to investigate the behavior of the benzils at the dropping mercury cathode. Buchta and Evans[51] had reported the polarography of benzil in dimethylsulfoxide, indicating two waves, at 1.04 v and 1.76 v. An esr spectrum was published for the product after the first half-wave, but no conclusions were drawn by them concerning its interpretation.

A systematic analysis of the relationship between the structure of organic molecules and their observed polarographic behavior was begun quite early in the development of polarography. Heyrovsky[52,53] deduced from early data that polarographic reduction becomes easier as the extent of conjugation in the molecule is increased. Shikata and Tachi[54] first described substituent effects on half-wave potentials of organic compounds and postulated the "electronegativity rule" which states that the more electronegative the substituent, the more positive the half-wave

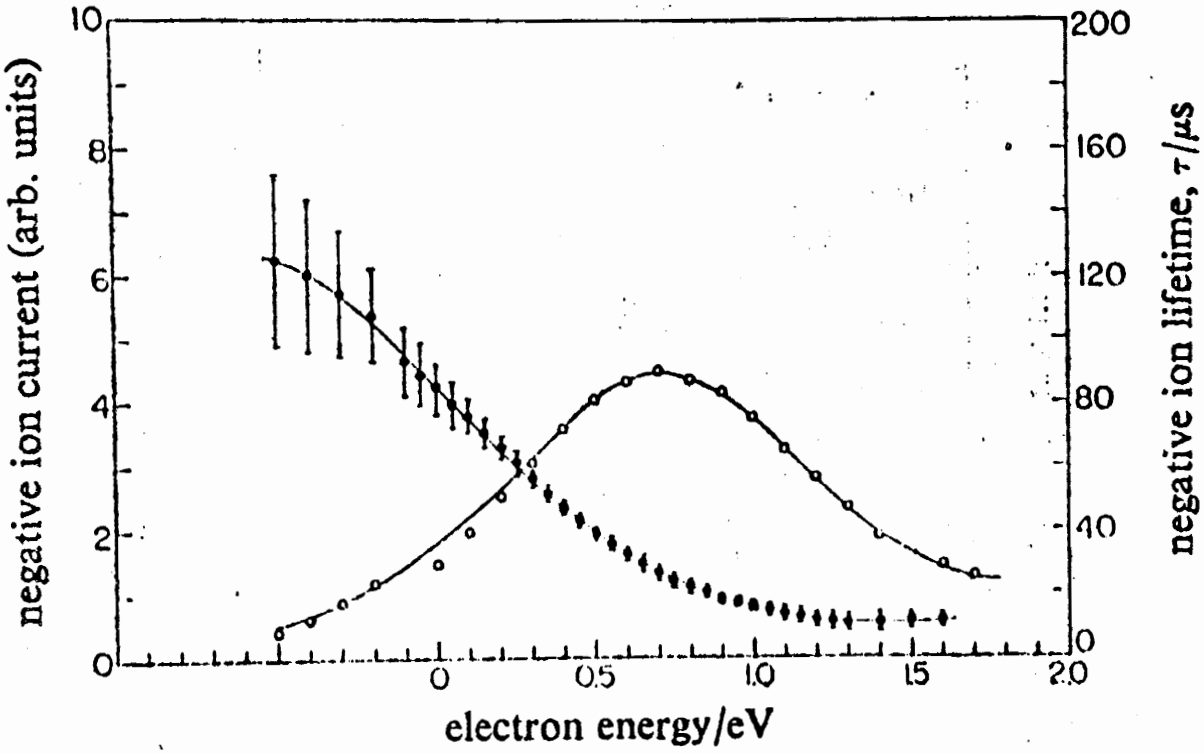

FIGURE 1. Negative Ion Current and Negative Ion Lifetime for Benzil

(From L. G. Christophorou, A. Hadjiantoniou and J. G. Carter, J. Chem. Soc., Far. Trans. II, 69, 1713 (1973).)

potential. Zuman[55,56] has postulated two empirical rules which relate the observed half-wave potential to inductive (I) and tautomeric (T) effects:

> "(1) Groups with -I and -T effects shift the half-wave potentials toward more positive values. Groups with +I and +T effects shift the half-wave potentials toward more negative values. (2) In the absence of other effects, the reduction of benzene derivatives with a reducible group in the side chain and a -T substituent in the ortho or para position occurs at more positive potentials than that of the meta isomer. On the other hand, in the presence of a +T group, the reduction of the meta derivatives takes place at a more positive potential than that of the ortho or para isomer."

Quantitative treatments based on substituent effects were found to be best approached in terms of the structure of the molecular framework because the reaction mechanism is often determined by the framework and not the substituent. Structural changes may cause shifts in the half-wave potentials through changes in the mechanism of the reduction, the reversibility, or the rate of the electrode process, or may affect the diffusion coefficient as seen in changes in the limiting current. The effect of the substituent may be to change the electroactive group, analogous to a change in chromaphores in electronic spectra, or merely to alter the electron density at the electroactive site, analogous to the effect of auxochromes. The former effect is observed in situations where there is an extension of conjugation or where the substituent itself is electroactive, while the latter effect is a true substituent effect amenable to quantitative treatment and Hammett correlations because the electrode process is the same for all members of the series and because variations in the value of the transfer coefficient are minimized.

The shape of the wave and the total (or limiting) current that flows at the plateau of a wave can be used to gain an insight into the reduction process. The wave height is defined as "the difference between the total current and the residual current, and is the current due to the presence of the substance of interest."[57] The wave height is related to the number of electrons (n) involved in the reduction by the Ilkovic[57] Equation (8):

$$i_d = 607\ n\ D^{1/2}\ C\ m^{2/3}\ t^{1/6} \qquad (8)$$

where i_d is the diffusion current (or wave height), D is the diffusion coefficient of the electroactive substance, C is its concentration, m is the flow rate of the capillary, and t is the drop lifetime. For organic compounds of similar structure and molecular weight in identical media, the ratio of wave heights provides the ratio of electrons involved in a reduction. For compounds which can be reduced in stages, the relative wave heights for each step indicate the relative number of electrons involved in each step.

The slope of a given wave can be used as an indication of the reversibility of an electrode reduction process without recourse to cyclic voltametry. For the reversible reduction formally described by Equation 9:

$$O_x + ne = R \qquad (9)$$

the Nernst[57] Equation 10:

$$E_{d.e.} = E_s^0 - \frac{RT}{nF} \ln \frac{f_R\, C_R^0}{f_{O_x}\, C_{O_x}^0} \qquad (10)$$

where E_s^0 is the standard potential for the couple, f is the activity coefficient, and C^0 is the molar concentration of each species at the surface of the drop, is obeyed at every instant. To relate current to concentration, let $i = k_{0_x}(C_{0_x} - C^0_{0_x})$, and $i_d = k_{0_x} C_{0_x}$ where i is the current at a point on the wave, i_d is the current at the plateau (the diffusion current), and $k_{0_x} = 607\, n_{0_x} D_{0_x}^{1/2}\, m^{2/3}\, t^{1/6}$. Subtracting, $i_d - i = k_{0_x} C^0_{0_x}$. Since the system is reversible, i also equals $-k_R C^0_R$. Substituting into the Nernst Equation 10:

$$E_{d.e.} = E_s^0 - \frac{RT}{nF} \ln \left(\frac{f_R k_{0_x}}{f_{0_x} k_R}\right) - \frac{RT}{nF} \ln \frac{i}{i_d - i} \qquad (11)$$

at the half-wave potential

$$E_{d.e.} = E_{1/2} = E_s^0 - \frac{RT}{nF} \ln \left(\frac{f_R k_{0_x}}{f_{0_x} k_R}\right) \qquad (12)$$

or

$$E_{d.e.} = E_{1/2} - \frac{RT}{nF} \ln \frac{i}{i_d - i} \qquad (13)$$

at one quarter of the height of the wave ($E_{1/4}$)

$$E_{1/4} = E_{1/2} - \frac{0.059}{n} \log \frac{i_d/4}{i_d - i/4} = E_{1/2} - \frac{0.059}{n} \log 1/3 \qquad (14)$$

analogously,

$$E_{3/4} = E_{1/2} - \frac{0.059}{n} \log 3$$

subtracting yields

$$E_{3/4} - E_{1/4} = -\frac{0.059}{n} \log 9 = -\frac{0.056}{n} \qquad (15)$$

therefore, for a reversible cathodic wave, the difference in voltages

between $E_{3/4}$ and $E_{1/4}$ should be -56.4/n mV. Obviously, many factors affect the slope of the wave, including maxima, the use of maximum suppressants, damping in the recorder circuitry and changes in drop time. However, the slope test is useful as an exclusion test, and waves which have a slope significantly (ca. 10 mV) different from this value are almost certainly irreversible. Waves with a slope indicating reversibility cannot be reported as reversible without other evidence, but the likelihood of their reversibility is rather high. An irreversible wave for a benzil suggests significant structural changes in the molecule, while a reversible wave suggests slight changes in bond distances or geometric isomerism or a redistribution of energy levels.

The benzil system, therefore, should possess properties well suited to a comparison of substituent effects in positive and negative ion mass spectra, and to a correlation of these effects with properties in solution. Specifically, the benzils are easily synthesized, are indicated to have predictable positive ion spectra which are demonstrably related to the effect of the para substituent on the bond strength of the parent ion and/or to the stability of the daughter ion, and they have adjacent carbonyls, rendering them ideal for the formation of negative ions in both gas phase and in solution. This investigation constitutes an attempt to characterize the positive and negative spectra of a series of para substituted benzils by analysis of the spectra and the appearance potentials of all major ions formed, and to compare these with the results obtained from polarography and other solution phenomena as indicated by the Hammett substituent functions. The process of negative ion formation, the interaction of the carbonyl groups under different

energetic conditions, and the mode of product control were subsidiary issues whose determination was indicated to be possible at the conclusion of the investigation.

SECTION III

EXPERIMENTAL

A. PREPARATION OF MATERIALS

1. 4-Nitrobenzil

Benzil is commercially available from a number of sources, and a large number of substituted benzils are readily synthesized. A list of 4- and 4,4'-substituted benzils, with references to published syntheses, is found in Appendix 1. This preparation is based on that of Womack, Campbell, and Dodds.[58] Into a 150 ml flask fitted with an overhead stirrer was placed 100 g (0.472 mol) of benzoin and 500 ml of acetic anhydride, and the suspension was cooled to 0° with an ice-water bath. With stirring, 100 ml (1.88 mol) of concentrated sulfuric acid, then 55 g (0.495 mol) of potassium nitrate were slowly added, and the suspension was allowed to warm slowly to room temperature. Only after reaching room temperature did all of the potassium nitrate go into solution. The solution was stirred for 48 hrs, then poured into 500 ml of water. A yellow oil formed immediately and was separated in a separatory funnel. The aqueous layer was extracted once with 100 ml of ether, and the ether combined with the oil. The ether-oil fraction was then repeatedly extracted with 150 ml portions of water, then dried over magnesium sulfate. The ether was removed on a rotary evaporator, leaving a viscous brown oil which did not crystallize on standing for 5 days. The oil was placed in a 50 ml boiling flask, 7 ml of

concentrated nitric acid was added, and the solution heated gently for 1 hr. While still hot, the mixture was poured into water, and a yellow semi-solid was formed which remained after the decantation of the water layer. The yellow material was dissolved in 25 ml of acetic acid and recrystallized to give a yellow solid, mp 132-137°. Recrystallization from absolute ethanol afforded a yellow solid, mp 134-137°. Sublimation and recrystallization from 25 ml of benzene-absolute ethanol afforded 2.1 g (0.82 mol, 6%) of 4-nitrobenzil, mp 139.5-140.5°.

Analysis calculated for $C_{14}H_9NO_4$: C, 65.88; H, 3.53; N, 5.49

Found: C, 65.84; H, 3.62; N, 5.65

2. 4-Chlorobenzil

a. p'-Chlorodesoxybenzoin:

In a 100-ml, three-necked flask, equipped with a stirrer, a nitrogen inlet tube, an addition funnel and a reflux condenser was prepared p-chlorobenzylmagnesium chloride from 16.0 g of p-chlorobenzyl chloride and 2.4 g of magnesium in 50 ml of dry ether. After the bright green reagent had formed (about one hour) a small Soxhlet extractor, containing 3.0 g of dry benzamide was placed between the reactor flask and the condenser. The ether solution was heated under reflux with constant stirring for three days during which time the benzamide was extracted completely into the solution. A constant pressure of dry nitrogen was maintained over the reaction mixture. After hydrolysis

of the reaction complex with aqueous hydrochloric acid, the ketone was recovered from ethanol-water solution. Drying afforded 4.5 g (0.019 mol, 78%) of white crystals, mp 130-132°. [Lit[59] 132°].

b. p-Chlorobenzil:

One gram of p'-chlorodesozybenzoin was dissolved in 4 ml of acetoc anhydride to which was added 0.86 g of selenium dioxide. The solution was heated at 140° for three hours, removed from the precipitated selenium with a micropipet and heated with 5 ml of water and 0.1 g of charcoal. The hot solution was filtered through a small Buchner funnel and the crude product was obtained on cooling. The yellow crude product was removed by filtration and recrystallized twice from aqueous ethanol and dried in vacuo to yield 1.2 g (0.005 mol, 96%) of yellow crystals, mp 72-73°. [Lit[60] 73°].

Analysis calculated for $C_{14}H_9ClO_2$: C, 68.71; H, 3.68

Found: C, 68.79; H, 3.60

3. 4-Methylbenzil

This procedure was adapted from that of Allen and Barker.[61] To a dry, 1 three-necked round-bottomed flask fitted with a condenser and Teflon-coated magnetic stirrer was added 184 g (2.02 mol) of toluene and 75 g (0.561 mol) of anhydrous aluminum chloride and, finally, 154 g (1.10 mol) of phenylacetylchloride dropwise. It was necessary to cool

the reaction mixture to moderate the rate of boiling at the start. After the addition was complete, the solution was refluxed for 1 hr, cooled, and poured onto a mixture of 500 g cracked ice and 200 ml of concentrated hydrochloric acid. The oily product which resulted was extracted into 500 ml of ether, the ether was extracted repeatedly with 100 ml aliquots of water, dried over magnesium sulfate, and evaporated. The crude benzyl-p-tolyl ketone product was recrystallized once from ca. 100 ml of methanol to give 42.5 g (2.02 mol, 18.5%), mp 106°, [Lit[62] 109-110°]. Into a 100 ml three-necked round-bottomed flask fitted with a condenser and a Teflon stirring bar was placed 20.0 g (0.09 mol) of benzyl-p-tolyl ketone, 22.2 g (0.20 mol) of selenium dioxide, and 50 ml of glacial acetic acid. The solution was refluxed overnight, poured into cold water, and extracted into 100 ml of ether. The ether was washed repeatedly with 100 ml portions of water and dried over magnesium sulfate. The ether was evaporated to leave a yellow oil which was distilled under vacuum (136-140°/3 mm). The oil failed to crystallize neat or after trituration with methanol. Pmr spectroscopy in carbon tetrachloride indicated peaks at 2.26 (s, 3, CH_3) and 7.10-8.00 (distorted quintuplet, 9, ArH). The ratio of areas on two successive sweeps was 1.32:1 and 1.32:1; theoretical 1.30:1.

Analysis calculated for $C_{15}H_{12}O_2$: C, 80.36; H, 5.36

Found: C, 80.59; H, 5.48

4. 4-Methoxybenzil

This is essentially the procedure of C. R. Kinney.[63] To a 1.5 ℓ flask fitted with a condenser and a stirrer were added 25 g (0.395 mol)

of potassium cyanide in 175 ml of water, 136 g (1.00 mol) of anisaldehyde, 106 g (1.00 mol) of benzaldehyde, and 350 ml of 95% ethanol. The mixture was refluxed with stirring for 1.5 hr. The oily product obtained was steam distilled from the reaction mixture, the aqueous layer drawn off, and the product cooled to yield 51 g of crude p-methoxybenzoin. Successive recrystallizations from ca. 125 ml of absolute ethanol afforded 46 g (0.19 mol, 19%) of pure white p-methoxybenzoin, mp 102-103°.

To a stirred, refluxing solution of 37 g (0.23 mol) of cupric sulfate in 50 g of pyridine and 20 ml of water was added 24.2 g (0.10 mol) of p-methoxybenzoin. After 2 hrs, the mixture was poured into a separatory funnel and the $CuSO_4$-pyridine solution drawn off. The product was then washed with 10 ml portions of 10% 6N HCl in ether until no pyridine odor remained. The crude product was then recrystallized from 50 ml of 80% ethanol to give 18.2 g (0.07 mol, 75%) mp 62°, [Lit[64] 61-62°].

5. 4-Methylthiobenzil

The following procedure for the preparation of α-phenyl-4-methylthioacetophenone is essentially that of Becker et al.[65] To a stirred solution of 13.0 g (0.106 mol) of thioanisol (methyl phenyl sulfide, Eastman Chemical Co.) and 18.0 g (0.129 mol) of phenylacetyl chloride in 75 ml of anhydrous, freshly distilled 1,1,2,2-tetrachloroethane (bp 146°) was added, portionwise, 14.5 g (1.10 mol) of aluminum chloride, while maintaining the temperature at 0-5° with an ice-bath. The solution first turned brown, then brilliant green. Three hours after the aluminum chloride had been added, the stirrer was turned off and the solution allowed to stand overnight. The mixture was then poured over a mixture of 500 g

of ice and 500 ml of concentrated hydrochloric acid. The resultant oil was separated from the water in a separatory funnel, washed several times with 150 ml portions of water, dried over magnesium sulfate, and evaporated to near dryness on a rotary evaporator. When the product failed to crystallize, the oil was vacuum distilled to remove the last traces of 1,1,2,2-tetrachloroethane. The remaining solid was crystallized from 30 ml of absolute ethanol to yield 13.0 g (0.055 mol, 53%) of glistening yellow powdery α-phenyl-4-methylthioacetophenone, mp 98-100°. Into a 50 ml boiling flask, fitted with a Teflon stirring bar and a reflux condenser, was added 3.0 g (0.0127 mol) of α-phenyl-4-mercaptoacetophenone, 1.38 g (1.24 mol) of selenium dioxide, and 10 ml of acetic acid. The solution was heated to reflux, stirred overnight, then dumped into cold water. The water was extracted with 100 ml of ether, and the ether solution dried over magnesium sulfate and evaporated. Several recrystallizations from ca. 50 ml of absolute ethanol afforded 1.9 g (0.0073 mol, 60%) of 4-methylmercaptobenzil, mp 58-60°.

6. 4-Dimethylaminobenzil

Using the method of Staudinger,[66] to a 125 ml three-necked round-bottomed flask equipped with a Teflon stirring bar and a cold-finger condenser were added 10.6 g (10.2 ml, 0.10 mol) of benzaldehyde and 14.9 g (0.10 mol) of p-dimethylaminobenzaldehyde in 40 ml of 95% ethanol. To this stirred mixture was added a solution of 2.0 g (0.31 mol) of potassium cyanide in 20 ml of water. The reaction mixture was refluxed with stirring for 1 hr, then cooled. The resulting precipitate was filtered from the solution, and the solution returned to the reaction

vessel with an additional 2.0 g of potassium cyanide in 20 ml of water and refluxed for another hour. Upon cooling and filtration, the second precipitate was added to the first and the product recrystallized once from methanol to give 22.4 g (0.088 mol, 88%) of p-dimethylaminobenzoin, mp 162-164°. The p-dimethylaminobenzoin was split into two 10 g (0.039 mol) portions, one of which was treated by the method of Weiss and Appel[67] (cf. p. 30) and gave none of the desired product; the other portion was treated in a method analogous to that of Boesler[68] and yielded a product with the reported melting point. Into a 126 ml Erlenmeyer flask was placed a stirring bar, 10 g of p-dimethylaminobenzoin, and enough 95% ethanol (ca. 30 ml) to dissolve the p-dimethylaminobenzoin when heated gently. To this hot solution was added 50 ml of Fehling's solution. (Fehling's solution was prepared by mixing immediately before use equal volumes of the following: Solution A, 34.6 g copper sulfate in 500 ml of water; Solution B, 173 g sodium potassium tartrate and 70 g of sodium hydroxide in 500 ml of water). The reaction mixture was stirred with heating until the solution was a deep blue and a red precipitate of cuprous oxide was visible. The mixture was cooled, filtered, and concentrated to yield some greenish-yellow crystals. The precipitate from the reaction mixture was extracted with hot ethanol, and the crystals added to the ethanol. Crystallization afforded 7.1 g (0.027 mol, 70%) of bright yellow prismatic crystals, mp 115-117°, [Lit[58] 115-117, [69] 101°].

Analysis calculated for $C_{16}H_{15}NO_2$: C, 75.85; H, 5.94; N, 5.58

Found: C, 75.91; H, 6.00; N, 5.94

7. 4,4'-Dinitrobenzil

a. 4,5-Diphenylglyoxalone:

The preparation was based on the work of Chattaway and Coulson.[70] Into a 500 ml three-necked round-bottomed flask fitted with a magnetic stirrer and a condenser were placed 50 g (0.236 mol) of benzoin, 26 g (0.435 mol) of urea, and 200 ml of glacial acetic acid. The mixture was refluxed for 6 hrs and cooled to yield crude crystalline 4,5-diphenylglyoxalone which was filtered, washed with cold acetic acid, and recrystallized from ca. 70 ml of acetic acid to yield 40 g (0.177 mol, 75.6%) of colorless needles, mp 324°.

b. 4,4'-Dinitrobenzil:

Into a 500 ml three-necked round-bottomed flask were placed 27 g (0.144 mol) of 4,5-diphenylglyoxalone and 315 g of concentrated sulfuric acid. When solution had been effected, the solution was cooled in an ice-salt bath to -5° and 57 ml of fuming nitric acid was slowly added. The mixture was allowed to warm slowly to room temperature and allowed to stand for three days, during which time a flocculant yellow mass separated from the solution. The whole solution was then poured onto ice, and the resulting yellow solid was boiled with water, drained, and recrystallized three times from acetic acid to yield 4.5 g (0.015 mol, 10%) of deep yellow crystals, mp 212-213.5°, [Lit[70] 213°, [69] 209°].

8. 4,4'-Dichlorobenzil

a. 4,4'-Dichlorobenzoin:

This is essentially the procedure of Lutz and Murphy.[71] For best results, the p-chlorobenzaldehyde should be purified before use, and all

unreacted p-chlorobenzaldehyde had to be removed from the initial reaction product before final oxidation to the benzil. The purification procedure was as follows: dissolve 500 g (3.35 mol) of commercial p-chlorobenzaldehyde (Eastman Chemical Co.) in 800 ml of ether and extract three times with a total of 800 ml of 10% sodium carbonate solution. The resulting ether solution was washed with 200 ml of water, dried over sodium sulfate, and the ether removed by distillation. Vacuum distillation of the resulting oil ($78^{\circ}/5$ mm) afforded 92% recovery of pure p-chlorobenzaldehyde.

Into a 500 ml one-necked round-bottomed flask was placed 300 g (2.15 mol) of purified p-chlorobenzaldehyde, 300 ml of methanol, 5 g of a saturated aqueous solution of potassium cyanide, and the solution heated to reflux. When the solution had turned a dark red (about 20 min) the flask was placed on a rotary evaporator and the methanol removed under vacuum. The resultant red paste was taken up in 250 ml of benzene and extracted three times with 100 ml portions of 20% aqueous sodium bisulfite solution. This treatment turned the red benzene solution yellow-green. The third sodium bisulfite wash solution was tested by adding aqueous sodium hydroxide solution (a clouding of the solution indicates the presence of p-chlorobenzaldehyde). When all p-chlorobenzaldehyde had been removed, the benzene solution was washed twice with 100 ml portions of water, dried over magnesium sulfate, and the benzene removed on the rotary evaporator. The thick orange oil resulting from this treatment was taken up in 1 ℓ of pentane, heated, filtered, and allowed to stand overnight in the refrigerator. This afforded 80 g (0.285 mol, 26.5%) of white 4,4'-dichlorobenzoin, mp $87-88^{\circ}$, [Lit[71] $87-88^{\circ}$].

b. 4,4'-Dichlorobenzil:

This procedure is essentially that of Weiss and Appel.[67] Into a 1 ℓ one-necked round-bottomed flask equipped with a magnetic stirrer were placed 80 g (0.285 mol) of 4,4'-dichlorobenzoin, 30 g (0.375 mol) of cupric acetate monohydrate, and 350 ml of 80% acetic acid, and the mixture was allowed to reflux with stirring for 1.5 hr. At this point, the hot solution was transferred to a beaker where it solidified. It was then filtered, washed with cold 80% acetic acid, and finally with water. This treatment afforded 73.8 g (0.26 mol, 92%) of bright yellow crystals, mp 194-195°, [Lit[72,73] 195-196°, [74] 200°]. Recrystallization from 2.5 ℓ of n-butanol containing 1 ℓ of ethanol afforded a 96% recovery of pure yellow crystals of 4,4'-dichlorobenzil, mp 197-198.5°.

9. 4,4'-Dimethylbenzil

a. 4,4'-Dimethylbenzoin:

Into a 1 ℓ , three-necked round-bottomed flask equipped with a reflux condenser and a mechanical stirrer was placed 30 g (0.46 mol) of potassium cyanide and 150 ml of water, and the solid dissolved with stirring. When solution was effected, 178 g (1.5 mol) of p-tolualdehyde and 300 ml of 95% ethanol were added. The solution was refluxed for 3 hrs and cooled with stirring to yield an oil which descended to the bottom of the flask. Continued stirring at room temperature afforded crystallization of the oil. The crystals were filtered, washed with cold 95% ethanol, and pressed dry to yield 151 g (0.675 mol, 90%) of white, crystalline 4,4'-dimethylbenzoin, mp 87.5-88.5°, [Lit[75] 88-89°].

b. 4,4-Dimethylbenzil:

This is essentially the oxidation procedure of Weiss and Appel.[67] Into a 1 ℓ three-necked round-bottomed flask fitted with a magnetic stirrer and two Fredericks condensers were placed the 151 g (0.675 mol) of 4,4'-dimethylbenzoin produced supra., 72.3 g (0.93 mol) of ammonium nitrate, 1.5 g (0.007 mol) of cupric acetate monohydrate, and 520 ml of 80% acetic acid, and the resulting solution was washed with cold 80% acetic acid, affording 142.8 g (0.56 mol, 88%) of yellow crystals, mp 101-103°. Recrystallization from 350 ml of 95% ethanol afforded 96% recovery of pure yellow 4,4'-dimethylbenzil, mp 102.6-103.2°, [Lit[75] 104-105°].

10. 4,4'-Dimethoxybenzil

The oxidation procedure of Weiss and Appel[67] was used to oxidize commercial p-anisoin. Into a 500 ml, one-necked round-bottomed flask equipped with a mechanical stirrer was placed 100 g (0.368 mol) of p-anisoin, 34.9 g (0.436 mol) of ammonium nitrate, 0.872 g (0.0044 mol) of cupric acetate monohydrate, 303 ml of 80% acetic acid, and the resulting solution was refluxed for 2 hrs. At this point the solution was cooled, the solid filtered, washed with cold 80% acetic acid and then water. This afforded 85 g (0.313 mol, 85%) of yellow 4,4'-dimethoxybenzil, mp 130-131°. Recrystallization from 1400 ml of 95% ethanol afforded 81.2 g (0.300 mol, 95.5% recovery) of pure product, mp 131.4-132.4°, [Lit[67] 132° [76] 133°].

11. 4,4'-Dimethylthiobenzil

a. p-Methylmercaptobenzaldehyde:

Into a 3 ℓ, three-necked round-bottomed flask equipped with a stirrer, thermometer, reflux condenser with a drying tube, and a gas inlet tube were placed 346 g (3.10 mol) of zinc cyanide, 242 g (1.95 mol) of thioanisol (Aldrich Chemical Co.) and 700 ml of dry benzene. The flask was then cooled in an ice bath to 5°, and a swift stream of dry hydrogen chloride gas passed into the solution for 0.75 hr, during which time the temperature rose to 15°. With continuous stirring and cooling, 343 g (2.57 mol) of anhydrous aluminum chloride was added over a period of 10 min. The reaction was then allowed to stir for 8.5 hrs while the temperature rose to room temperature. During this time the solution turned dark green. One liter of 18% hydrochloric acid was then added with stirring, and the mixture allowed to stand overnight. The mixture was then refluxed for 4 hrs and steam distilled until clear (ca. 25 ℓ). The distillate was extracted twice with ether and the ether dried over anhydrous sodium sulfate. The ether was then removed on the rotary evaporator and the oil distilled to yield 122.7 g (0.806 mol, 41.4%) of p-methylmercaptobenzaldehyde, bp 118-120°/4 mm, [Lit[77] 153°/17 mm, [78,79] 273°].

b. 4,4'-Dimethylthiobenzoin:

Into a 1 ℓ flask equipped with a reflux condenser was placed 100 g (0.656 mol) of p-methylmercaptobenzaldehyde, 30 g (0.461 mol) of potassium cyanide dissolved in 150 ml of water, and 350 ml of 95% ethanol. The solution was refluxed for 2 hrs and allowed to cool slowly to room temperature, during which time a red oil deposited which later turned to a light yellow solid. The reaction was cooled in ice, filtered, and the precipitate was washed repeatedly with cold 95% ethanol, and then dried

in air. The crude product was used as obtained in the next reaction, and the yield was not recorded at this point.

c. 4,4'-Dimethylthiobenzil:

The 4,4'-dimethylthiobenzoin produced *supra* was oxidized to the corresponding benzil according to the procedure of Weiss and Appel.[67] Into a 1 ℓ, three-necked round-bottomed flask equipped with a stirrer and two Fredericks condensers was placed the crude 4,4'-dimethylthiobenzoin, 32.8 g (0.420 mol) of ammonium nitrate, 0.655 g (32.8 mol) of cupric acetate monohydrate, and 230 ml of 80% acetic acid. The solution was refluxed for 3 hrs and allowed to stand overnight. It was refluxed for an additional hour, cooled, filtered, and the precipitate washed with 50% acetic acid, then water, and dried. There was obtained 61.9 g (0.205 mol, 62.4%) of crude 4,4'-bismethylmercaptobenzil, mp 140-145°. Recrystallization from 95% ethanol afforded yellow needles, mp 161-162°.

Analysis calculated for $C_{16}H_{14}O_2S_2$: C, 63.54; H, 4.67; S, 21.21

Found: C, 63.35; H, 4.64; S, 21.17

12. 4,4'-Bis(dimethylamino)benzil

This preparation is based on that of Tuzun, Ogliaruso, and Becker.[80] Into a 3 ℓ , three-necked round-bottomed flask equipped with a high-torque stirrer, reflux condenser with a calcium chloride drying tube, thermometer, and a dropping funnel was placed 133 g (1.00 mol) of anhydrous aluminum chloride and 200 ml of dry carbon disulfide. The mixture was cooled in an ice bath and stirred while 182 g (1.50 mol) of *N*,*N*-dimethylaniline was slowly added through the dropping funnel during a 0.25 hr period. The dropping funnel was then washed with 20 ml of dry

carbon disulfide, which was then added to the reaction mixture. At this point the reaction mixture consisted of a white solid slurried in a light-green liquid.

The reaction mixture was then cooled to 5-10° in an ice-salt bath, and with continuous stirring 31.7 g (21.3 ml, 0.25 mol) of oxalyl chloride in 200 ml of dry carbon disulfide was added dropwise over a 20 min period. The resulting thick black mixture was allowed to warm slowly to room temperature, refluxed for 1 hr, and then cooled to 0-5° in an ice bath, all while stirring continuously. To the mixture was then added 100 g of ice, followed by 400 ml of cold water. The flask was then set for steam distillation and so distilled until all unreacted N,N-dimethylaniline and the carbon disulfide had been removed and the green-black aluminum chloride complex had decomposed to leave a blue-green solid (ca. 2 hrs). The mixture was cooled to 50° and the crude product filtered out. The crude product was slurried in 200 ml of water at 50° and filtered to remove impurities, then washed with 50° water and then cold methanol. The air-dried product, 47 g, mp 190-192°, was then dissolved in 500 ml of chloroform, extracted three times with 400 ml portions of 6% hydrogen peroxide containing 1.0 g of sodium hydroxide, then 500 ml of cold water. The combined aqueous layers were heated to drive off chloroform, then filtered. The solid so obtained was added to the chloroform fraction. The chloroform was distilled off and the residue dissolved in 1.5 ℓ of acetone under reflux. The acetone solution was filtered, then cooled overnight in a refrigerator. The yellow crystals were filtered, washed with cold methanol, and air dried to yield 27 g (0.0891 mol, 36%) of product, mp 199-200°, [Lit[80] 199-200°].

B. EQUIPMENT AND TECHNIQUES

The mass spectral studies were carried out using an Hitachi Perkin-Elmer RMU-7 double focusing mass spectrometer. Solid benzils (vide supra) were introduced into the ionization chamber using the direct inlet probe. Gaseous samples were metered from an external manifold into an all-glass heated manifold and allowed to diffuse through a molecular leak into the ionization chamber. Liquid samples were injected through a septum into the aforementioned heated manifold. The ionization chamber was maintained at 140-150°, and the solid inlet heater and liquid manifold temperatures were adjusted between 50° and 120° so as to maintain an analyzer tube pressure between 1.0 and 3.0 x 10^{-6} torr in all experiments. It is assumed that the pressure in the ionization chamber differed by less than an order of magnitude from the analyzer tube. No investigations were performed in the range of 1 x 10^{-4} torr, and no data are therefore available concerning reactions between ions and molecules produced in the ionization chamber.

For positive ion spectra and energetics measurements, the energy of the electron beam, emitted thermionically from a 7 mil diameter rhenium filament heated by approximately 3.1 amperes of current, is controlled by a variable d.c. potential between filament and chamber. The resultant electron beam is not monoenergetic since electrons emitted from the heated filament have appreciable thermal energies, producing a distribution of energies above the measured voltage difference. To obviate both this problem and the difficulties raised by the fact that ionization efficiency curves for different compounds often do not have the same

shape,[81] all experimental ionization (IP) and appearance (AP) potentials must be adjusted by use of an internal calibrant, in these studies, Xe-129, with an I.P. of 12.13 eV.[82] Target potential is regulated at approximately 7 V. above the chamber voltage.

An ionization efficiency curve is a plot of the variation of the intensity of an observed ion (the ion current) as a function of the energy of the ionizing electron. The type of curve obtained for benzils is typical of singly-charged positive ions in the range from 0 to 50 eV (Figure 2) and consists of three sections: a) a "foot," a curved portion for approximately one volt above the threshold energy, and an indication of both the nonhomogeniety of the electron beam and of the population of states lying close in energy to the ground state; b) a linear portion for the next 10-20 eV; and c) a plateau region where the curve approaches 100% asymptotically. Figure 2 shows a plot of the ionization efficiency curves of Xe-129, the calibrant, and m/e 139 formed by fragmentation of 4,4'-dichlorobenzil. The difference in the slope in the linear region (b) is the result of the presence of several energy levels in the positive ion close to its ground state, on the kinetic energy released on rupture of the carbonyl-carbonyl bond, and on the cross-section of the particular ion. The slope becomes more horizontal in the ionization efficiency curves of smaller and smaller fragments from the same parent molecule. Because of the differences in slopes, the simplest analytical method for determining A.P.'s from ionization efficiency curves, the semi-log plot, should not be used here because the distortion of the curve is greatest in the foot region (a), the region where the semi-log method measures the difference in potential between ion and calibrant.

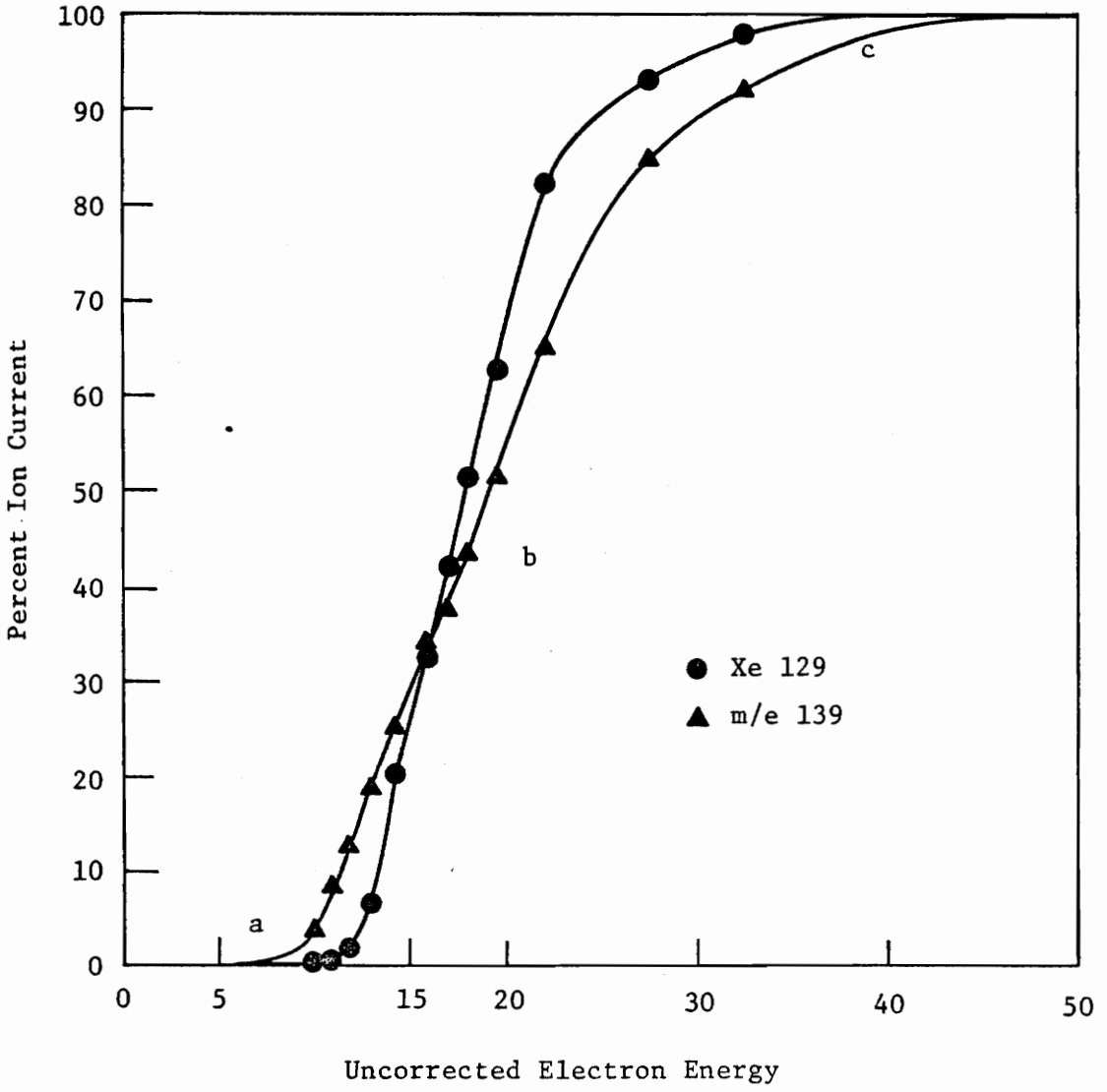

FIGURE 2. Ionization Efficiency Curves for Xe-129 and m/e 139 from 4,4'-Dichlorobenzil

a. foot region
b. linear region
c. plateau region

On the assumption that the ionization and fragmentation processes for the benzils would be similar to each other, and that the ionization efficiency curves would not vary measurably for a given process, the Warren method for determining the appearance potentials was chosen. In the Warren method,[83] the ion current scales are adjusted so as to make the linear portions (b) of the ionization efficiency curves of the sample and the calibrant ion parallel. This is done by applying a correction factor to all points on the ionization efficiency curve of the fragment ion. The differences in voltages (ion versus calibrant) at various ion currents are determined from the corrected curves, and these differences are plotted as a function of the ion current. The resulting curve is extrapolated to zero ion current, and the value obtained is alegbraically added to the ionization potential of the calibrant to obtain the appearance (or ionization) potential of the sample ion. Calibrant ionization efficiency curves were reproducible to ± 0.05 eV on successive determinations. A.P.'s of fragments, especially secondary fragment ions, were less reproducible, and the precision of the measurement may depend on the condition of the source, especially the cleanliness of the insulators. The variation in A.P.'s explains, in large part, the variation in ratios of relative abundances. All A.P. values are expressed in terms of one standard deviation.

Negative ion spectra and ionization efficiency curves were obtained by reversing the polarity of the chamber relative to the exit accelerating slit, and by reversing the polarity of the sector and magnet. Repeller voltages were trimmed to zero. Because the large thermal distribution of the electron beam produces electrons of several eV at nominally zero

chamber voltage, the instrument was modified so that the electron energy was controlled by three 10.3 V mercury batteries and a ten-turn Helipot precision potentiometer which allowed a positive bias to be applied on the electron-accelerating circuit (Figure 3). The result is effectively to allow only electrons with energy greater than the bias to enter the ionizing chamber, i.e. to produce zero energy electrons so as to allow measurement of the complete electron capture curve.

The instrument was focused on SF_6^-, produced from SF_6 by electron capture,[50] to produce an electron capture ionization efficiency curve with a width at half-height of 0.18 to 0.50 eV. A filament current of 2.6 to 2.8 amperes was found to afford the best curves (Figure 4).

Ionization efficiency curves for the parent and fragment ion peaks were obtained by recording the ion current at 0.15 eV increments, beginning at a voltage at least 0.5 eV before onset and calibrating by comparison with the SF_6^- curve determined by the same method immediately afterward. Reported values are for voltages corresponding to the maximum ion current recorded for the ion, and also for the onset voltage as determined by the vanishing current method. Both methods are reproducible to $\pm$0.10 eV.

Positive and negative ion spectra were obtained at nominal energies of 50 eV. The most intense ion peak in the mass spectrum is denoted the "base peak" and assigned the arbitrary intensity value of 100.0%. Spectra are reported as observed with no correction for isotopic abundances. The intensities of all other peaks are given values relative to the base peak. Positive ions are detectable under normal conditions to 0.001% of the base peak, but ions of less than 0.5% are not included in the reported

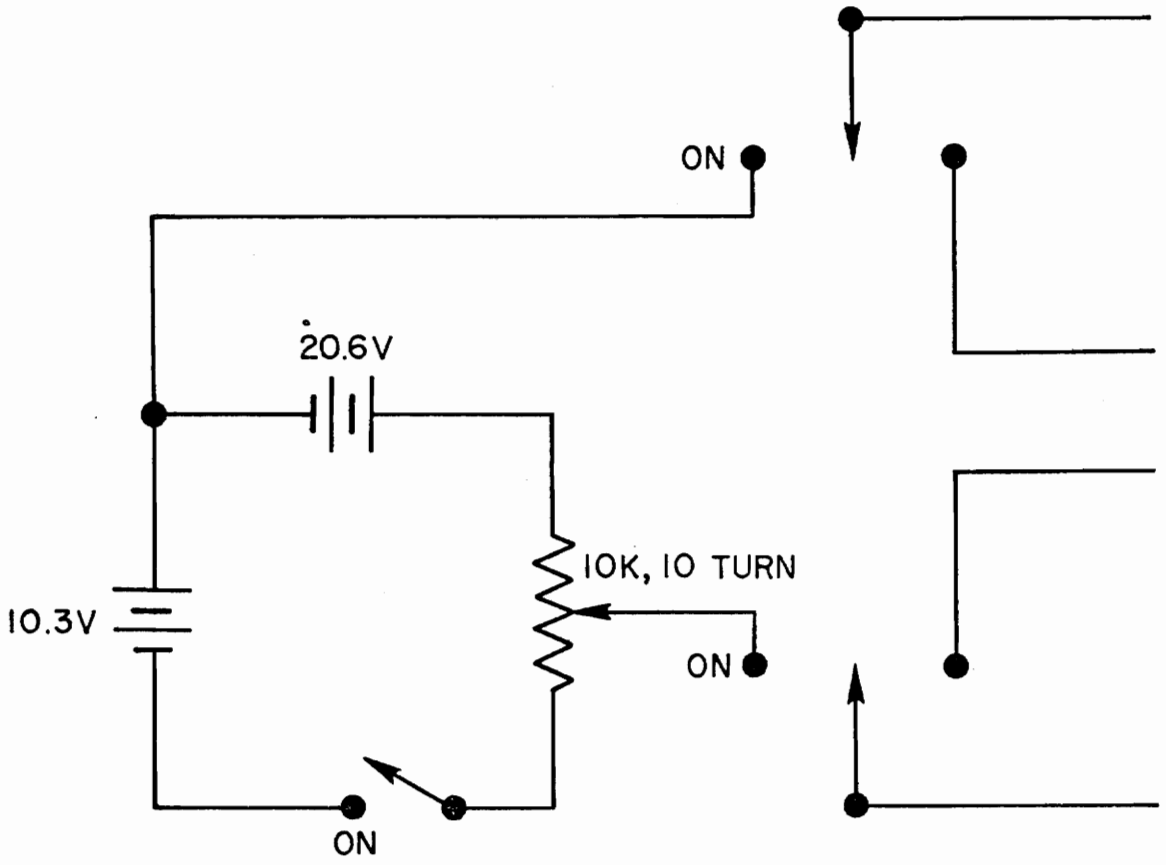

FIGURE 3. Modified Electron Energy Supply Control Circuit

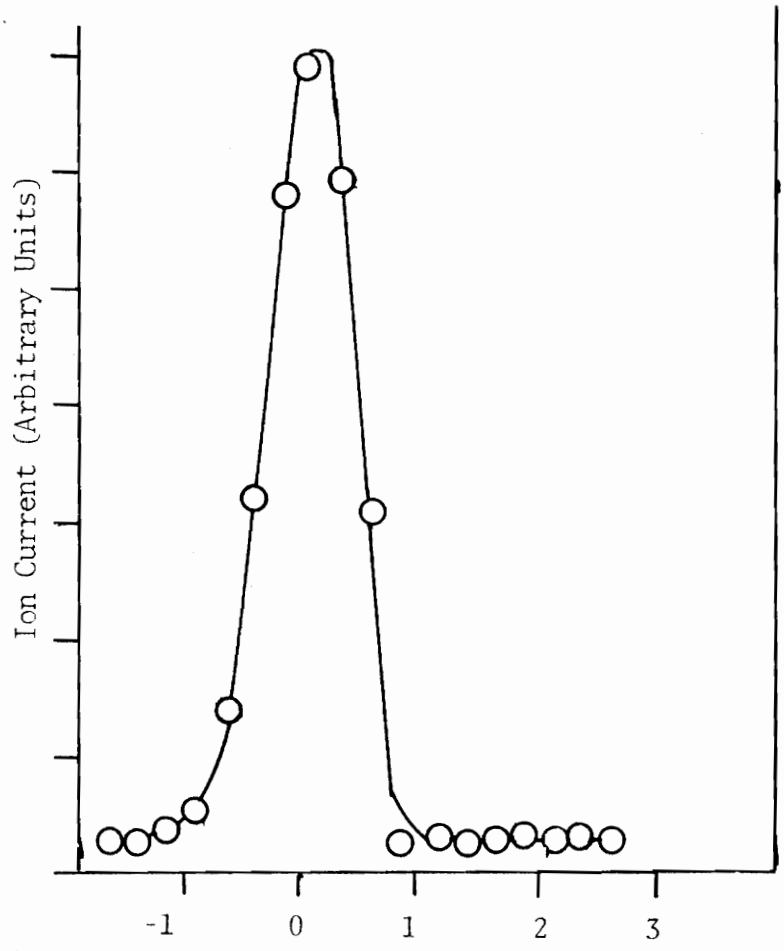

Figure 45. Ionization Efficiency Curve for SF_6^-

spectra. Metastable ions with relative abundances of ca. 0.1% or less were amplified to determine their position and shape. Negative ions are present at much lower abundance than positive ions, and ions of less than 1% relative abundance are normally not clearly separable from the background noise.

Metastable peaks are ions which are formed by fragmentation of an ion somewhere along its path of flight from the source into the analyzer tube.[84] It is presumed that these fragments are produced by the same processes as those occurring in the ion source before acceleration. The result is an ion which is accelerated as though it had one mass, but is focused at a lower mass, and explains the characteristic features of metastable peaks in spectra. The peaks are of relatively low intensity, generally 1% or less of the base peak. They are likely to occur at non-integral masses, and they tend to be broad and "out of focus." Because metastable peaks are dependant for their abundance upon the abundance of the precursor ion, metastable peaks for the decomposition of low intensity ions are often not detectable, and negative inferences based on the absence of a metastable peak are suspect. Metastable peaks appear at, or around, an m/e described by Equation 16,[84]

$$m^* = m^2/m_0 \qquad (16)$$

where m* is the m/e of the observed metastable, m is the mass of the daughter ion, and m_0 is the mass of the precursor ion. Metastable peaks are, therefore, more likely to appear at non-integral masses[84] and avoid being lost in the integral mass peaks, but half-masses and high intensity ions often do obscure low intensity metastables. Finally, metastable ion peaks are broad, from 0.25 m/e to several mass units, because the

instrument is focused for a different velocity to charge ratio, because the decomposition may occur over a greater distance than the "normal" decomposition, and because the kinetic energy lost almost always will affect the focus of the ion. While the positioning of the focusing slits has some effect on both the intensity and shape of the metastable peak, the ions can usually be characterized according to peak shapes, "Gaussian" (approximately rounded and symmetrical), or "flat-topped" (which may or may not be symmetrical). Flat-topped metastables are almost always broader than the Gaussian metastables in the same spectrum, and the shape is characteristic of a greater number of energy states in the precursor from which energy is converted into kinetic energy upon the formation of the daughter.

Decomposition of the benzils in the source of the RMU-7 was not a problem, but the chloro-substituted benzils caused instrumental instability after about 0.5 hr, probably by deposition on parts in the source. Spectra run at different times after varied by 5% in relative abundances, and the I.P. of Xe-129 regularly varied by 0.5 eV on different days. The latter problems are ascribable to changes in some conditions as the result of daily use and were also observed by Einolf and Munson.[19] Metastables are presented as calculated values to 0.01 mass units, although spectra are not amenable to determinations more accurate than 0.1 mass units.

Mass calibration at 50 eV was accomplished by introducing perfluorokerosene (PFK) into the mass spectrometer simultaneously with the compounds studied. The identity of the ionic species was established by comparing

the spectrum of PFK[85] with that of the compound of interest. Resolution for the RMU-7 ($\Delta H/H$) is at least 1 x 10^{-3} for all spectra.

All polarographic data were obtained on a unit consisting of a Heathbuilt Model EUA-19-2 Polarography Module, an Heathbuilt amplifier, and a Sargent Model SR strip-chart recorder (equipment courtesy of Dr. John G. Mason, V.P.I. & S.U.). Mercury column pressure was kept constant by using an adjustable-height bulb to maintain a constant mercury column height above the capillary dropping tube. Voltages were measured against a silver/silver perchlorate electrode and were corrected to benzil as the standard.[51] Solutions were 1 x 10^{-3} M in the appropriate benzil (dried overnight in an Abderhalden drying pistol at the boiling point of ethanol, and 0.5 mm Hg using P_2O_5 as the desiccant) and 0.2 M in tetra-(n-butyl)-ammonium perchlorate (obtained as polarographic grade from the G. F. Smith Chemical Co., and dried by the same method as the benzils). Dimethyl sulfoxide (Fisher), freshly distilled from calcium hydride, was the solvent. Dissolved oxygen was removed by bubbling dry nitrogen through the polarographic cell for 2 min before each series of runs was begun, and each run was made under a head of dry nitrogen gas. Reported potentials are the average of at least two successive determinations. Reproducibility on successive determinations is within 0.02 v, and error after correction to the benzil standard is estimated to be $\pm$ 0.05 v. Evaluation of $E_{3/4} - E_{1/4}$ was made by using the tops of the respective currents to determine wave height, and interpolating between voltages at the end of successive drops.

SECTION IV

POLAROGRAPHY

A. RESULTS

The values for the half-wave potentials of the benzils are listed in Table 1. The observed values are versus a silver-silver perchlorate electrode and adjusted for slight variations in the observed half-waves of the standard, benzil. Figures 5 and 6 are plots of the observed half-waves versus the Hammett ; Figures 7 through 10 are similar plots versus σ^+ and σ^I (c f. Appendix 2 for a list of Hammett substituent constants used). The apparent best fit is obtained with σ. Several anomalies are present which may severely compromise the validity of the correlation line shown in these plots or, for that matter, any correlation line. It is observed that the values for the first half-wave potentials for the nitro- and chloro-substituted benzils are significantly more positive than any other values. The differences between the first and second half-wave potentials for these compounds is under 0.4 v, compared to a difference of 0.6-0.7 V for the other benzils. The values in Table 1 and the plots in Figures 5 through 10 suggest that for the electron withdrawing substituents, and particularly for the chlorobenzils, the observed half-wave potentials do not exhibit true substituent effects but may be the result of a change in the polarographically active group.

The values for $E_{3/4} - E_{1/4}$ are listed in Table 2. Values are taken from chart readings at a rate of 100 mv per 0.5 in. and are uncorrected for uncompensated IR drop so that any error in the observed value is toward higher voltages. Values for the first half-wave indicate possible

TABLE 1

POLAROGRAPHIC HALF-WAVE POTENTIALS
FOR BENZILS

R_1-$C_6H_4COCOC_6H_4$-R_2

R_1	R_2	$E_{1/2}$ 1st wave (v)	$E_{1/2}$ 2nd wave (v)
H	NO_2	0.64	0.98
H	Cl	0.70	0.88
H	CH_3S	1.02	1.74
H	H	1.04	1.76
H	CH_3	1.07	1.76
H	CH_3O	1.11	1.86
H	$(CH_3)_2N$	1.20	1.79
NO_2	NO_2	0.64	1.00
Cl	Cl	0.68	0.94
CH_3S	CH_3S	1.02	1.67
CH_3	CH_3	1.11	1.86
CH_3O	CH_3O	1.17	1.88
$(CH_3)_2N$	$(CH_3)_2N$	1.39	1.94

All voltages relative to benzil standard, 1.04 v and 1.76 v, as reported by R. C. Buchta and D. H. Evans, Anal. Chem., 40, 2181 (1968).

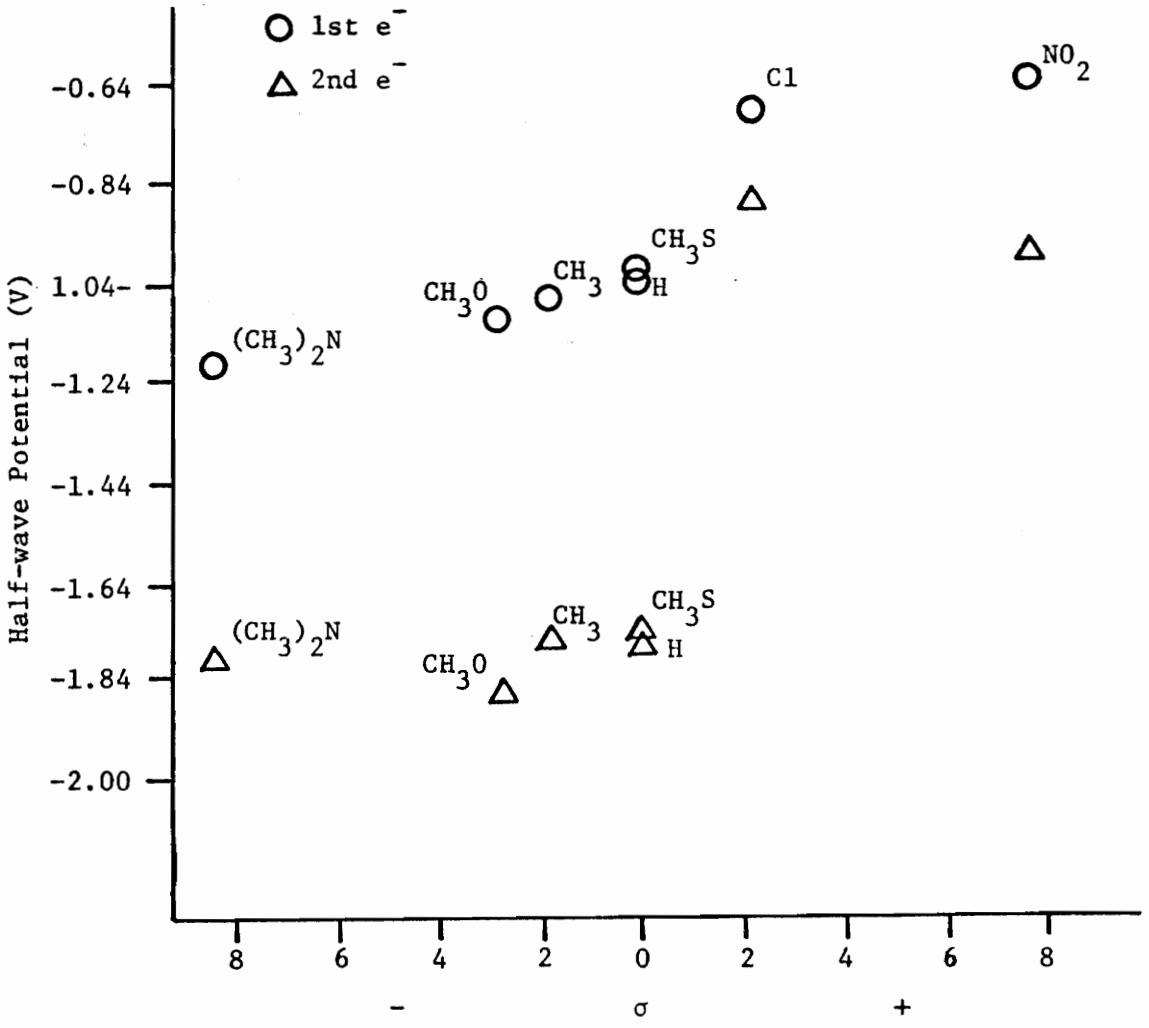

FIGURE 5. Hammett Plot: $E_{1/2}$ for Monosubstituted Benzils vs. σ

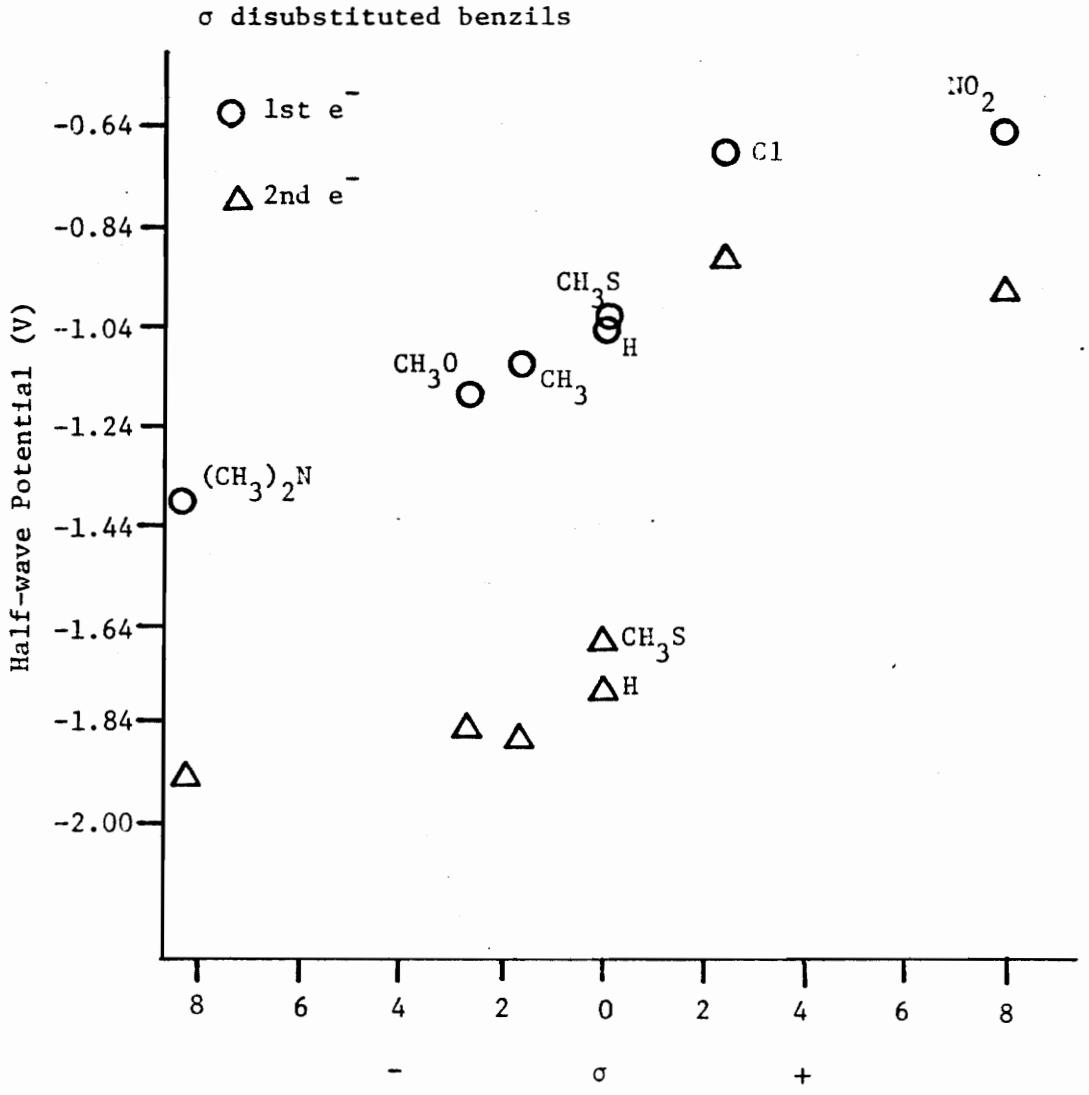

FIGURE 6. Hammett Plot: $E_{1/2}$ for Disubstituted Benzils vs. σ

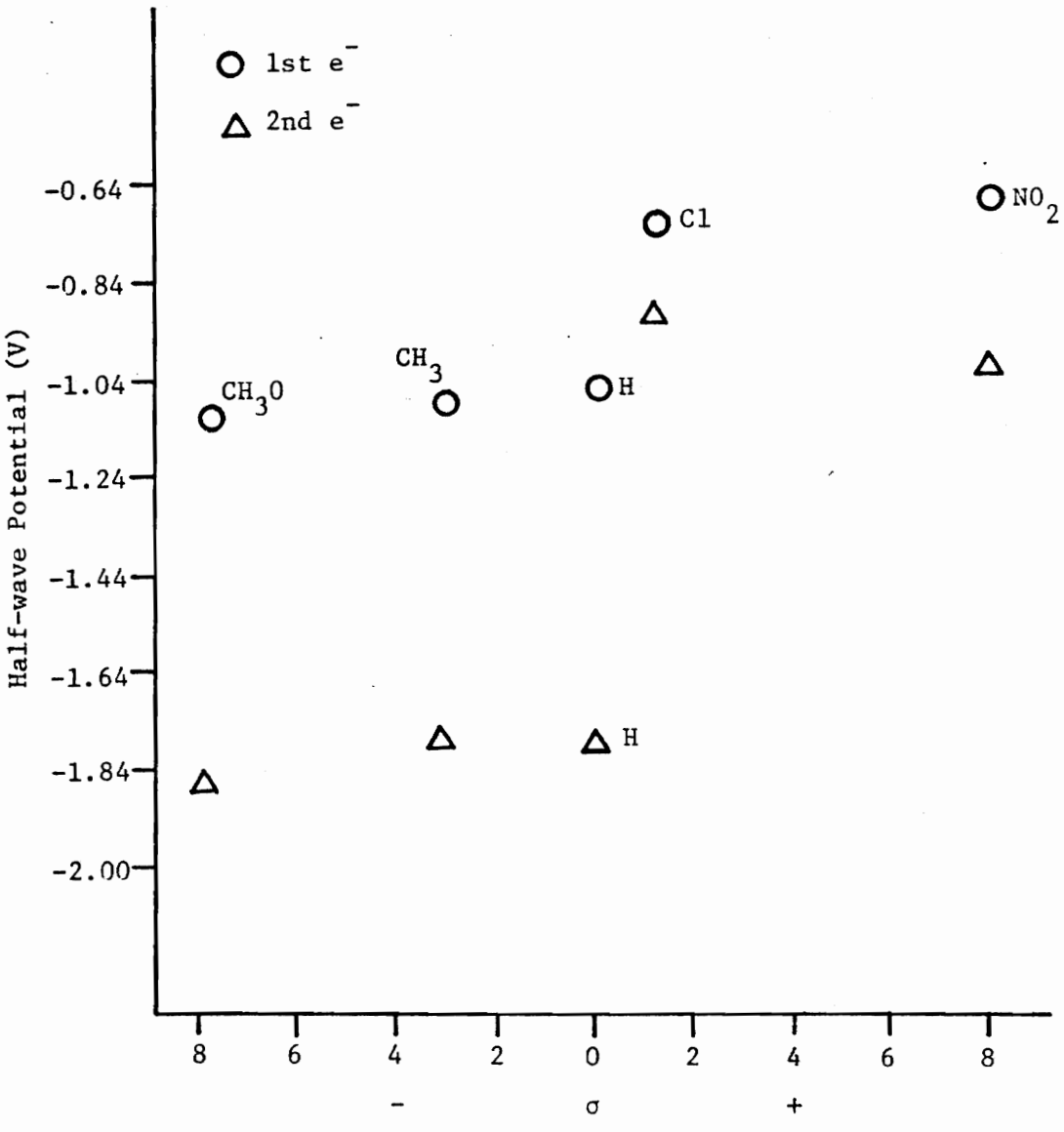

FIGURE 7. Hammett Plot: $E_{1/2}$ for Monosubstituted Benzils vs. σ^+

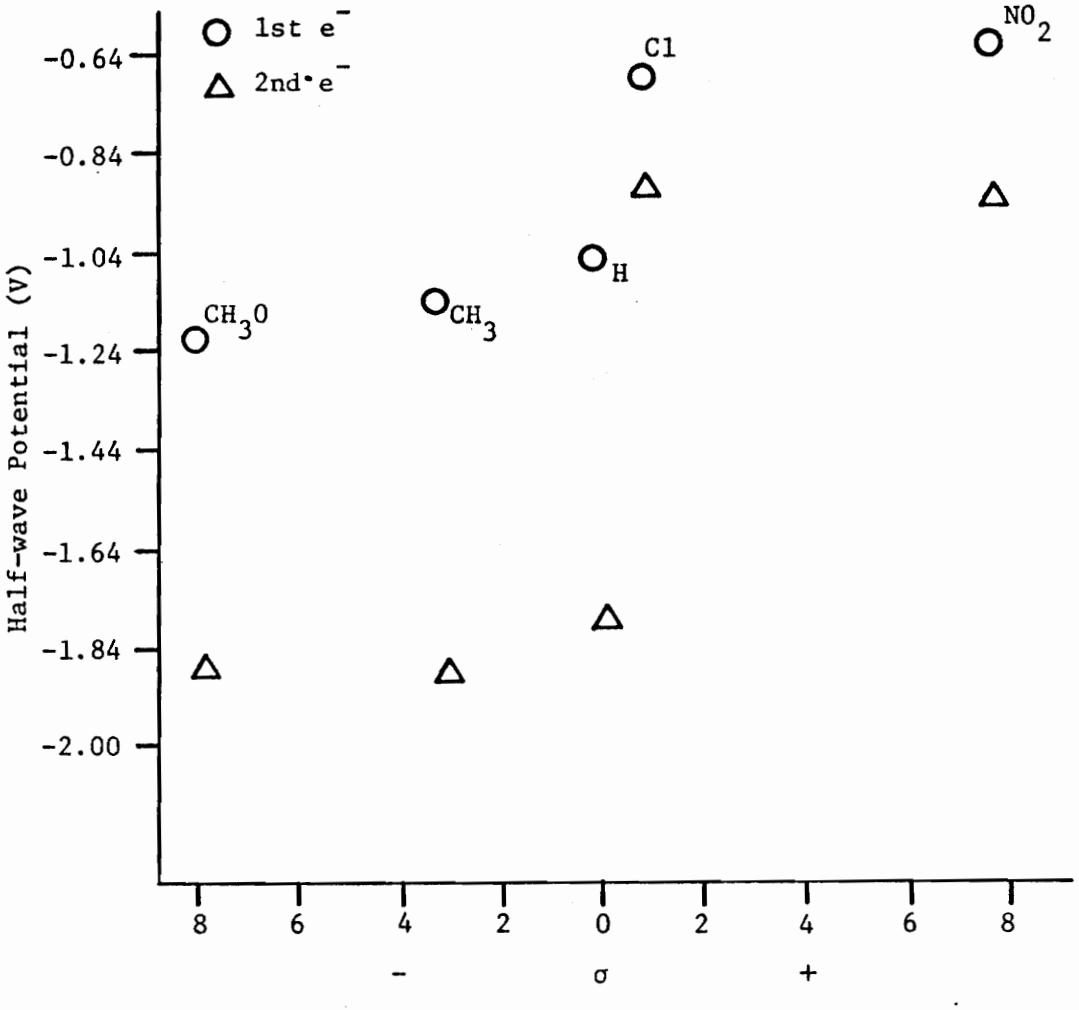

FIGURE 8. Hammett Plot: $E_{1/2}$ for Disubstituted Benzils vs. σ^+

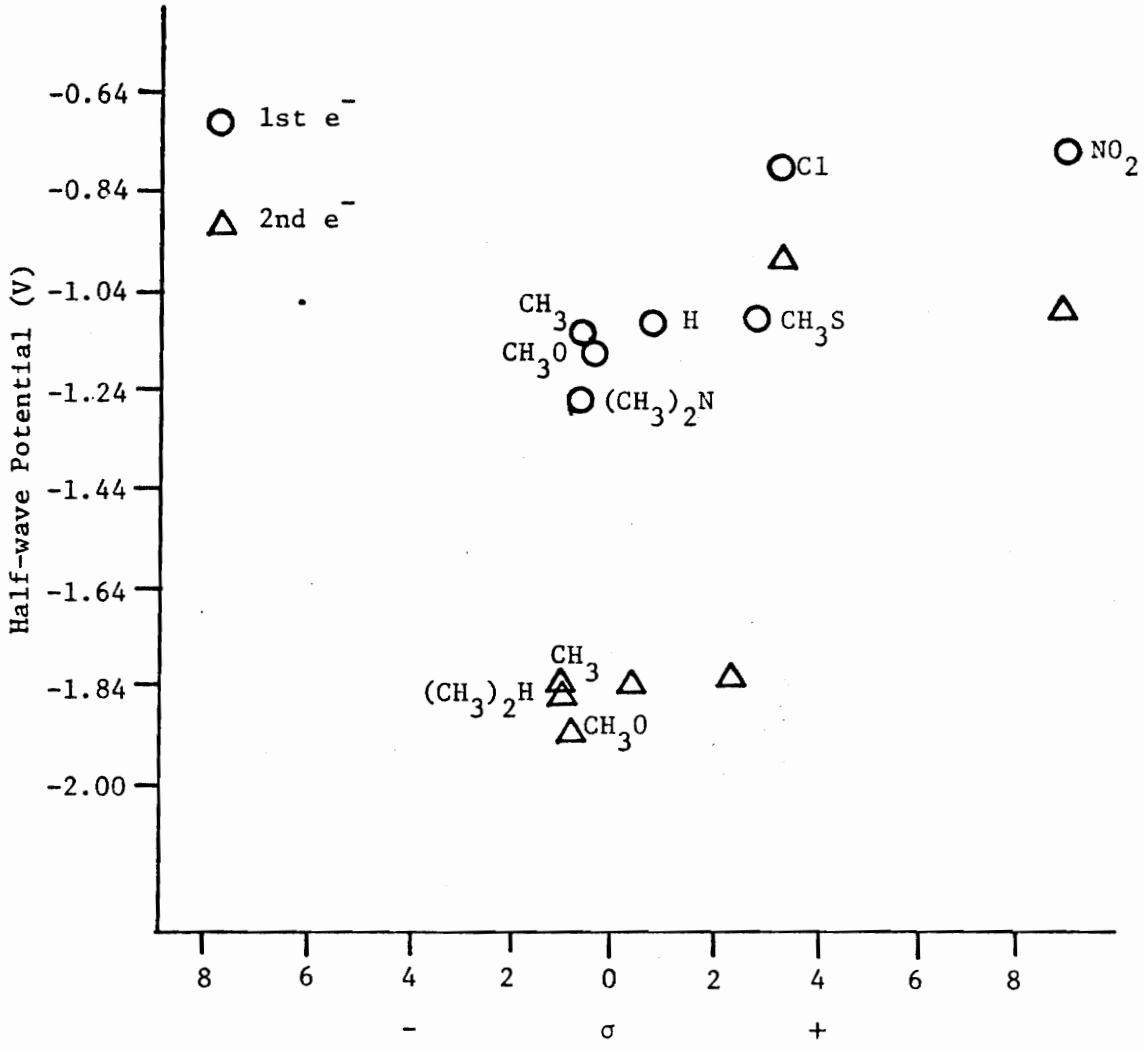

FIGURE 9. Hammett Plot: $E_{1/2}$ for Monosubstituted Benzils vs. σ^I

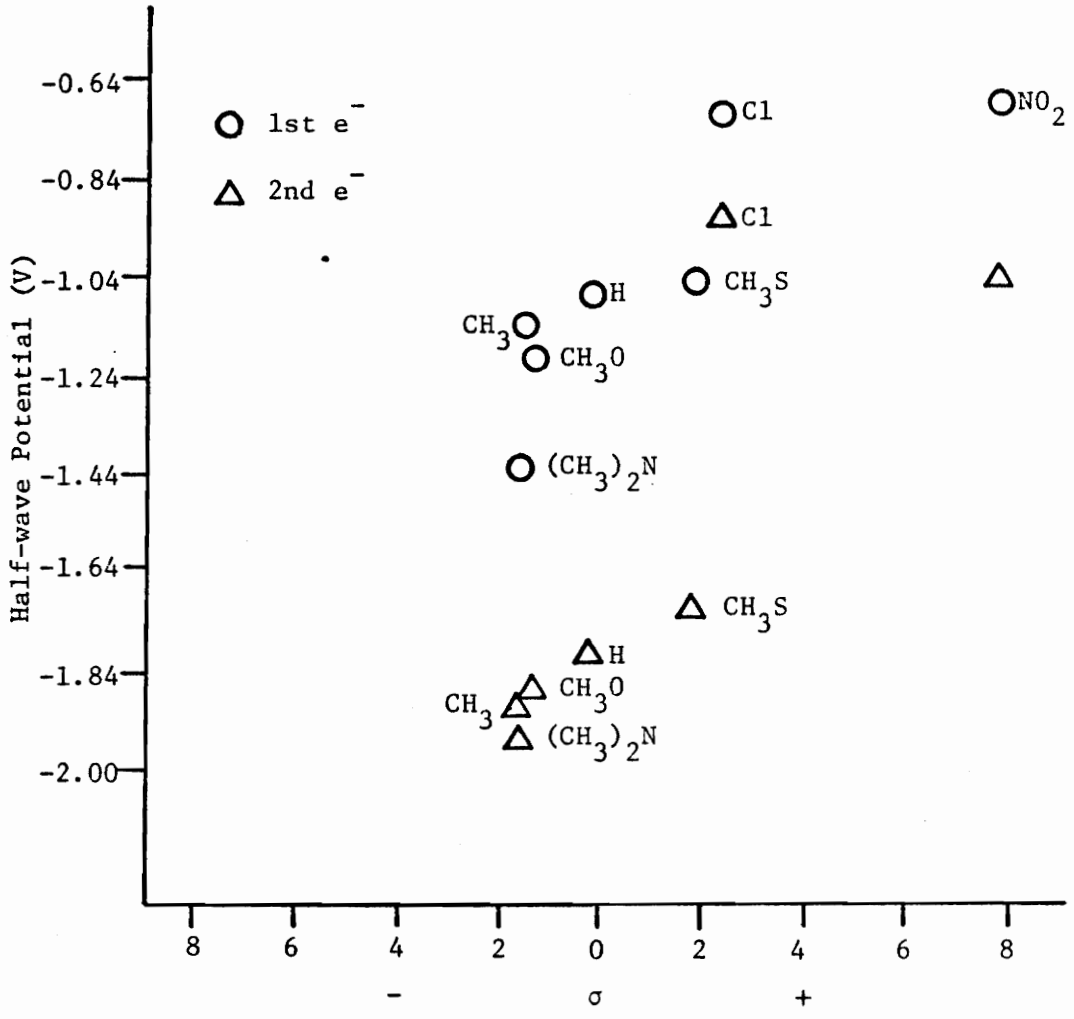

FIGURE 10. Hammett Plot: $E_{1/2}$ for Disubstituted Benzils vs. σ^I

TABLE 2

$E_{3/4} - E_{1/4}$ FOR POLAROGRAPHIC WAVES FOR BENZILS

$R_1\text{-}C_6H_4COCOC_6H_4\text{-}R_2$

R_1	R_2	$E_{3/4} - E_{1/4}$, 1st wave (mv)	$E_{3/4} - E_{1/4}$, 2nd wave (mv)
H	NO_2	70	62
H	Cl	80	65
H	CH_3S	80	85
H	H	55	130
H	CH_3	65	65*
H	CH_3O	57	100
H	$(CH_3)_2N$	60	115
NO_2	NO_2	59	58
Cl	Cl	100	50
CH_3S	CH_3S	62	200
CH_3	CH_3	65	110
CH_3O	CH_3O	110	115
$(CH_3)_2N$	$(CH_3)_2N$	55	82

* This wave exhibits a maximum.

reversibility for all waves except those of the 4-chlorobenzil, 4,4'-dichlorobenzil, 4-nitrobenzil, 4-methylthiobenzil, and 4,4'-dimethoxybenzil. The shape of the first wave of 4-methylthiobenzil indicates that an impurity in the solution may be expanding the wave, thereby accounting for the high value for $E_{3/4} - E_{1/4}$, but the shape and high value of the wave for 4,4'-dimethoxybenzil was readily reproducible and showed no signs of impurities in the solution. The only second waves which appear to be possibly reversible are those for the mono- and dinitrobenzils, and mono- and dichlorobenzil. The value of 65 mV for the 4-methylbenzil is the result of a maximum for this wave which leads to a slightly higher value by distorting the top of the wave. The only second waves which appear to possibly be reversible occur within a range of 0.12 V and are between 0.16 and 0.04 V more positive than the first half-wave potential for benzil. All second half waves are slightly less high than their corresponding first wave, although the difference is small. All waves appear to be of the same relative height, presumably indicating the uptake of one electron per wave per molecule as the data of Buchta and Evans[51] suggest and the calculations of Bauld[30] indicate to be possible.

DISCUSSION

The values for $E_{3/4} - E_{1/4}$ and the correlation line for the plot of $E_{1/2}$ vs σ indicate that the "normal" mode of reduction of benzils involves the reversible addition of one electron to form a radical anion, followed by an irreversible step to form a dianion at a potential ca. 0.6-0.8 V more negative. This process is that observed by Bauld[30] for reduction with metals and is supported by the esr spectrum reported by Buchta and Evans.[51] Based on Bauld's[30] calculations and the distorted 21 line esr spectrum of Buchta and Evans,[51] the radical is planar and probably cis. No evidence of an equilibrium between radical anion and dianion, as noted by Bauld,[30] is directly obtainable from the wave shapes alone.

Chloro-substituted benzils are anomalous, the half-wave potential for the first waves are clearly not reversible; they fit no correlation line. The second waves closely fit the correlation line for the first waves of the other benzils. Cleavage of the chlorine-carbon bond followed by abstraction of a proton from the solvent is one rationalization which has been invoked to explain the behavior of p-chlorobenzophenone under similar circumstances.[86] The nitro-substituted compounds are more troubling since the $E_{3/4} - E_{1/4}$ values are near enough to 56.4 mV to suggest that the reduction is reversible. If this be true, and both reductions are reversible, the nitrobenzils are reduced by a different path, and probably a different mechanism, than any of the other benzils. Under any interpretation, the benzils with electron-withdrawing substituents appear to have polarographically active groups which are somewhat

different from that present in the other benzils studied.

A comparison of the free energies ($\Delta G = nFE$) of the radical anions of the benzils with neutral and electron donating substituents, relative to benzil, is presented in Table 3. Also listed in Table 3 is a similar comparison for both waves of the nitrobenzils and for the second wave of the chlorobenzils. Dimethoxybenzil, dimethylbenzil, and bis(dimethylamino) benzil each have values approximately twice that of their monosubstituted analogues. The 4-methylthiobenzil and the 4,4'-dimethylthiobenzil have identical values, as would be expected with a σ value of zero. The range of values for the first and second waves for the nitro-substituted benzils and for the second waves for the chloro-substituted benzils indicate that the second waves are more likely to correspond to a reduction process similar to that involved in the first reduction of the other benzils.

The apparent additivity of the substituent effect for the neutral and electron-donating substituents indicates that the effects of the second substituent are transmitted across the carbon-carbon bond. This means that the carbonyls are either parallel for a significant time or locked into a planar radical anion. The 21 lines in the esr spectrum published by Buchta and Evans[51] indicates that the latter to be the more likely.

TABLE 3

COMPARATIVE FREE ENERGIES FOR FORMATION OF RADICAL ANIONS FORMED IN THE POLAROGRAPHIC REDUCTION OF BENZILS

$R_1 - C_6H_4COCOC_6H_4-R_2$

R_1	R_2	ΔG_f, 1st wave kcal/mol	ΔG_f, 2nd wave kcal/mol
H	CH_3S	+1.930	-------
H	CH_3	-2.895	-------
H	CH_3O	-6.754	-------
H	$(CH_3)_2N$	-15.438	-------
CH_3S	CH_3S	+1.930	-------
CH_3	CH_3	-6.754	-------
CH_3O	CH_3O	-12.544	-------
$(CH_3)_2N$	$(CH_3)_2N$	-34.770	-------
H	NO_2	+38.595	+5.789
NO_2	NO_2	+38.595	+3.859
H	Cl	-------	+15.438
Cl	Cl	-------	+9.649

SECTION V

POSITIVE ION SPECTRA

The positive ion spectra of 4-methylbenzil, 4-chlorobenzil, 4-methoxybenzil, 4-methylmercaptobenzil, and 4-dimethylaminobenzil are shown in Figures 11 through 15. At 50 eV, the parent-molecule ion appears at very low abundance, and the predominant ions are benzoyl and substituted benzoyl ions, phenyl and substituted phenyl ions. These spectra are in agreement with the observations of Natalis and Franklin,[33] Scheppele et al.,[34] and Einolf and Munson[22] that the principle ions in the spectrum of the benzils are the benzoyls and their daughter ions. In each case, the observed spectrum can be rationalized to result from a fragmentation scheme proposed by Scheppele et al.[34] as depicted in Figure 16. Evidence in support of this scheme comes from the relative abundances of the principle fragment ions, the appearance potentials of the various fragment ions (c.f. Section VI, pages 75 through 112), and the metastable data in Tables 4 through 8.

A metastable peak of relatively low intensity is present for the formation of $C_6H_5CO^+$ directly from benzil and 4-methylbenzil. No corresponding metastable is found in the 50 eV spectra of 4-methoxybenzil, 4-methylthiobenzil, 4-chlorobenzil, or 4-dimethylaminobenzil. The absence of such a metastable is ascribed to the relatively low abundance of a parent ion in the spectra of these compounds as compared to benzil and 4-methylbenzil and to the fact that, in the 4-methoxybenzil and 4-methylthiobenzil, the metastables corresponding to the formation of $C_6H_5CO^+$ occur at near-even masses where they are easily obscured by ions of

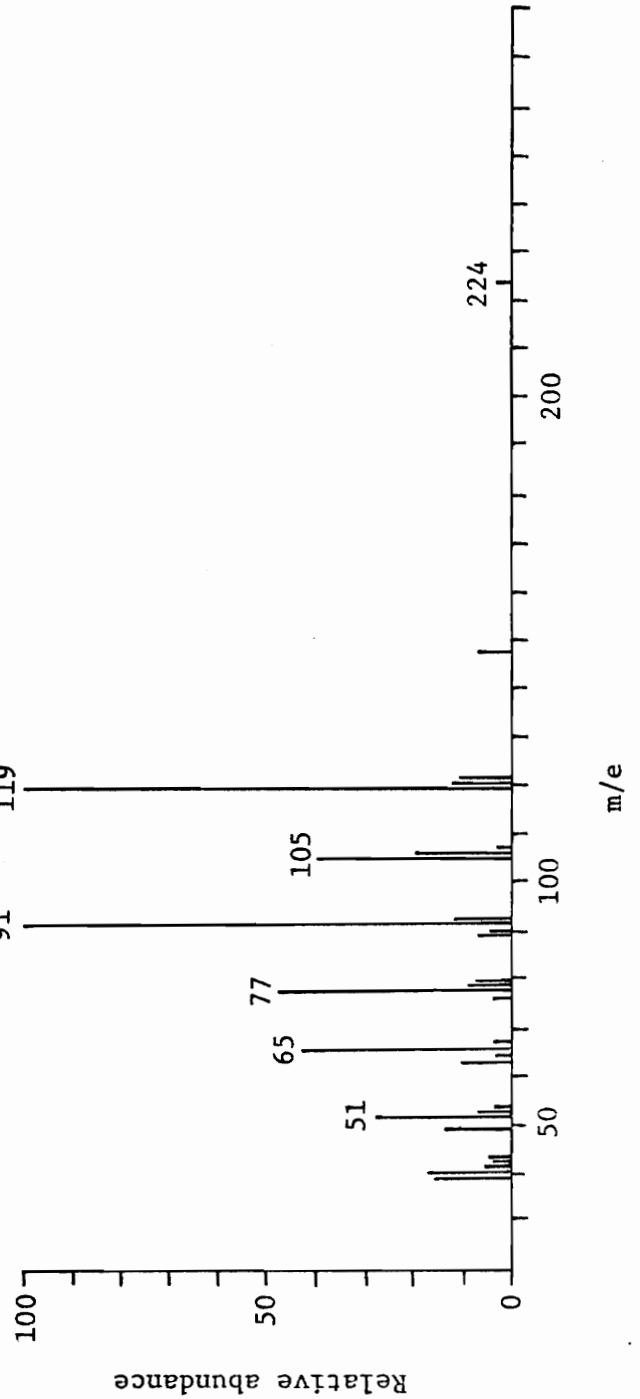

FIGURE 11. Positive Ion Mass Spectrum of 4-Methylbenzil (50 eV)

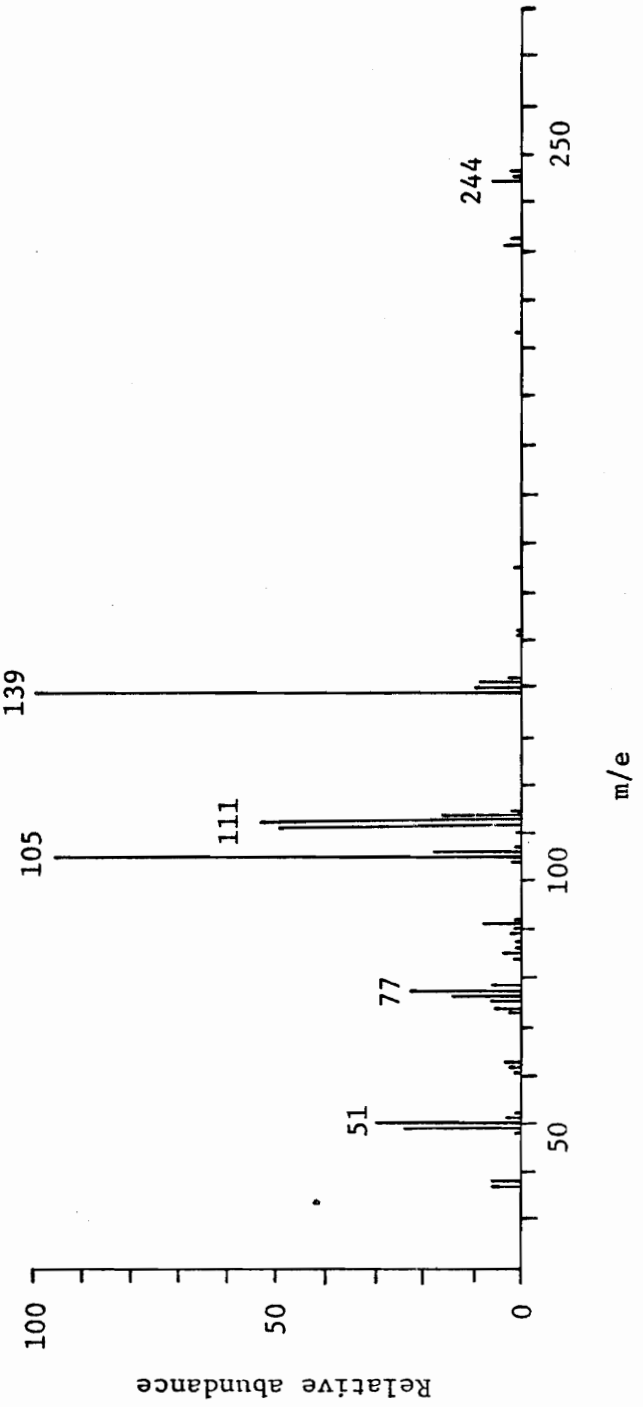

FIGURE 12. Positive Ion Mass Spectrum of 4-Chlorobenzil (50 eV)

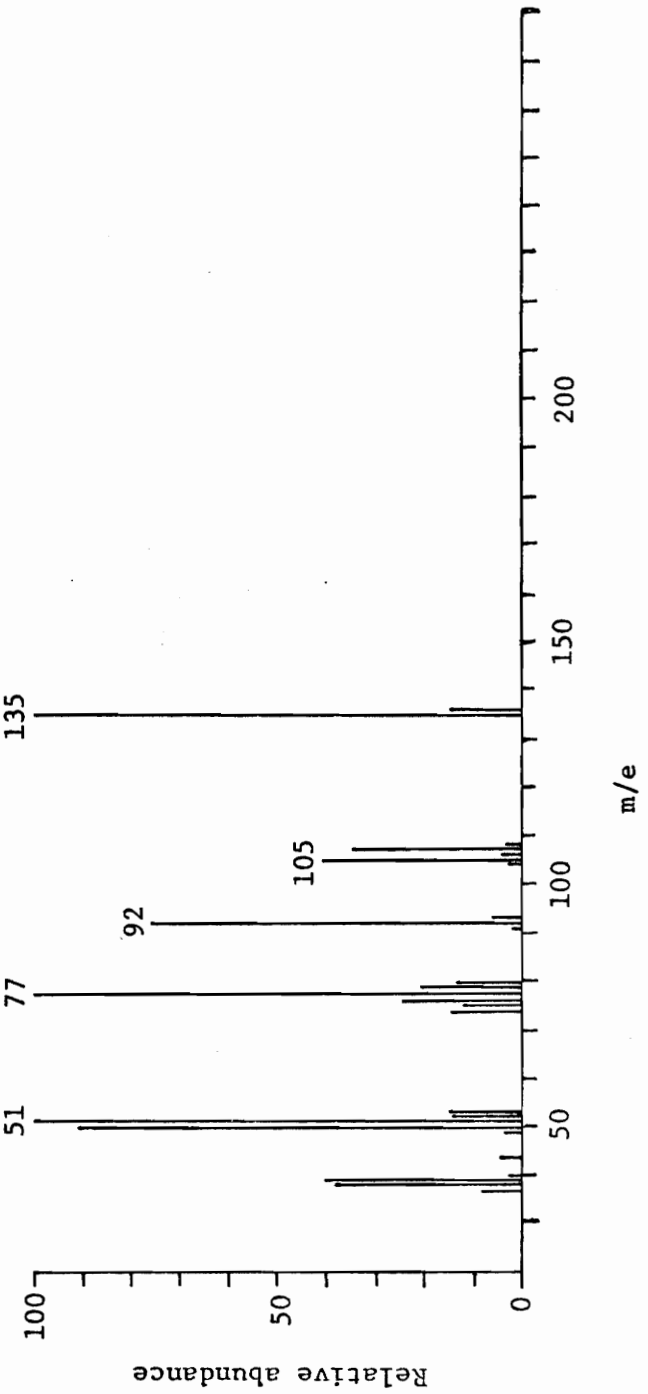

FIGURE 13. Positive Ion Mass Spectrum of 4-Methoxybenzil (50 eV)

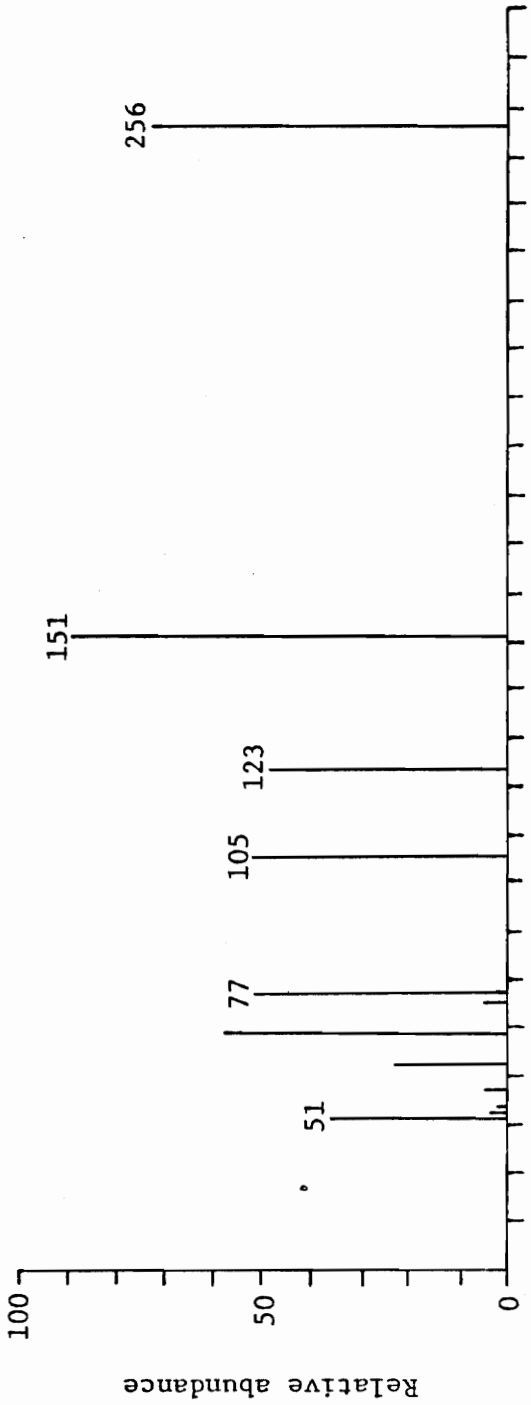

FIGURE 14. Positive Ion Mass Spectrum of 4-Methylmercaptobenzil (50 eV)

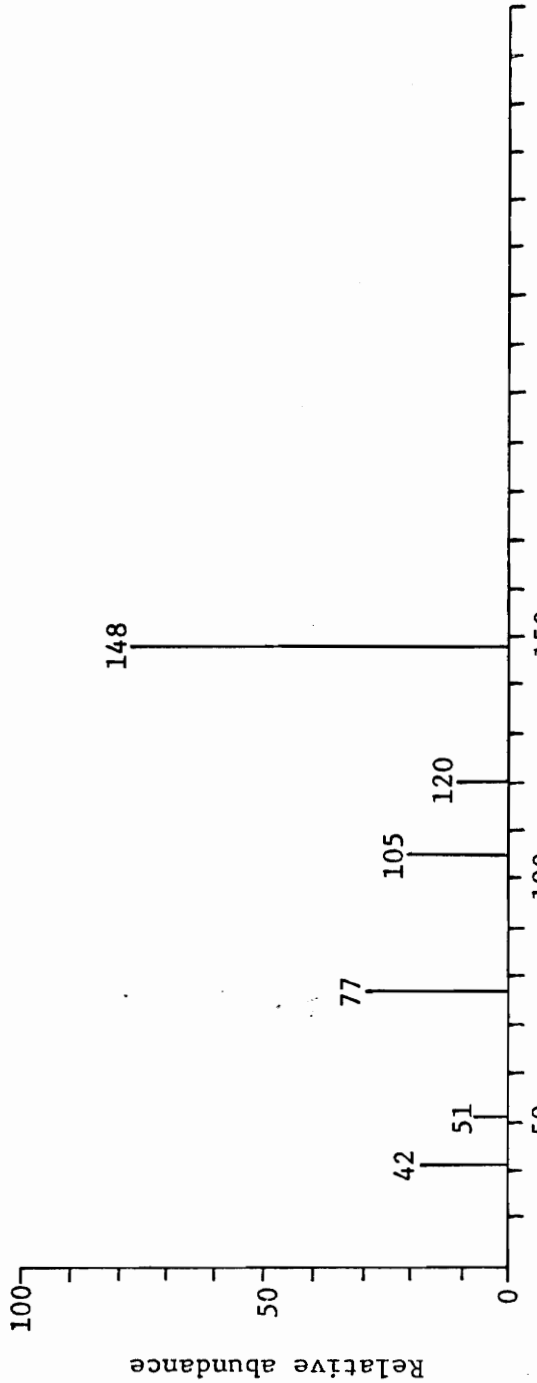

FIGURE 15. Positive Ion Mass Spectrum of 4-Dimethylaminobenzil (50 eV)

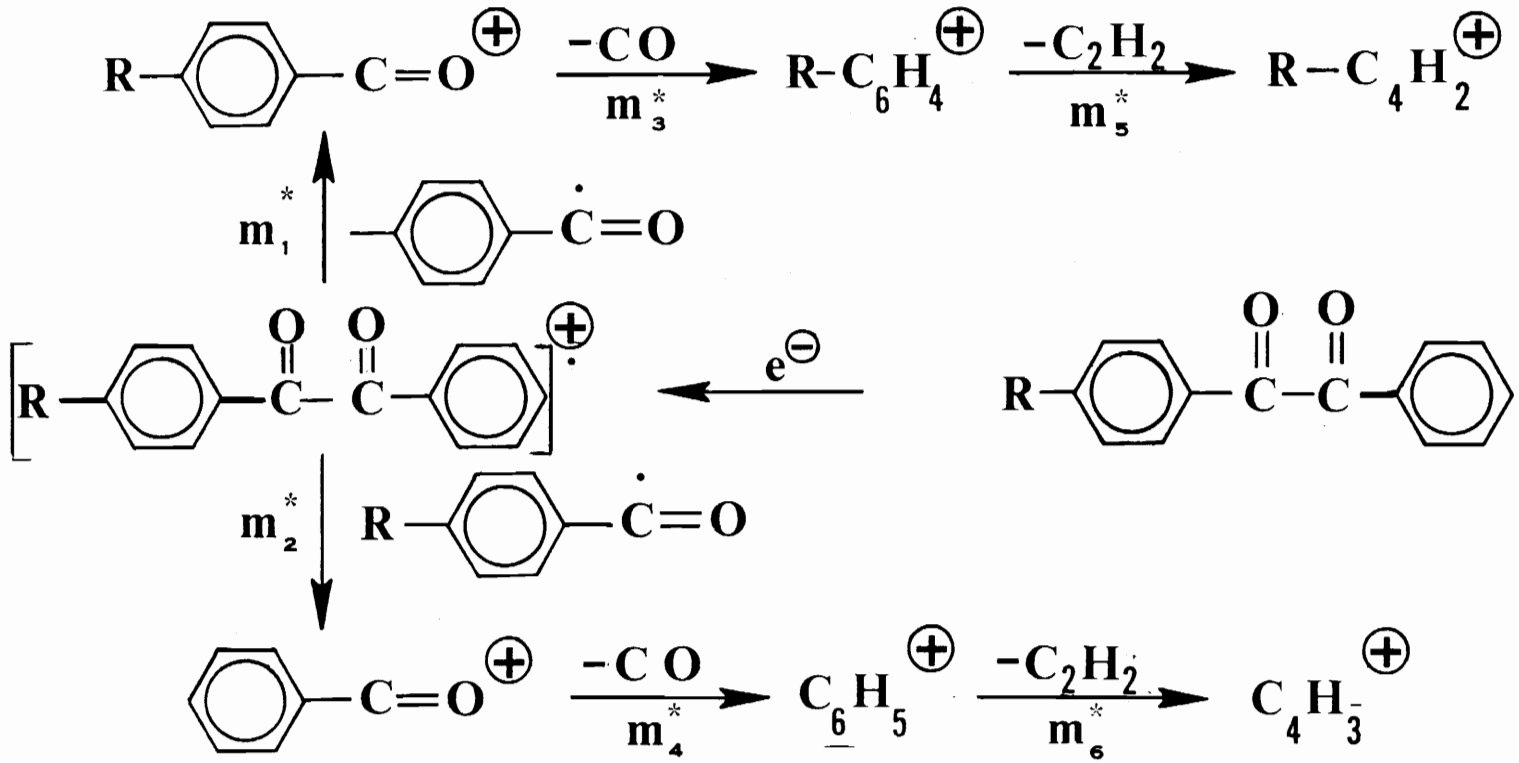

FIGURE 16. Monosubstituted Benzils Fragmentation Pattern and Metastables

m_1^* R=H, CH_3, $(CH_3)_2N$, NO_2 m_2^* R=H, CH_3, NO_2 m_3^* R=H, CH_3, CH_3O, CH_3S, Cl, $(CH_3)_2N$

m_4^* R=H, CH_3, CH_3O, CH_3S, Cl, $(CH_3)_2N$, NO_2 m_5^* R=H, CH_3 m_6^* R=H, CH_3, CH_3O, CH_3S, $(CH_3)_2N$, NO_2

TABLE 4

METASTABLE IONS

From Positive Ion Fragmentation Processes of $R_1\text{-}C_6H_4COCOC_6H_4\text{-}R_2$

PARENT R_1	PARENT R_2	PROCESS	METASTABLE m/e calc. (obs.)	intensity	shape
H	H	$C_6H_5COCOC_6H_5^{+\cdot} \longrightarrow C_6H_5CO^+ + C_6H_5CO\cdot$ m/e=210 m/e=105	52.50 (52.5)	n.o.	g
		$C_6H_5CO^+ \longrightarrow C_6H_5^+ + CO$ m/e=105 m/e=77	56.47 (56.3-56.6)	s	f.t.
		$C_6H_5^+ \longrightarrow C_4H_3^+ + C_2H_2$ m/e=77 m/e=51	33.78 (33.8)	w	g
CH_3	CH_3	$CH_3\text{-}C_6H_4COCOC_6H_4\text{-}CH_3^{+\cdot} \longrightarrow CH_3\text{-}C_6H_4CO^+ + CH_3\text{-}C_6H_4CO\cdot$ m/e=238 m/e=119	59.50 (59.5)	w	g
		$CH_3\text{-}C_6H_4CO^+ \longrightarrow CH_3\text{-}C_6H_4^+ + CO$ m/e=119 m/e=91	69.59 (69.1-70.1)	s	f.t.
		$CH_3\text{-}C_6H_4^+ \longrightarrow C_5H_5^+ + C_2H_2$ m/e=91 m/e=65	46.43 (46.1-46.8)	s	g
		$P^{+\cdot} \longrightarrow CH_3\text{-}C_6H_4^+ + CH_3\text{-}C_6H_4COCO\cdot$ m/e=238 m/e=91	34.79	n.o.	

s=strong, w=weak, n.o.=not observed, g=gaussian, f.t.=flat-topped, *-may be observed.

TABLE 5

METASTABLE IONS

From Positive Ion Fragmentation Processes of R_1-$C_6H_4COCOC_6H_4$-R_2

PARENT R_1	PARENT R_2	PROCESS	m/e calc. (obs.)	METASTABLE intensity	METASTABLE shape
H	CH_3	$P^{+\cdot}$ (224) $\longrightarrow$ CH_3-$C_6H_4CO^+$ (119) + $C_6H_5CO\cdot$	63.22 (63.2)	w	g
		CH_3-$C_6H_4CO^+$ (119) $\longrightarrow$ CH_3-$C_6H_4^+$ (91) + CO	69.59 (69.6)	s	f.t.
		CH_3-$C_6H_4^+$ (91) $\longrightarrow$ $C_5H_5^+$ (65) + C_2H_2	46.43 (46.3)	w	g
		$P^{+\cdot}$ (224) $\longrightarrow$ CH_3-$C_6H_4^+$ (91) + $C_6H_5COCO\cdot$	36.97*	n.o.	
		$P^{+\cdot}$ (224) $\longrightarrow$ $C_6H_5CO^+$ (105) + CH_3-$C_6H_4CO\cdot$	49.22 (49.2)	w	g
		$C_6H_5CO^+$ (105) $\longrightarrow$ $C_6H_5^+$ (77) + CO	56.47 (56.4–56.6)	w	f.t.
		$C_6H_5^+$ (77) $\longrightarrow$ $C_4H_3^+$ (51) + C_2H_2	33.78 (33.8)	w	g
		$P^{+\cdot}$ (224) $\longrightarrow$ $C_6H_5^+$ (77) + CH_3-$C_6H_4COCO\cdot$	26.47	n.o.	

TABLE 6

METASTABLE IONS

From Positive Ion Fragmentation Processes of $R_1-C_6H_4COCOC_6H_4-R_2$

PARENT R_1	PARENT R_2	PROCESS	METASTABLES m/e calc. (obs.)	intensity	shape
H	CH_3O	$P^{+\cdot}$ (240) $\longrightarrow$ $CH_3O-C_6H_4CO^+$ (135) + $C_6H_5CO^+$	75.94*	n.o.	
		$CH_3O-C_6H_4CO^+$ (135) $\longrightarrow$ $CH_3O-C_6H_4^+$ (107) + CO	84.81 (84.7-85.0)	s	f.t.
		$CH_3O-C_6H_4^+$ (107) $\longrightarrow$ $C_5H_5C^+$ (81) + C_2H_2	61.32	n.o.	
		$P^{+\cdot}$ (240) $\longrightarrow$ $CH_3O-C_6H_4^+$ (107) + $C_6H_5COCO\cdot$	42.40	n.o.	
		$P^{+\cdot}$ (240) $\longrightarrow$ $C_6H_5CO^+$ (105) + $CH_3O-C_6H_4CO\cdot$	45.94*	n.o.	
		$C_6H_5CO^+$ (105) $\longrightarrow$ $C_6H_5^+$ (77) + CO	56.47 (56.4-56.7)	w	f.t.
		$C_6H_5^+$ (77) $\longrightarrow$ $C_4H_3^+$ (51) + C_2H_2	33.78 (33.8)	w	g
		$P^{+\cdot}$ (240) $\longrightarrow$ $C_6H_5^+$ (77) + $CH_3O-C_6H_5COCO\cdot$	24.71	n.o.	

TABLE 7

METASTABLE IONS

From Positive Ion Fragmentation Processes of R_1-$C_6H_4COCOC_6H_4$-R_2

PARENT R_1	PARENT R_2	PROCESS	m/e calc. (obs.)	METASTABLES intensity	METASTABLES shape
H	CH_3S	$P^{+\cdot}$ (256) $\longrightarrow$ CH_3S-$C_6H_4CO^+$ (151) + $C_6H_5CO\cdot$	89.07*	n.o.	
		CH_3S-$C_6H_4CO^+$ (151) $\longrightarrow$ CH_3S-$C_6H_4^+$ (123) + CO	100.19 (100.2)	w	f.t.
		CH_3S-$C_6H_4^+$ (123) $\longrightarrow$ $C_5H_5S^+$ (96) + C_2H_2	74.93*	n.o.	
		$P^{+\cdot}$ (256) $\longrightarrow$ CH_3S-$C_6H_4^+$ (123) + $C_6H_5COCO\cdot$	59.10	n.o.	
		$P^{+\cdot}$ (256) $\longrightarrow$ $C_6H_5CO^+$ (105) + CH_3S-$C_6H_4\cdot$	43.07*	n.o.	
		$C_6H_5CO^+$ (105) $\longrightarrow$ $C_6H_5^+$ (77) + CO	56.47 (56.5)	s	f.t.
		$C_6H_5^+$ (77) $\longrightarrow$ $C_4H_3^+$ (51) + C_2H_222	33.78 (33.7)	s	g
		$P^{+\cdot}$ (256) $\longrightarrow$ $C_6H_5^+$ (77) + CH_3S-$C_6H_4COCO\cdot$	23.16	n.o.	

TABLE 8

METASTABLE IONS

From Positive Ion Fragmentation Processes of $R_1-C_6H_4COCOC_6H_4-R_2$

PARENT R_1	R_2	PROCESS	m/e calc. (obs.)	METASTABLES intensity	shape
H	$(CH_3)_2N$	$P^{+\cdot}$ (253) $\longrightarrow$ $(CH_3)_2N-C_6H_4CO^+$ (148) + $C_6H_5CO\cdot$	86.58 (86.6)	w	g
		$(CH_3)_2N-C_6H_4CO^+$ (148) $\longrightarrow$ $(CH_3)_2N-C_6H_4^+$ (120) + CO	97.30 (97.3)	s	g
		$(CH_3)_2N-C_6H_4^+$ (120) $\longrightarrow$ $C_6H_8N^+$ (94) + CO	73.63*	n.o.	
		$P^{+\cdot}$ (253) $\longrightarrow$ $(CH_3)_2N-C_6H_4^+$ (120) + $C_6H_5COCO\cdot$	56.92*	n.o.	
		$P^{+\cdot}$ (253) $\longrightarrow$ $C_6H_5CO^+$ (105) + $(CH_3)_2N-C_6H_4CO\cdot$	43.58	n.o.	
		$C_6H_5CO^+$ (105) $\longrightarrow$ $C_6H_5^+$ (77) + CO	56.47 (56.5)	w	g
		$C_6H_5^+$ (77) $\longrightarrow$ $C_4H_3^+$ (51) + C_2H_2	33.78 (33.8)	w	g
		$P^{+\cdot}$ (253) $\longrightarrow$ $C_6H_5^+$ (77) + $(CH_3)_2N-C_6H_4COCO\cdot$	23.48	n.o.	

near-integral masses. Analogously, the metastable for the formation of $R\text{-}C_6H_4CO^+$ from the parent-molecule ion is found for 4-methylbenzil but not for the others.

The metastables of greatest intensity, in each of the above spectra, correspond to the loss of neutral carbon monoxide from the benzoyl or substituted benzoyl ion to form the phenyl or substituted phenyl ion. Several of these metastables are flat-topped; all other metastables in the spectra are gaussian. Formation of the phenyl and substituted phenyl ions directly from the parent, as suggested by Natalis and Franklin,[33] cannot be conclusively eliminated by the lack of a corresponding metastable but appears to be an unlikely process in light of the intensity of the metastable for the competing process and the energetic data vide infra.

Metastables for the fragmentation of the phenyl ion into $C_4H_3^+$ (m/e 33.78) are observed in the spectra of benzil, 4-methylbenzil, 4-methoxybenzil, 4-methylmercaptobenzil, and 4-dimethylaminobenzil, but not in the spectra of 4-chlorobenzil (Table 9). The other product from this process is, presumably, neutral ethylene, and no significance is attached to the non-appearance of this metastable in the chloro case. A metastable for the formation of $R\text{-}C_4H_3^+$ is found for 4-methylbenzil, but not for any other monosubstituted benzil. Scheppele et al.[34] suggest that m/e 91 in the 4-methylbenzil spectrum may not be the tolyl ion, but rather the tropylium ion, and postulate that the rearrangement occurs prior to the loss of carbon monoxide by $CH_3\text{-}C_6H_4CO^+$. Since this lower energy pathway is not available to other monosubstituted benzoyl ions, it is not surprising that no significant peak is found in the spectra of the

TABLE 9

METASTABLE IONS

From Positive Ion Fragmentation Processes of $R_1\text{-}C_6H_4COCOC_6H_4\text{-}R_2$

PARENT R_1	PARENT R_2	PROCESS	METASTABLES m/e calc. (obs.)	METASTABLES intensity	METASTABLES shape
H	Cl	$P^{+\cdot}$ (224) $\longrightarrow$ $Cl\text{-}C_6H_4CO^+$ (139) + $C_6H_5CO\cdot$	79.18	n.o.	
		$Cl\text{-}C_6H_4CO^+$ (139) $\longrightarrow$ $Cl\text{-}C_6H_4^+$ (111) + CO	88.64 (88.7)	s	f.t.
		$Cl\text{-}C_6H_4^+$ (111) $\longrightarrow$ $C_4H_2Cl^+$ (63) + C_2H_2	35.76	n.o.	
		$P^{+\cdot}$ (224) $\longrightarrow$ $Cl\text{-}C_6H_4^+$ (111) + $C_6H_5COCO\cdot$	55.05	n.o.	
		$P^{+\cdot}$ (224) $\longrightarrow$ $C_6H_5CO^+$ (105) + $Cl\text{-}C_6H_4CO\cdot$	45.18	n.o.	
		$C_6H_5CO^+$ (105) $\longrightarrow$ $C_6H_5^+$ (77) + CO	56.47 (56.5)	s	g
		$C_6H_5^+$ (77) $\longrightarrow$ $C_4H_3^+$ (51) + C_2H_2	33.78	n.o.	
		$P^{+\cdot}$ (224) $\longrightarrow$ $C_6H_5^+$ (77) + $Cl\text{-}C_6H_4COCO\cdot$	24.30	n.o.	

other substituted benzils for $R\text{-}C_4H_3^+$ and that there is no metastable for such a process.

The spectra of 4,4'-dimethylbenzil, 4,4'-dichlorobenzil, and 4,4'-dimethoxybenzil, Figures 17 through 19, Tables 4, 10 and 11 all exhibit metastables for the formation of $R\text{-}C_6H_4CO^+$ from the parent-molecule ion. The comparable metastable for 4,4'-dimethylthiobenzil, Figure 20, Table 10, was not detected. The metastable for the formation of $(CH_3)_2N\text{-}C_6H_4CO^+$ from 4,4'-bis(dimethylamino)benzil, Figure 21, Table 11, is calculated to be m/e 74.00 and is probably obscured by the large peak at that mass. Intense metastables for the process

$$R\text{-}C_6H_4CO^+ \longrightarrow R\text{-}C_6H_4^+ + CO$$

are present in all spectra. No metastables are found for the formation of $R\text{-}C_6H_4^+$ from the parent molecule ion, and the conclusion drawn in the discussion of the monosubstituted benzils' spectra that this is an unlikely process seems applicable here as well.

An intense peak at m/e 65 is present in the spectrum of 4,4'-dimethylbenzil, and an intense metastable at m/e 46.43 is also present, indicating the formation of $C_5H_5^+$ from $C_7H_7^+$. Since no analogous ions or metastables are found in the other disubstituted benzils' spectra, Scheppele and coworkers'[34] suggestion that a tropylium intermediate is involved may well be valid for the 4,4'-dimethylbenzil as well. The generalized scheme, analogous to Figure 16, for the decomposition of the disubstituted benzils is shown in Figure 22.

The spectra of the 4-nitrobenzil and 4,4'-dinitrobenzil are unique among the benzils studied. Figures 23 and 24 illustrate the spectra, and

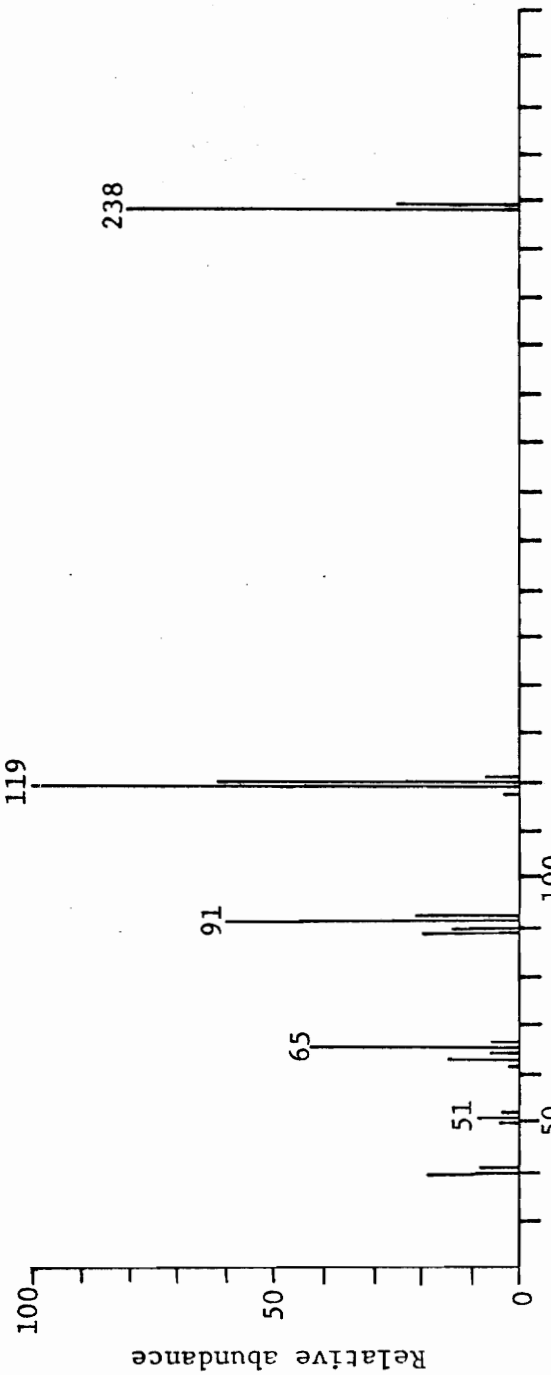

FIGURE 17. Positive Ion Mass Spectrum of 4,4'-Dimethylbenzil (50 eV)

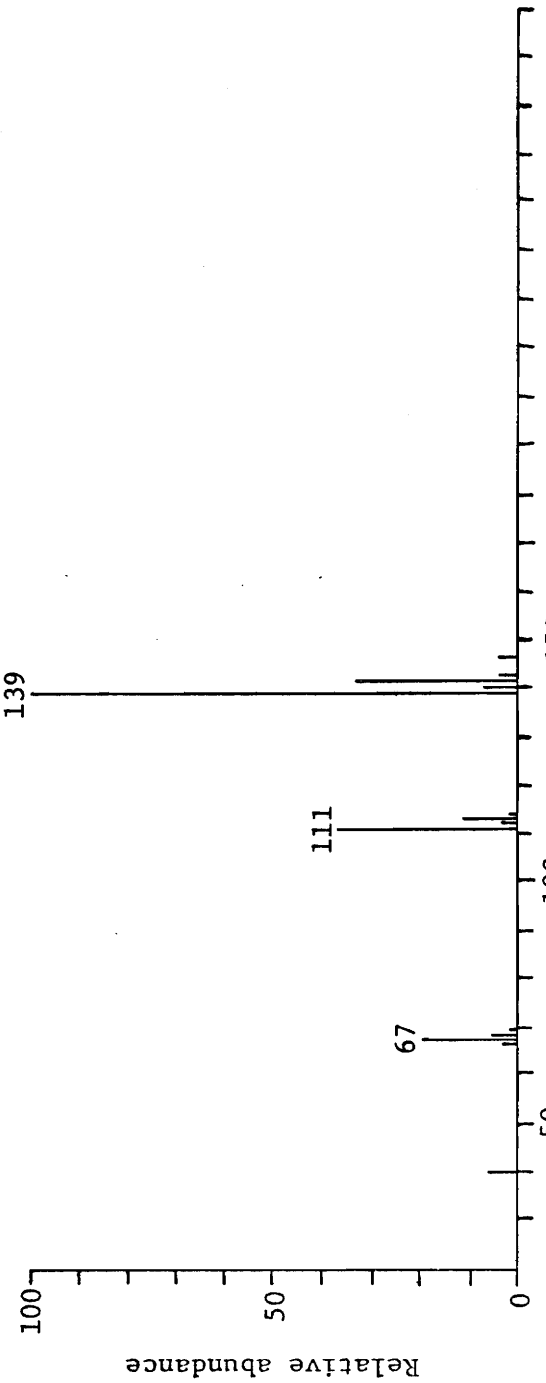

FIGURE 18. Positive Ion Mass Spectrum of 4,4'-Dichlorobenzil (50 eV)

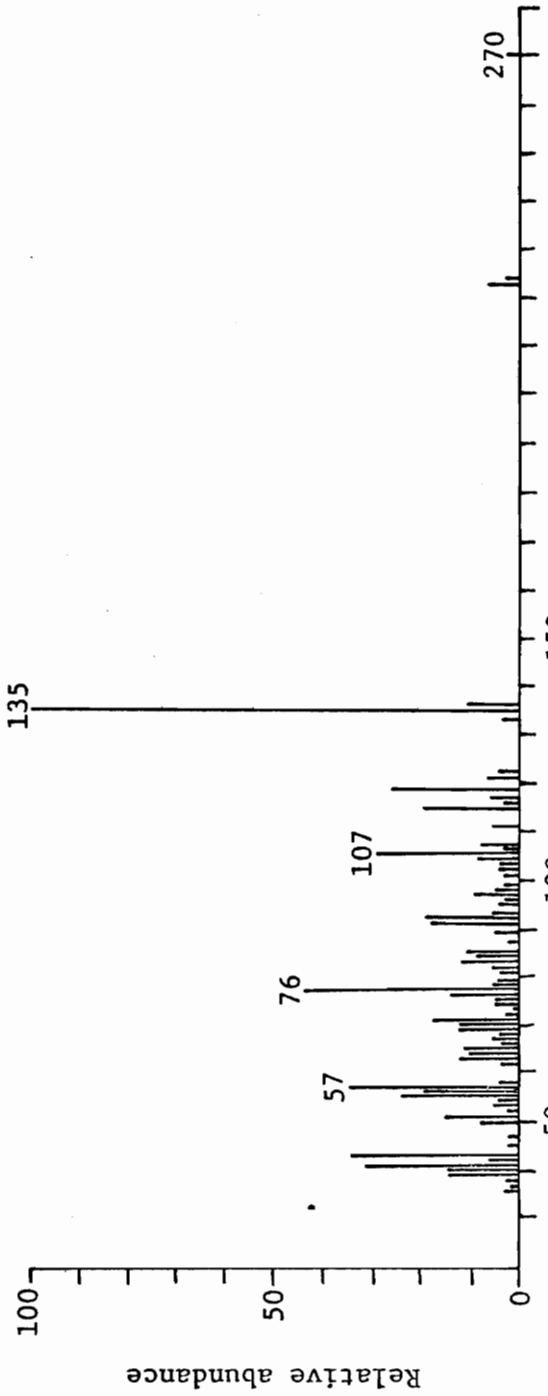

FIGURE 19. Positive Ion Mass Spectrum of 4,4'-Dimethoxybenzil (50 eV)

TABLE 10

METASTABLE IONS

From Positive Ion Fragmentation Processes of R_1-$C_6H_4COCOC_6H_4$-R_2

PARENT R_1	PARENT R_2	PROCESS	METASTABLES m/e calc. (obs.)	intensity	shape
CH_3O	CH_3O	$P^{+\cdot}$ (270) $\longrightarrow$ CH_3O-$C_6H_4CO^+$ (135) + CH_3O-$C_6H_4CO\cdot$	67.50 (67.5)	w	g
		CH_3O-$C_6H_4CO^+$ (135) $\longrightarrow$ CH_3O-$C_6H_4^+$ (107) + CO	84.81 (84.7-85.0)	s	f.t.
		CH_3O-$C_6H_4^+$ (107) $\longrightarrow$ $C_5H_5O^+$ (81) + C_2H_2	61.32	n.o.	
		$P^{+\cdot}$ (270) $\longrightarrow$ CH_3O-$C_6H_4^+$ (107) + CH_3O-$C_6H_4COCO\cdot$	42.40	n.o.	
CH_3S	CH_3S	$P^{+\cdot}$ (302) $\longrightarrow$ CH_3S-$C_6H_4CO^+$ (151) + CH_3S-$C_6H_4CO\cdot$	75.50	n.o.	
		CH_3S-$C_6H_4CO^+$ (151) $\longrightarrow$ CH_3S-$C_6H_4^+$ (123) + CO	100.19 (100.1-100.4)	s	f.t.
		CH_3S-$C_6H_4^+$ (123) $\longrightarrow$ $C_5H_5S^+$ (96) + C_2H_2	74.93	n.o.	
		$P^{+\cdot}$ (302) $\longrightarrow$ CH_3S-$C_6H_4^+$ (123) + CH_3S-$C_6H_4COCO\cdot$	50.10	n.o.	

TABLE 11

METASTABLE IONS

From Positive Ion Fragmentation Processes $R_1-C_6H_4COCOC_6H_4-R_2$

PARENT R_1	PARENT R_2	PROCESS	METASTABLES m/e calc.	m/e (obs.)	intensity	shape
$(CH_3)_2N$	$(CH_3)_2N$	$P^{+\cdot}$ (296) $\longrightarrow$ $(CH_3)_2N-C_6H_4CO^+$ (148) + $(CH_3)_2N-C_6H_4CO$	74.00*		n.o.	
		$(CH_3)_2N-C_6H_4CO^+$ (148) $\longrightarrow$ $(CH_3)_2N-C_6H_4^+$ (120) + CO	97.30	(97.3)	s	g
		$(CH_3)_2N-C_6H_4^+$ (120) $\longrightarrow$ $C_6H_8N^+$ (94) + C_2H_2	73.63		n.o.	
		$P^{+\cdot}$ (296) $\longrightarrow$ $(CH_3)_2N-C_6H_4^+$ (120) + $(CH_3)_2N-C_6H_4COCO\cdot$	48.65		n.o.	
Cl	Cl	$P^{+\cdot}$ (278) $\longrightarrow$ $Cl-C_6H_4CO^+$ (139) + $Cl-C_6H_4CO\cdot$	69.50		n.o.	
		$Cl-C_6H_4CO^+$ (139) $\longrightarrow$ $Cl-C_6H_4^+$ (111) + CO	88.64	(88.5-88.9)	s	f.t.
		$P^{+\cdot}$ (278) $\longrightarrow$ $Cl-C_6H_4^+$ (111) + $Cl-C_6H_4COCO\cdot$	44.32		n.o.	
		$Cl-C_6H_4^+$ (111) $\longrightarrow$ $C_4H_2Cl^+$ (63) + C_2H_4	35.76		n.o.	

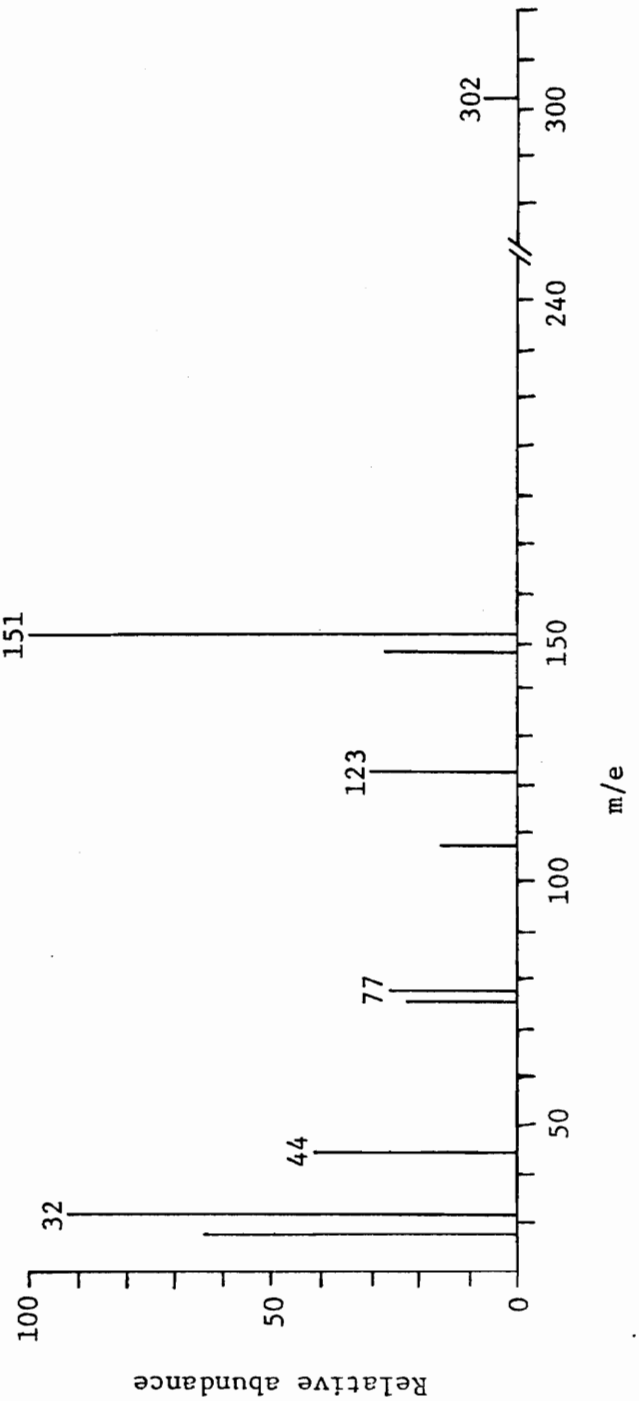

FIGURE 20. Positive Ion Mass Spectrum of 4,4'-Bismethylmercaptobenzil (50 eV)

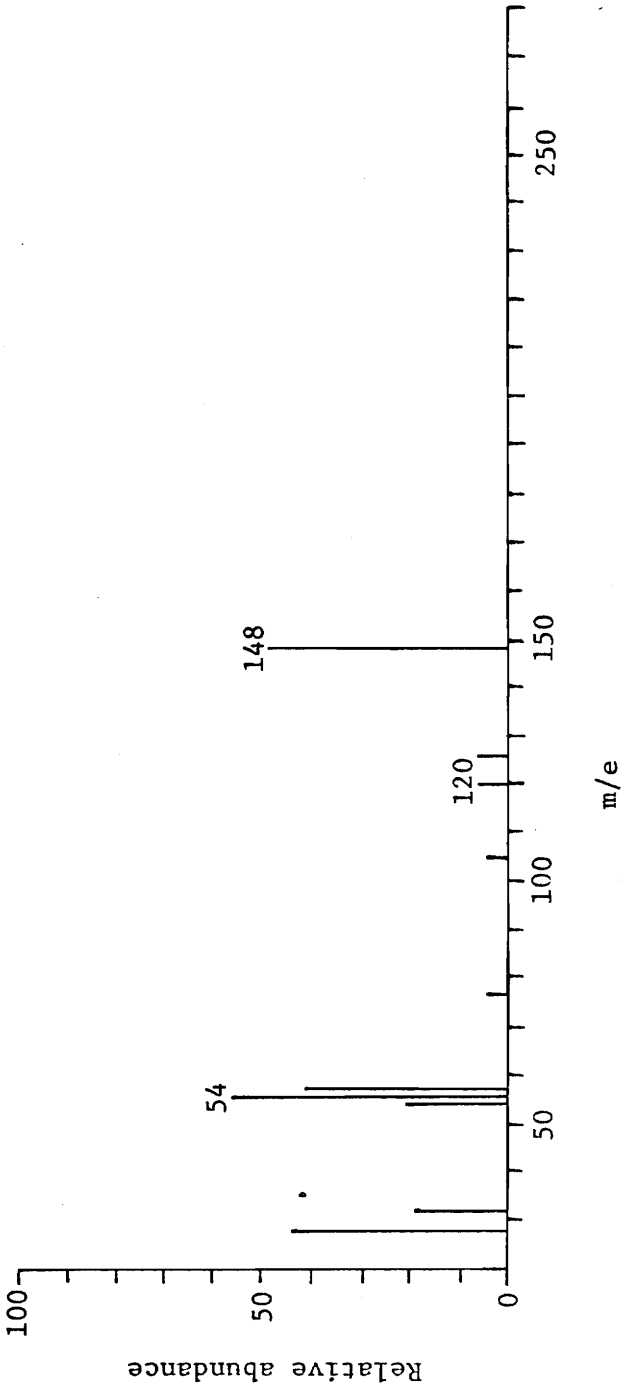

FIGURE 21. Positive Ion Mass Spectrum of 4,4'-Bis(dimethylamino)benzil (50 eV)

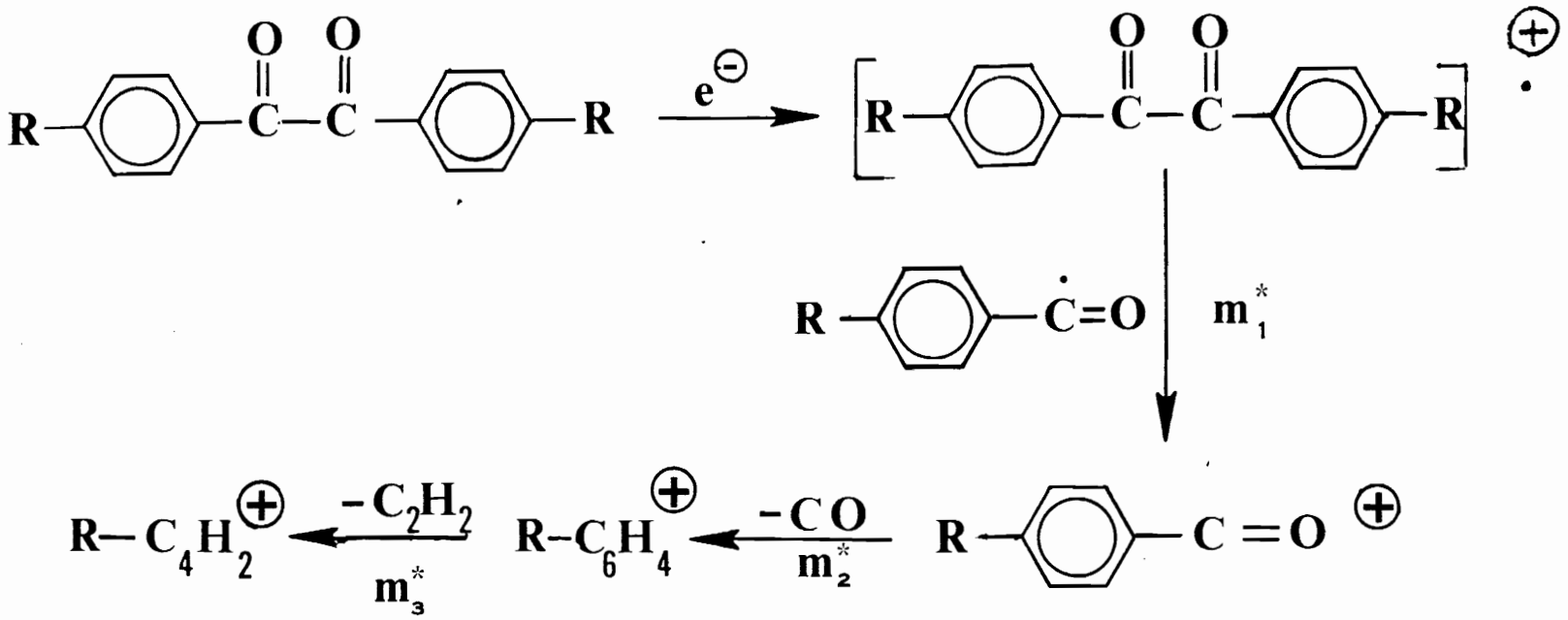

FIGURE 22. Disubstituted Benzils Fragmentation Pattern and Metastables

m_1^* R=H, CH_3, CH_3O, NO_2 m_2^* R=H, CH_3, CH_3O, CH_3S, Cl, $(CH_3)_2N$ m_3^* R=H, CH_3

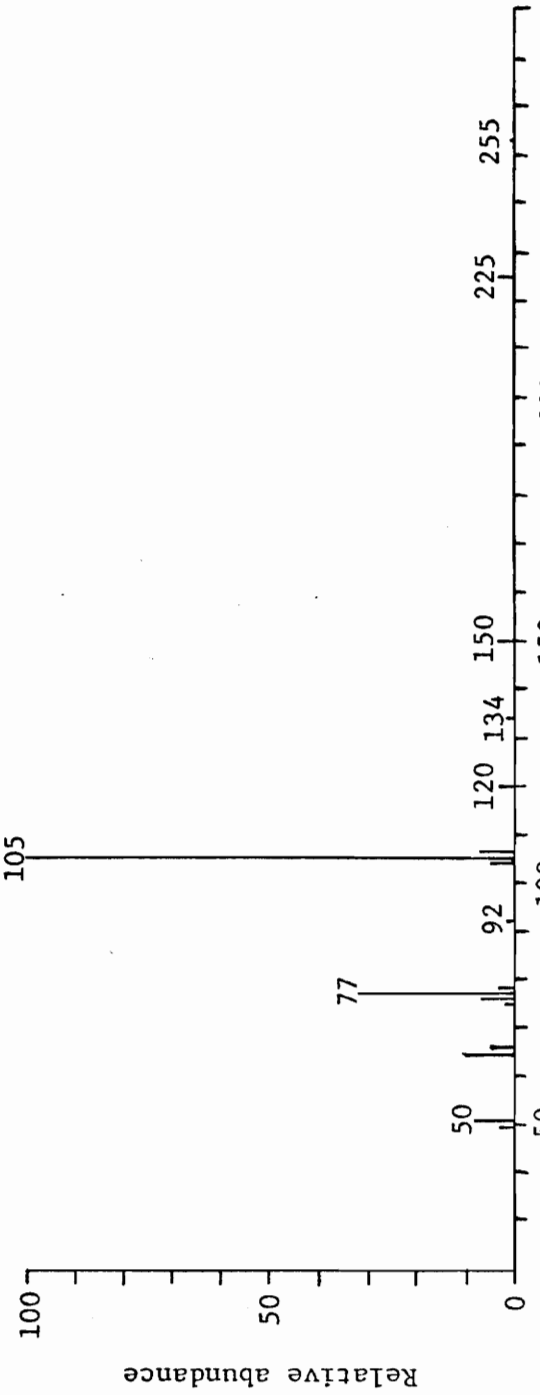

FIGURE 23. Positive Ion Mass Spectrum of 4-Nitrobenzil (50 eV)

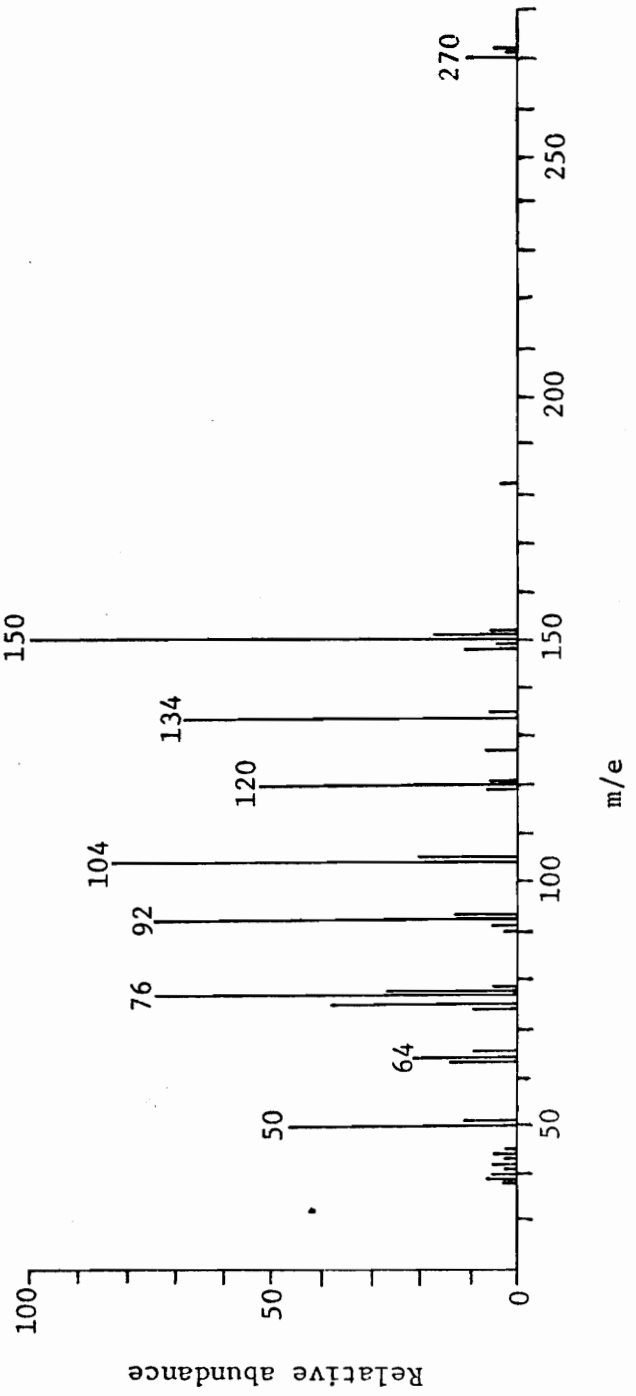

FIGURE 24. Positive Ion Mass Spectrum of 4,4'-Dinitrobenzil (50 eV)

TABLE 12

IDENTIFICATION OF THE MAJOR IONS IN THE POSITIVE ION SPECTRUM OF 4-NITROBENZIL

m/e	STRUCTURE	PRECURSOR	m* Calc.	m* Exp.
255	$O_2N\text{-}C_6H_4COCOC_6H_5^{+\cdot}$	---	---	---
225	$O\text{-}C_6H_4COCOC_6H_5^{+}$	$O_2N\text{-}C_6H_4COCOC_6H_5^{+\cdot}$	198.53	198.5
150	$O_2N\text{-}C_6H_4CO^{+}$	$O_2N\text{-}C_6H_4COCOC_6H_5^{+\cdot}$	88.23	88.2
134	$ON\text{-}C_6H_4CO^{+}$	?	---	---
120	$O\text{-}C_6H_4CO^{+}$	$O_2N\text{-}C_6H_4CO^{+}$	96.00	96.1
105	$C_6H_5CO^{+}$	$O_2N\text{-}C_6H_4COCOC_6H_5^{+\cdot}$	(43.24)	---
104	$C_6H_4CO^{+}$	$ON\text{-}C_6H_4CO^{+}$	80.72	80.5-90.0
92	$O\text{-}C_6H_4^{+}$	$O\text{-}C_6H_4CO^{+}$	(70.53)	---
77	$C_6H_5^{+}$	$C_6H_5CO^{+}$	56.47	56.5
76	$C_6H_4^{+}$	$C_6H_4CO^{+}$	55.54	55.5
64	?	$O\text{-}C_6H_4^{+}$	(44.52)	---

TABLE 12 (cont'd.)

m/e	STRUCTURE	PRECURSOR	m* Calc.	m* Exp.
51	$C_4H_3^+$	$C_6H_5^+$	33.76	33.8
50	$C_4H_2^+$	$C_6H_4^+$	(32.89)	---

Values in parentheses indicate metastables (m*) found in analogous spectra which are not detected in the spectrum of 4-nitrobenzil.

TABLE 13

IDENTIFICATION OF THE MAJOR IONS IN THE POSITIVE ION SPECTRUM OF 4,4'-DINITROBENZIL

m/e	STRUCTURE	PRECURSOR	m* Calc.	m* Exp.
300	$O_2N\text{-}C_6H_4COCOC_6H_4\text{-}NO_2^{+\cdot}$	---	---	---
270	$O_2N\text{-}C_6H_4COCOC_6H_4\text{-}O^+$	$O_2N\text{-}C_6H_4COCOC_6H_4\text{-}NO_2^{+\cdot}$	243.00	243.0
240	$O\text{-}C_6H_4COCOC_6H_4\text{-}O^+$	$O_2N\text{-}C_6H_4COCOC_6H_4\text{-}O^+$	---	---
150	$O_2N\text{-}C_6H_4CO^+$	$O_2N\text{-}C_6H_4COCOC_6H_4\text{-}NO_2^{+\cdot}$	75.00	75.0[1]
134	$ON\text{-}C_6H_4CO^+$	?	---	---
120	$O\text{-}C_6H_4CO^+$	$O_2N\text{-}C_6H_4CO^+$	96.00	96.0
104	$C_6H_4CO^+$	$ON\text{-}C_6H_4CO^+$	80.72	80.5-90.0
92	$O\text{-}C_6H_4^+$	$O_2N\text{-}C_6H_4^+$	69.38	69.2-71.5[2]
		$O\text{-}C_6H_4CO^+$	70.53	
76	$C_6H_4^+$	$C_6H_4CO^+$	55.54	55.6

TABLE 13 (cont'd.)

m/e	STRUCTURE	PRECURSOR	m* Calc.	m* Exp.
64	?	$o\text{-}C_6H_4^+$	44.52	44.2-44.7
50	$C_4H_2^+$	$C_6H_4^+$	32.89	32.9

---

[1]Broad bottom of $C_6H_5^+$ fragment ion peak.

[2]Overlapping strong m*.

Tables 12 and 13 list the major ions in the spectrum, indicating probable structure and origin, and the metastables supporting the process. The characteristic difference between the nitrobenzils and other benzils is the ready loss of NO• to yield ions unique to these benzil systems. As a result, the nitrobenzils are the only benzils to yield an ion apparently not generated from benzoyl or a substituted benzoyl ($P\cdot^+ \longrightarrow P\text{-}NO\cdot$) and the only benzils which do not form an ion from the loss of CO from $R\text{-}C_6H_4CO^+$. The mechanism for the loss of NO• will be discussed in Section VIII in comparison with a similar phenomenon in the negative ion spectra. The mechanism is undoubtedly a free radical one and involves a rearrangement. The ion of undetermined structure or origin, at m/e 134, which is present at low abundance in the spectra of both nitro-substituted benzils, may be a by-product of the loss of NO from $NO_2\text{-}C_6H_4CO^+$, but does not appear to be part of the primary decomposition pathway. The anomalous ion at m/e 64, which is apparently formed from $O\text{-}C_6H_4^+$, is tentatively assigned the formula $C_5H_4^+$ and is probably formed by loss of CO from its precursor.

The low relative abundance, ca. 3%, of the $NO_2\text{-}C_6H_4CO^+$ ion, in the 4-nitrobenzil spectrum agrees with the observations of Einolf and Munson[22] who found a relative abundance of 3.7% at 70 eV, up from 0.79% at 15 eV. Contrasted with the ratio of relative abundances found for the 4-dimethylaminobenzil, these data indicate that the effect of an electron-withdrawing substituent is to diminish the formation of a benzoyl ion on the carbonyl nearest it, as opposed to augmentation of the decomposition of said benzoyl. This conclusion is not surprising, in that it is the basis of Einolf and Munson's[22] analysis, but the effect of the low abundance will

be seen in Section VI on the shape of the ionization efficiency curves.

SECTION VI

POSITIVE ION ENERGETICS

A. RESULTS

In order to obtain an estimate of the ionization potentials for the benzils, and to determine what differences in ionization and appearance potentials should be expected from the addition of a second substituent to the parent, several simple calculations were performed.

Heats of formation of the benzils were calculated in the following way. The group equivalent method of Franklin[82,87] was used to obtain an estimate of the heat of formation. The value used for benzil is -19.22 kcal/mol, which is somewhat less than the normally accepted value of -21.8 kcal/mol.[88] Following the method of Scheppele et al.,[34] two "difference methods" based on analogous systems were also employed to estimate the heat of formation. For monosubstituted benzils, the difference between the group equivalents value for the 4-substituted benzaldehyde and the experimental heat of formation of benzaldehyde[82] was added to the accepted value for benzil. For both mono- and di-substituted benzils, the difference between the group equivalents value of the 4-(mono) or 4,4'-(di)substituted benzophenones and benzophenone[82] was added to the accepted value for benzil. The values obtained in this manner are presented in Table 14. The average value for the heat of formation is used in subsequent calculations. It is noted that the values calculated by the various methods do not vary by more than 4 kcal/mol with one exception, that of 4-methoxybenzil. The heat of formation calculated using the difference between group equivalents value for 4-methoxybenzophenone and the experimental value for benzophenone differs by 22.3 kcal/mol from the values

TABLE 14

HEATS OF FORMATION OF BENZILS $R_1\text{-}C_6H_4COCOC_6H_4\text{-}R_2$

COMPOUND R_1	COMPOUND R_2	$\Delta\Delta H_f$ Group Equivalents (kcal/mol)	$\Delta\Delta H_f$[1] Benzophenone (kcal/mol)	$\Delta\Delta H_f$[2] Benzaldehyde (kcal/mol)	$\Delta\Delta H_f$ Average (kcal/mol)
H	H	-19.2	-----	-----	-21.8[3]
H	CH_3	-28.3	-31.0	-32.3	-30.54 ± 1.36
H	Cl	-28.2	-30.9	-32.2	-30.43 ± 1.52
H	NO_2	-26.7	-29.4	-30.7	-28.93 ± 1.67
H	CH_3S	-16.7	-19.4	-20.7	-18.93 ± 1.67
H	CH_3O	-55.5	-33.2	-59.5	-49.40 ± 11.57
					(-57.5)[4] ± 2.00
H	$(CH_3)_2N$	-19.2	-21.9	-21.5	-20.87 ± 1.19
CH_3	CH_3	-37.4	-40.0	-----	-38.70 ± 1.30
Cl	Cl	-37.2	-39.9	-----	-38.55 ± 1.35
NO_2	NO_2	-34.2	-36.9	-----	-35.55 ± 1.35
CH_3S	CH_3S	-14.2	-16.9	-----	-15.55 ± 1.35
CH_3O	CH_3O	-91.8	-94.5	-----	-93.15 ± 1.35
$(CH_3)_2N$	$(CH_3)_2N$	-19.2	-21.9	-----	-20.55 ± 1.35

1. Calculated from differences in heats of formation of substituted and unsubstituted benzophenones.
2. Calculated from differences in heats of formation of substituted and unsubstituted benzaldehydes.
3. H. D. Springall and T.R.J. White, J. Chem. Soc., 2764 (1964).
4. Better value. N.b. low value from benzophenone method.

calculated by the other methods. The best value is considered to be the average of the values calculated by the other two methods. In subsequent calculations, values are determined using both averages, with the "best value" shown in parenthesis.

The heats of formation of the molecular ions of the benzils and the corresponding ionization potentials are shown in Table 15. The values for benzil are those of Scheppele et al.[34] and are used as the basis for all subsequent calculations, the results of which are also shown in this table. Where values exist[82] for the analogous 4-substituted benzophenone molecular ion, the difference between the heat of formation ($\Delta\Delta H_f$) of that substituted benzophenone molecular ion and the benzophenone molecular ion is used as the difference between the heats of formation of the substituted benzil molecular ion and the benzil molecular ion. Where values exist for the analogous 4-substituted benzaldehyde molecular ion, the same type of calculation is made to obtain a value for the difference between heats of formation of the substituted benzil molecular ion and the benzil molecular ion. The use of the benzaldehyde method is limited to the monosubstituted benzils calculations. Similarly, available values for the substituted benzene molecular ions were used to calculate $\Delta\Delta H_f$. Where no experimental values were available, the group equivalents method[82,87] was used. Whenever more than one method was available, the value shown in column three of Table 15 is the average of the methods used, and the appropriate methods are shown in column two. The value calculated for the heat of formation of the benzil is the sum of the average $\Delta\Delta H_f$ and the heat of formation of the benzil molecule ion. The value shown for the ionization potential of the molecule ion is obtained by subtracting

the calculated heat of formation found in Table 14 from the value for the heat of formation of the molecule ion in this table and dividing by 23.061 kcal/mol. Again, the value calculated for the 4-methoxybenzil is found to fit the data better when the benzophenone method is discarded.

Appearance potentials for the major fragment ions from the benzils were calculated on the assumption that the fragmentation patterns indicated in Figures 16 and 22, as supported by the 50 eV metastable data and discussion in Section V, are also valid for low energy processes. Initial cleavage of the carbonyl-carbonyl bond produces two fragments, one a positive ion and the other a neutral radical. Monosubstituted benzils generally produce two ions from this process, one containing the substituent and the other being the benzoyl ion. The substituted benzoyl ion is the only ion produced by this process in the disubstituted benzils.

The appearance potentials for the substituted benzoyl ions generated from the monosubstituted benzils were calculated from Equation 17 as suggested by Scheppele et al.[34]

$$A.P.(R\text{-}C_6H_4CO^+) = \frac{\Delta H_f(R\text{-}C_6H_4CO^+) + \Delta H_f(C_6H_5CO\cdot) - \Delta H_f(R\text{-}C_6H_4COCOC_6H_5)}{23.061} \quad (17)$$

The values for the heats of formation of the benzils were taken from Table 14. The heat of formation of the substituted benzoyl ions was calculated by adding the value for $\Delta\Delta H_f$ in column one of Table 15 to the accepted value for the formation of the benzoyl ion from benzil, 186 kcal/mol.[33] The value of 26.1 kcal/mol was used for the heat of formation of the benzoyl radical.[89] The calculated values are summarized in the top half of Table 16.

The appearance potentials for the benzoyl ions generated from the

TABLE 15

CALCULATED IONIZATION POTENTIALS FOR BENZILS

COMPOUND R_1	COMPOUND R_2	$\Delta\Delta H_f$ (kcal/mol)	Method	ΔH_f (kcal/mol)	I.P. (eV.)
H	H	0	1	182.5 ± 3.6	8.86 ± 0.14
H	CH_3	-14.5	2,3	168.0	8.61 ± 0.02
H	Cl	- 9.0	3,4	173.5	8.84 ± 0.02
H	NO_2	+ 9.5	3,4	192.0	9.58 ± 0.06
H	CH_3S	- 4.0	4	178.5	8.56
H	CH_3O	-59.5	3,4	123.0	7.48 ± 0.02
				(180.5)[6]	(7.83)[6] ± 0.02
H	$(CH_3)_2N$	-16.0	4	166.5	8.12
CH_3	CH_3	-34.0	4	148.5	8.12
Cl	Cl	-21.0	4	161.5	8.67
NO_2	NO_2	-17.0	5	165.5	8.72
CH_3S	CH_3S	+ 3.0	5	185.5	8.72
CH_3O	CH_3O	-74.6	5	107.9	8.72
$(CH_3)_2N$	$(CH_3)_2N$	-53.0	4	129.5	6.51

1. Value from Scheppele, et. al., J. Amer. Chem. Soc., 95, 5105 (1973).
2. Value calculated based on differences in heats of formation of substituted and unsubstituted benzophenone parent positive ions.
3. Value calculated based on differences in heats of formation of substituted and unsubstituted benzaldehyde parent positive ions.
4. Value calculated based on differences in heats of formation of substituted and unsubstituted benzene parent positive ions.
5. Value calculated using group equivalents.
6. Better value.

TABLE 16

CALCULATED APPEARANCE POTENTIALS FOR $R_2\text{-}C_6H_4CO^+$ GENERATED FROM $R_1\text{-}C_6H_4COCOC_6H_4\text{-}R_2$

R_1	R_2	ΔH_f (kcal/mol)	A.P. (eV)	Literature	Ref.
H	H	186	10.14	9.70	1
H	CH_3	171.5	9.89	9.73, 9.84	2
H	Cl	177.0	10.13		
H	NO_2	195.5	10.86		
H	CH_3S	182.0	9.84		
H	CH_3O	126.5	8.75 (9.02)		
H	$(CH_3)_2N$	170.0	9.41		
CH_3	CH_3	171.5	10.24/9.85[3]		
Cl	Cl	177.0	10.48/10.09[3]		
NO_2	NO_2	195.5	11.15/10.78[3]		
CH_3S	CH_3S	182.0	9.70/9.30[3]		
CH_3O	CH_3O	126.4	10.66/9.08[3]		
$(CH_3)_2N$	$(CH_3)_2N$	170.0	9.39/9.40[3]		

1. P. Natalis and J. L. Franklin, J. Phys. Chem., 69, 2943 (1965).
2. S. E. Scheppele, et. al., J. Amer. Chem. Soc., 95, 5105 (1973).
3. First value calculated using 26.1 kcal/mol for $R_1\text{-}C_6H_5CO\cdot$, second value using group equivalents to adjust this value. R. K. Solly and S. W. Benson, J. Amer. Chem. Soc., 93, 1592 (1971).

monosubstituted benzils were calculated from Equation 18.[34]

$$\text{A.P.}(C_6H_5CO^+) = \frac{\Delta H_f(C_6H_5CO^+) + \Delta H_f(R\text{-}C_6H_4CO\cdot) - \Delta H_f(R\text{-}C_6H_4COCOC_6H_5)}{23.061} \quad (18)$$

The value of 186 kcal/mol[33] was used for the heat of formation of the benzoyl ion. The values for the heats of formation of the benzils were taken from Table 14. Two values for the heat of formation of each substituted benzoyl radical were used. The first value was based on the conclusion of Solly and Benson[89] that "stabilization of formyl radicals, RCO·, is independent of R and is determined solely by conjugation of the unpaired carbon electron with the lone-pair oxygen electrons. Resonance structures in which the unpaired carbon electron is conjugated with a phenyl ring make no contribution to the stability of the benzoyl radical." The second value used added the group equivalent values[82] to the value of 27.1 kcal/mol. The calculated appearance potentials using the value of 26.1 kcal/mol are shown in column one of Table 17, and the values calculated using the group equivalents method are shown in column two.

The appearance potentials for the substituted benzoyl ions generated from the disubstituted benzils were calculated using Equation 19.

$$\text{A.P.}(R\text{-}C_6H_4CO^+) = \frac{\Delta H_f(R\text{-}C_6H_4CO^+) + \Delta H_f(R\text{-}C_6H_4CO\cdot) - \Delta H_f(R\text{-}C_6H_4COCOC_6H_4\text{-}R)}{23.061}$$

(19)

The values for the heats of formation of the ion are the same used for the ions in Equation 17. Values for the heats of formation of the benzils are taken from Table 14. Two values were again used in the calculation of the heats of formation of the benzoyl radicals, 26.1 kcal/mol for each radical[89] and 27.1 kcal/mol plus the group equivalent value. The results are

TABLE 17

CALCULATED APPEARANCE POTENTIALS FOR $C_6H_5CO^+$ GENERATED FROM $C_6H_5COCOC_6H_4$-R

R	$RC_6H_4CO\cdot$ = +26.1 kcal/mol (eV.)	A.P. Group Equiv. (eV.)	Lit.
H	10.14	-----	9.70[1]
CH_3	10.52	10.13	9.98[2]
Cl	10.52	10.13	
NO_2	10.45	10.13	
CH_3S	10.02	10.13	
CH_3O	11.34	9.77	
$(CH_3)_2N$	10.11	10.11	

1. P. Natalis and J. L. Franklin, J. Phys. Chem., 69, 2943 (1965).
2. S. E. Scheppele, et. al., J. Amer. Chem. Soc., 95, 5105 (1973).

summarized in this order in the bottom half of Table 16.

Appearance potentials for the ions formed by loss of neutral carbon monoxide from the benzoyl ions were calculated using Equations 20 and 21 for the monosubstituted benzils, and Equation 22 for the disubstituted benzils.

$$A.P.(R\text{-}C_6H_4^+) = \frac{\Delta H_f(R\text{-}C_6H_4^+) + \Delta H_f(C_6H_5CO\cdot) + \Delta H_f(CO) - \Delta H_f(R\text{-}C_6H_4COCOC_6H_5)}{23.061} \quad (20)$$

$$A.P.(C_6H_5^+) = \frac{\Delta H_f(C_6H_5^+) + \Delta H_f(R\text{-}C_6H_4CO\cdot) + \Delta H_f(CO) - \Delta H_f(R\text{-}C_6H_4COCOC_6H_5)}{23.061} \quad (21)$$

$$A.P.(R\text{-}C_6H_4^+) = \frac{\Delta H_f(R\text{-}C_6H_4^+) + \Delta H_f(R\text{-}C_6H_4CO\cdot) + \Delta H_f(CO) - \Delta H_f(R\text{-}C_6H_4COCOC_6H_4\text{-}R)}{23.061} \quad (22)$$

Values for the heats of formation of the molecules are taken from Table 14; values for the heats of formation of the benzoyl radicals are as described *supra.*; a value of -26.42 kcal/mol is used for $\Delta H_f(CO)$. A value of 299 kcal/mol is used for $\Delta H_f(C_6H_5^+)$, and literature values or group equivalents for $\Delta H_f(R\text{-}C_6H_4^+)$. It can be seen by inspection that the calculations are of minimal value since the effects of the substituents are self-canceling in Equation 22, the equations fail to take into account the kinetic energy involved in the cleavage process, and the values calculated via Equation 22 are dependent on ΔH_f for the substituted phenyl ion for which no good values exist. The calculated values are shown in Tables 18 and 19 along with the experimental values.

The calculated, experimental, and literature values for the appearance potentials of the benzoyl and substituted benzoyl ions formed from the

TABLE 18

POSITIVE ION APPEARANCE POTENTIALS FOR PHENYL AND SUBSTITUTED PHENYL IONS FORMED IN THE SECONDARY FRAGMENTATION OF MONOSUBSTITUTED BENZILS

SUBSTITUENT (R)	A. P. (eV) $C_6H_5^+$ Calculated[1]	$C_6H_5^+$ Experimental	$C_6H_5^+$ Lit.	A. P. (eV) $R\text{-}C_6H_4^+$ Calculated	$R\text{-}C_6H_4^+$ Experimental	$R\text{-}C_6H_4^+$ Lit.
H	14.17	13.58 ± 0.35	15.12[2] ± 0.2	-----	-----	-----
CH_3	13.88 (14.28)	14.37 ± 0.10	13.95[3] ± 0.66	10.98	12.51 ± 0.56	11.37[3] (12.5-13.0)[3]
Cl	13.88 (14.28)	14.07 ± 0.10	-----	10.98	13.91 ± 0.14	-----
NO_2	13.88 (14.28)	15.18 ± 0.80	-----	10.98	none	-----
CH_3S	13.88 (14.28)	14.83 ± 0.10	-----	10.98	13.72 ± 0.44	-----
CH_3O	13.88 (14.28)	14.98 ± 0.35	-----	11.05	13.10 ± 0.37	-----
$(CH_3)_2N$	13.88 (14.28)	15.03 ± 1.00	-----	10.95	11.06 ± 1.03	-----

1. First value calculated using group equivalents, second value calculated using 26.1 kcal/mol for $R\text{-}C_6H_4CO$. cf. Table 17.
2. P. Natalis and J. L. Franklin, J. Phys. Chem., 69, 2943 (1965).
3. S. E. Scheppele, R. K. Mitchum, K. F. Kinneberg, G. G. Meisels and R. H. Emmel, J. Amer. Chem. Soc., 95, 5105 (1973).

TABLE 19

POSITIVE ION APPEARANCE POTENTIALS FOR SUBSTITUTED BENZOYL IONS AND SUBSTITUTED PHENYL IONS PRODUCED BY PRIMARY AND SECONDARY FRAGMENTATION PROCESSES OF DISUBSTITUTED BENZILS

SUBSTITUENT (R)	A. P. (eV) $R\text{-}C_6H_4CO^+$			A. P. (eV) $R\text{-}C_6H_4^+$		
	Calculated[1]	Experimental	Lit.	Calculated[1,2]	Experimental	Lit.
CH_3	9.85 (10.24)	9.91 ± 0.34	----	10.93 - 14.02	14.09 ± 0.50	----
Cl	10.09 (10.48)	10.81 ± 0.35	----	10.85 - 14.01	13.15 ± 2.56	----
NO_2	10.78 (11.15)	10.63 ± 0.50	----	11.04 - 13.42	none	----
CH_3S	9.30 (9.70)	9.22 ± 0.10	----	11.73 - 13.03	13.72 ± 0.10	----
CH_3O	9.08 (10.66)	9.68 ± 0.21	----	10.11 - 14.79	13.90 ± 0.38	----
$(CH_3)_2N$	9.40	8.64 ± 0.10	----	9.82 - 12.76	12.97 ± 0.35	----

1. First value calculated using group equivalents, second value calculated using 26.1 kcal/mol for R-C6H4CO. cf Table 17.
2. Minimum and maximim values, depending on choice of ΔH_f for $R\text{-}C_6H_4^+$.

monosubstituted benzils are shown in Table 20. These values are plotted versus the Hammett σ values in Figures 25 and 28, and against σ^+ and σ^I values in Figures 26, 27, 29 and 30. The calculated and experimental appearance potential values for the substituted benzoyl ions generated from the disubstituted benzils are presented in Table 19 and plotted versus the Hammett σ values in Figure 31, and versus the σ^+ and σ^I values in Figures 32 and 33. The calculated and experimental and literature appearance potential values for the phenyl and substituted phenyl ions from monosubstituted benzils are presented in Table 18 and plotted versus the Hammett σ values in Figures 34 and 37 and versus the σ^+ and σ^I values in Figures 35, 36, 38 and 39. The calculated and experimental appearance potential values for the substituted phenyl ions generated by the secondary fragmentation of the disubstituted benzils are listed in Table 19 and plotted versus the Hammett σ values in Figure 40 and versus the σ^+ and σ^I values in Figures 41 and 42.

No experimental values were obtained for the ionization potentials of the parent-molecule ions because the ion current is so low at 50 eV that the Warren method is of no use in determining the true I.P. Inspection of Table 15 indicates that the differences in the ionization potentials obtained should be less than the experimental error for all but the extremes of substituents. The appearance potentials for the benzoyl and substituted benzoyl ions were generally obtained with a small correction factor, but the slope of the phenyl and substituted phenyl ions often required a large correction factor to make their slopes parallel to that of Xe-129. Another complicating factor which could rarely be predicted nor corrected for, was the condition of the source, which may be critical.

TABLE 20

POSITIVE ION APPEARANCE POTENTIALS FOR BENZOYL AND SUBSTITUTED BENZOYL IONS FORMED IN THE PRIMARY FRAGMENTATION OF MONOSUBSTITUTED BENZILS

SUBSTITUENT (R)	A. P. (eV) $C_6H_5CO^+$ Calculated[1]	Experimental	Lit.	A. P. (eV) $R\text{-}C_6H_4CO^+$ Calculated[1]	Experimental	Lit.
H	10.14	10.12 ± 0.10	9.70[2] ± 0.05	-----	-----	-----
CH_3	10.13 (10.52)	10.78 ± 0.10	9.98[3]	9.89	10.20 ± 0.25	9.84[3] ± 0.1
Cl	10.13 (10.52)	9.86 ± 0.13	-----	10.13	9.95 ± 0.13	-----
NO_2	10.13 (10.45)	10.06 ± 0.50	-----	10.86	12.60 ± 0.33	-----
CH_3S	10.13 (10.02)	11.08 ± 0.61	-----	9.84	10.02 ± 0.15	-----
CH_3O	9.77 (11.34)	10.51 ± 0.38	-----	9.02	9.66 ± 0.10	-----
$(CH_3)_2N$	10.11	12.62 ± 0.35	-----	9.41	8.69 ± 0.10	-----

1. First value calculated using group equivalents, second value calculated using 26.1 kcal/mol for $R\text{-}C_6H_4CO$. cf. Table 17.
2. P. Natalis and J. L. Franklin, J. Phys. Chem., 69, 2943 (1965).
3. S. E. Scheppele, R. K. Mitchum, K. F. Kinneberg, G. G. Meisels and R. H. Emmel, J. Amer. Chem. Soc., 95, 5105 (1973).

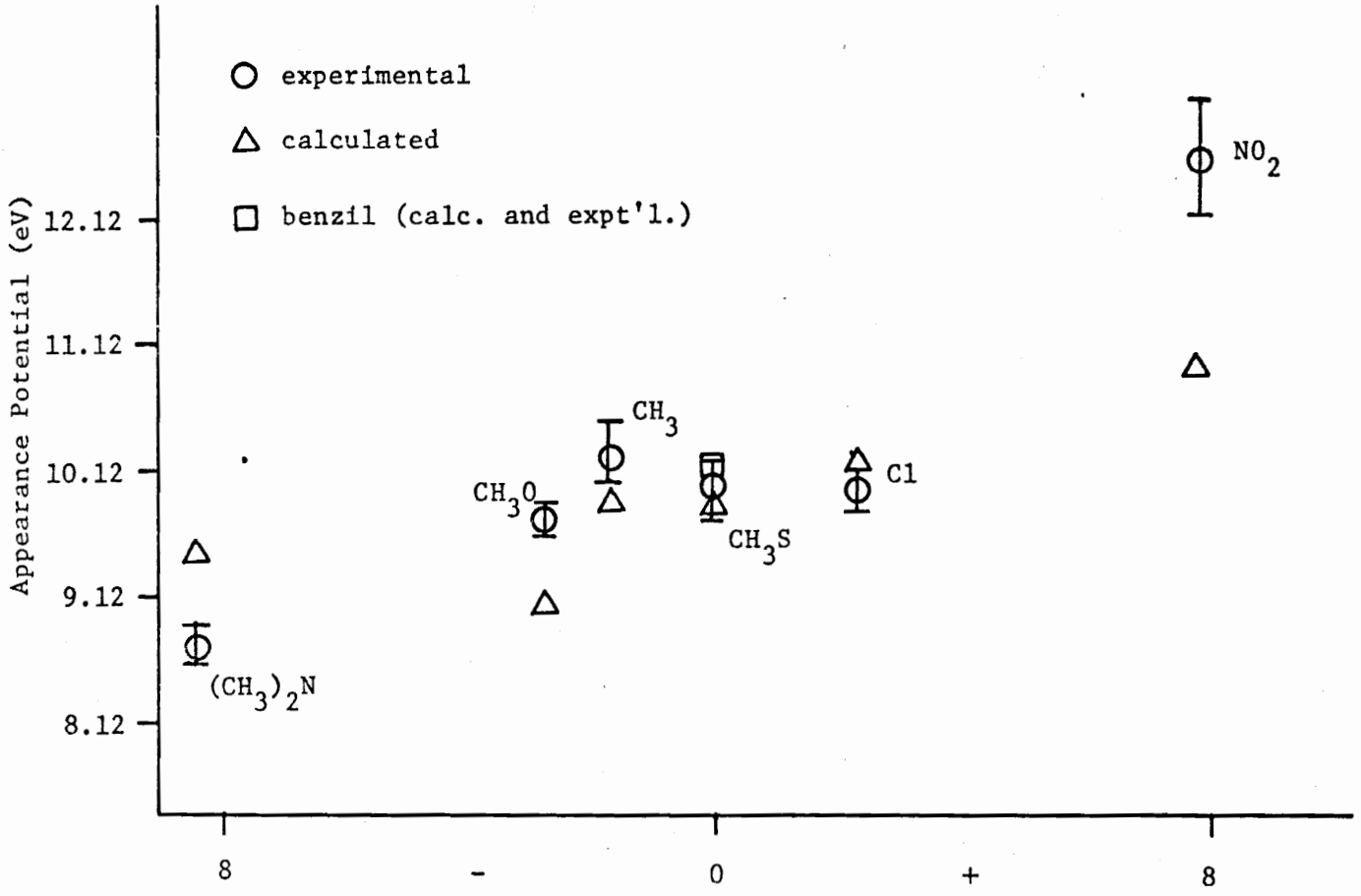

FIGURE 25. Appearance Potentials for Substituted Benzoyl Ions from Monosubstituted Benzils vs. σ

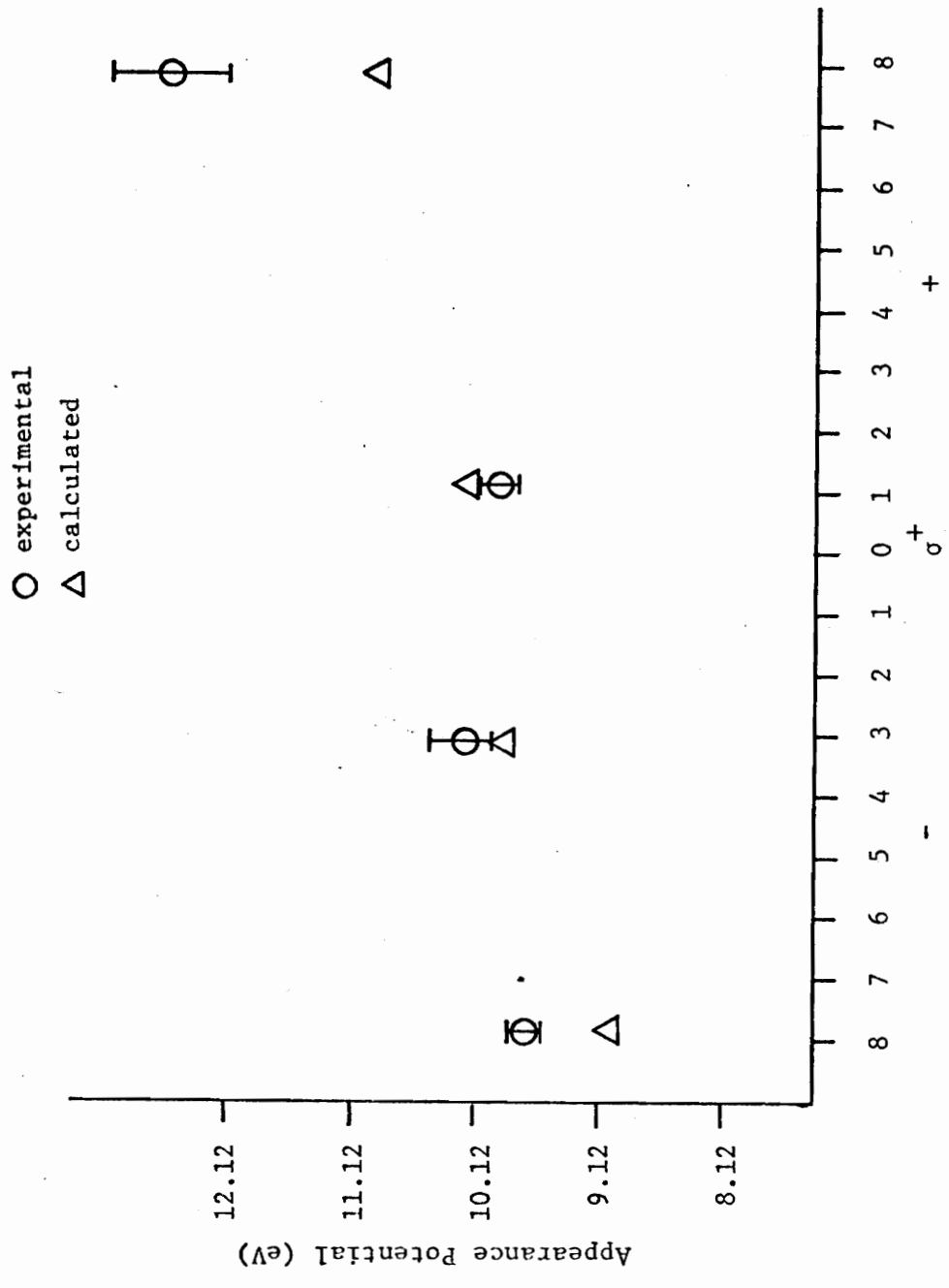

FIGURE 26. Appearance Potentials for Substituted Benzoyl Ions from Monosubstituted Benzils vs. σ^+

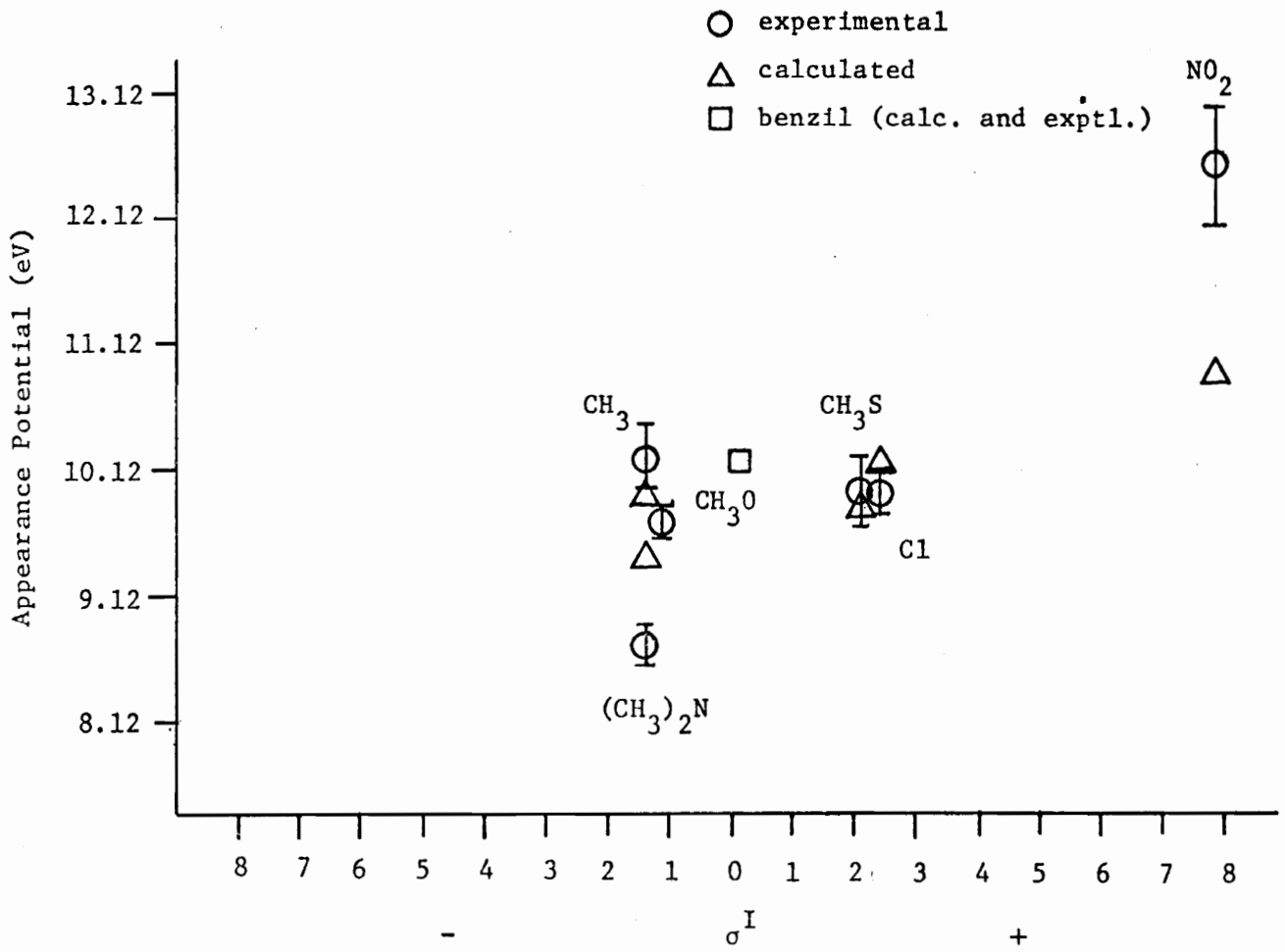

FIGURE 27. Appearance Potentials for Substituted Benzoyl Ions from Monosubstituted Benzils vs. σ^I

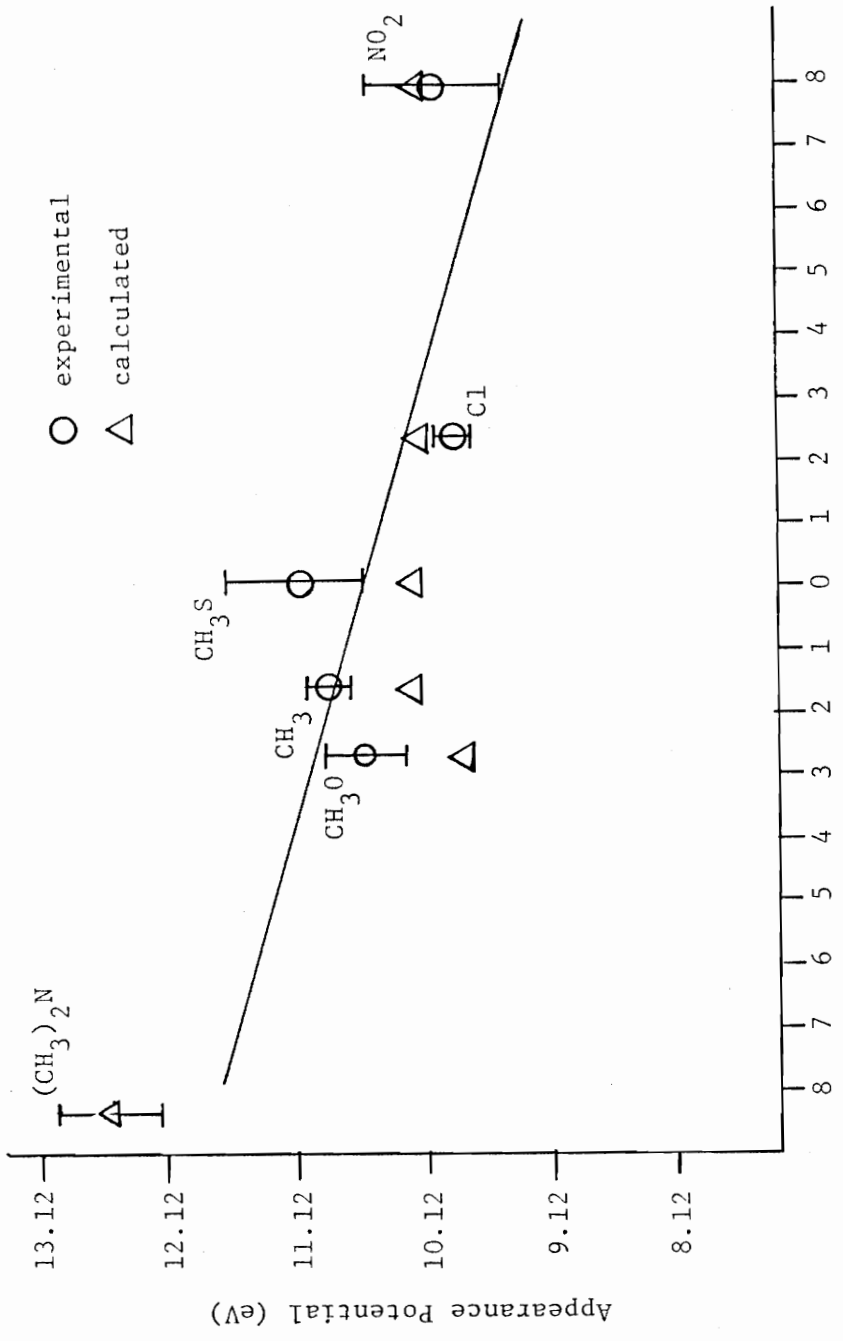

FIGURE 28. Appearance Potentials for Benzoyl Ions from Monosubstituted Benzils vs. σ

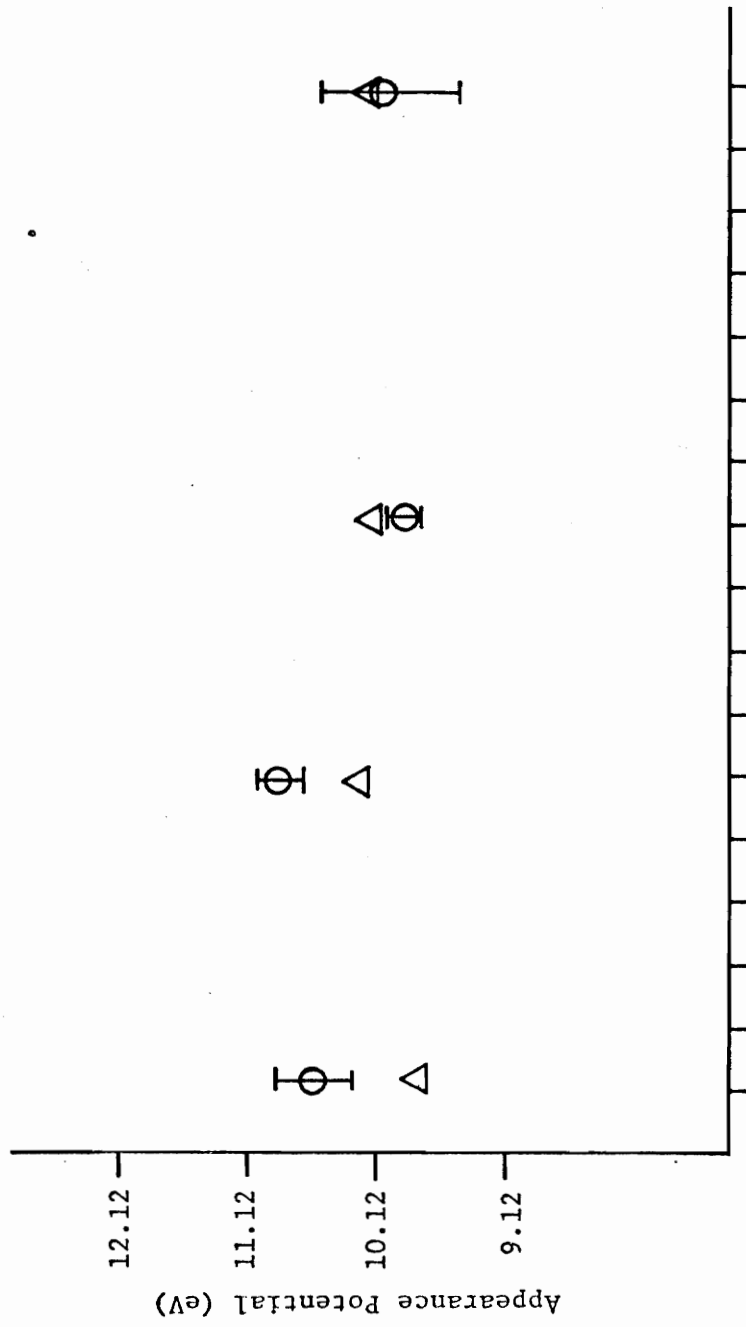

FIGURE 29. Appearance Potentials for Benzoyl Ions from Monosubstituted Benzils vs. σ^+

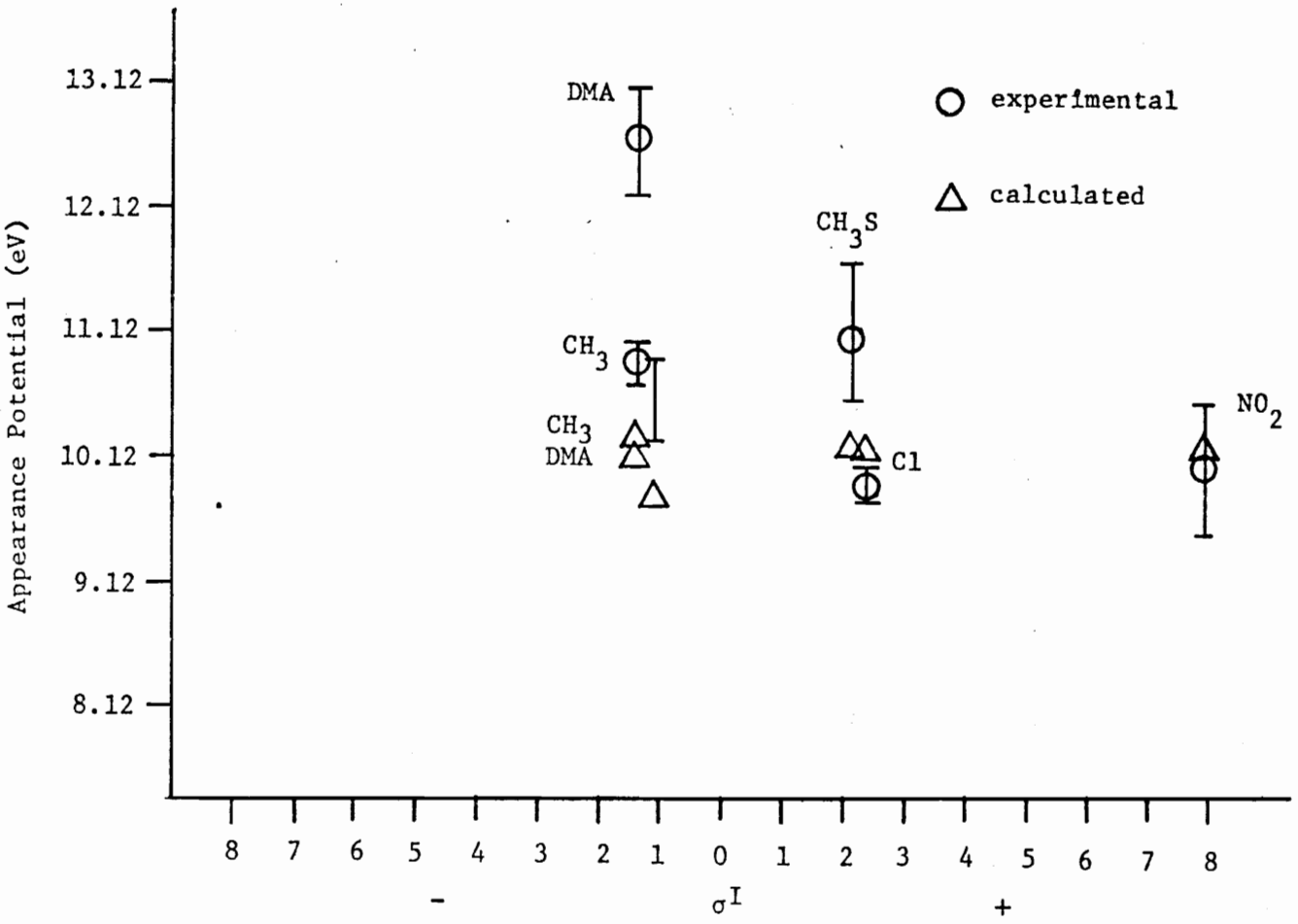

FIGURE 30. Appearance Potentials for Benzoyl Ions from Monosubstituted Benzils vs. σ^I

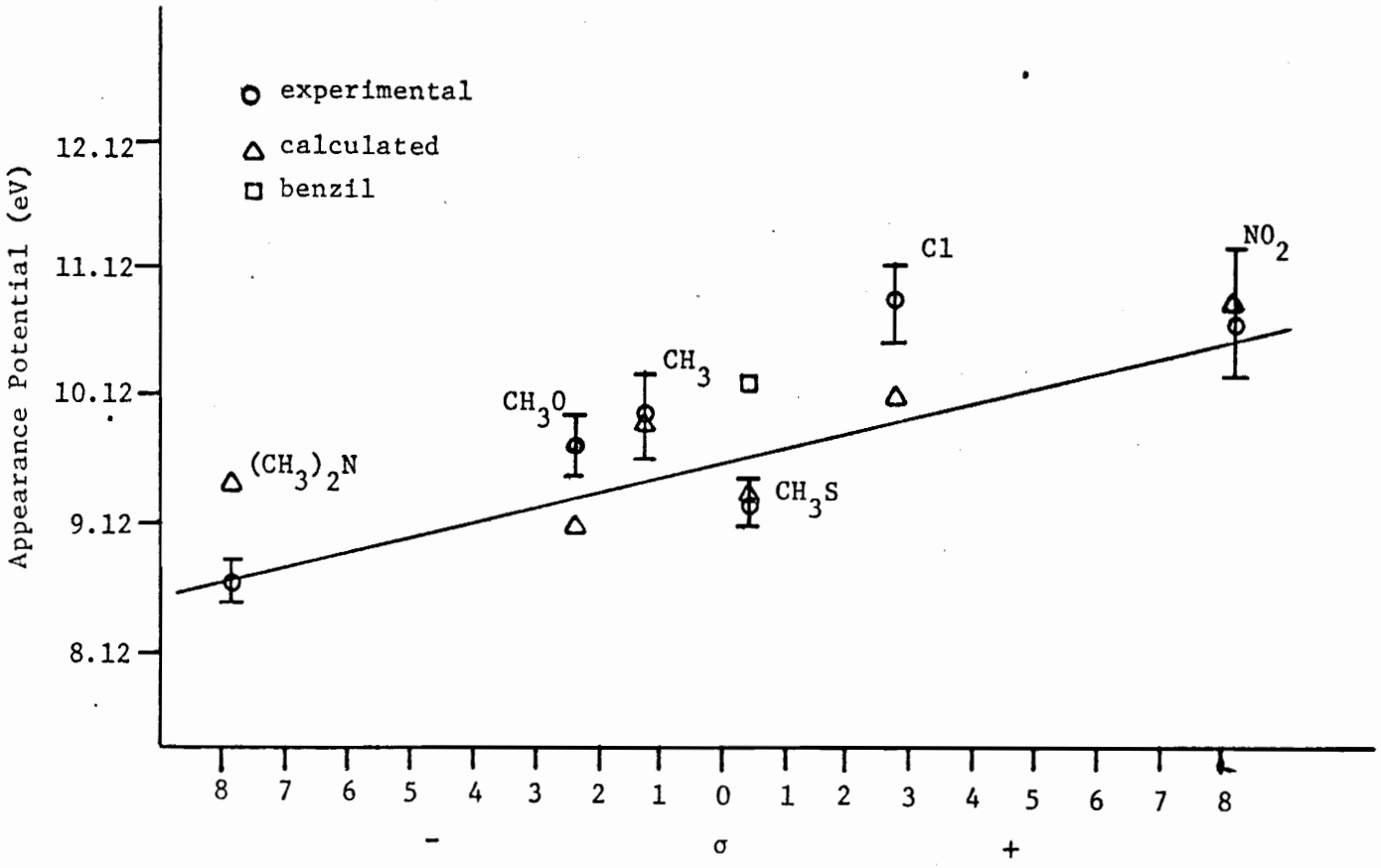

FIGURE 31. Appearance Potentials for Substituted Benzoyl Ions from Disubstituted Benzils vs. σ

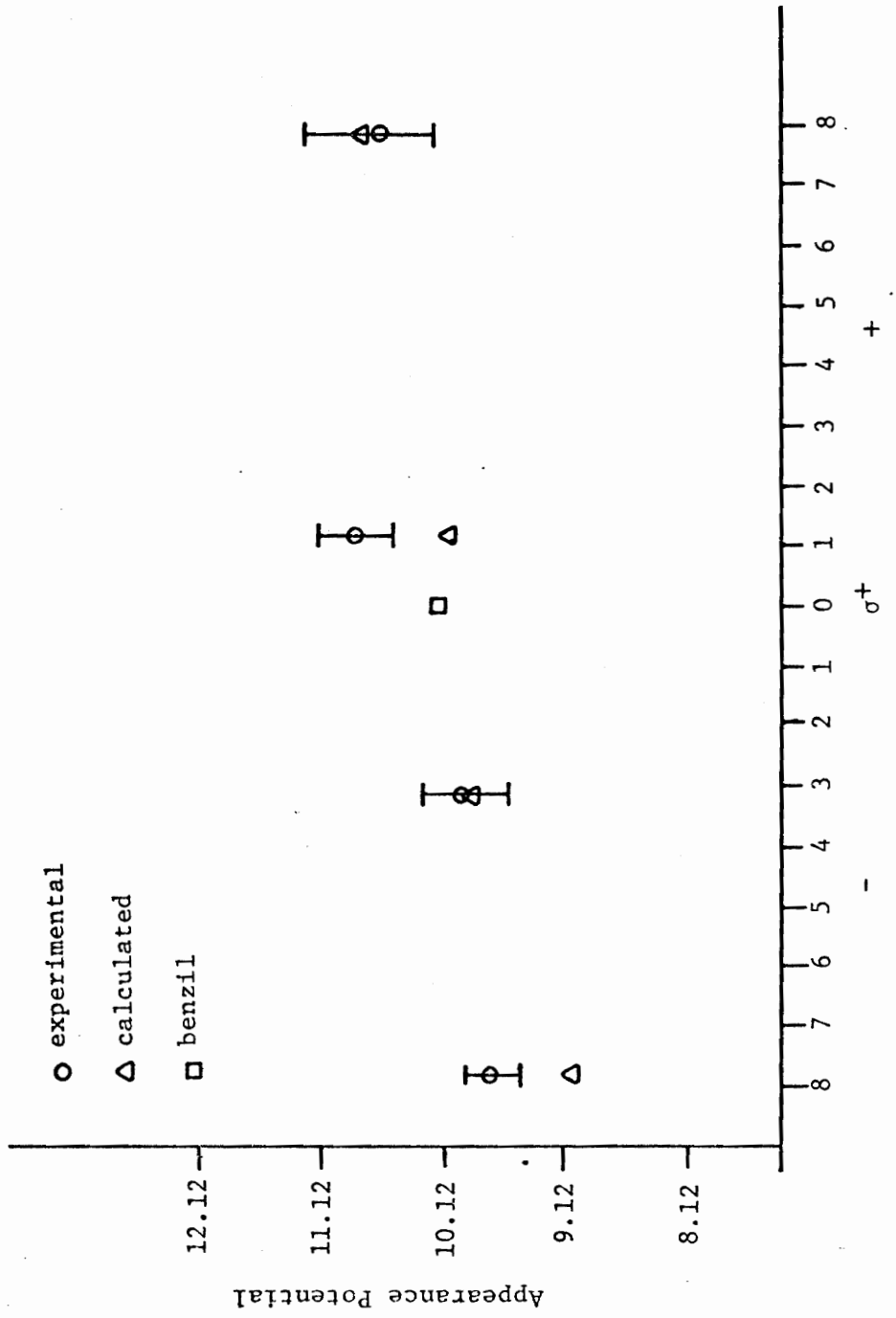

FIGURE 32. Appearance Potentials for Substituted Benzoyl Ions from Disubstituted Benzils vs. σ^+

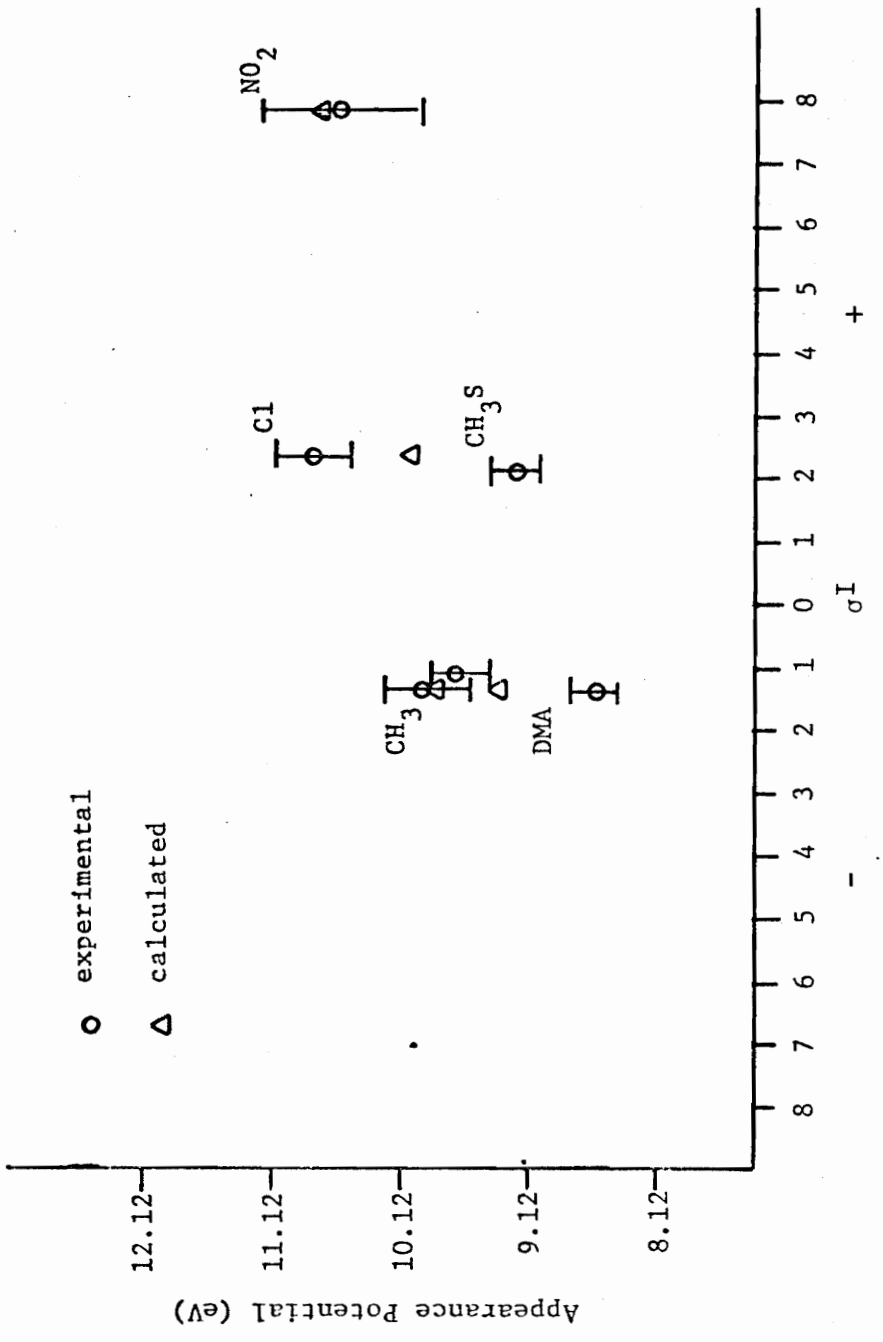

FIGURE 33. Appearance Potentials for Substituted Benzoyl Ions from Disubstituted Benzils vs. σ_I

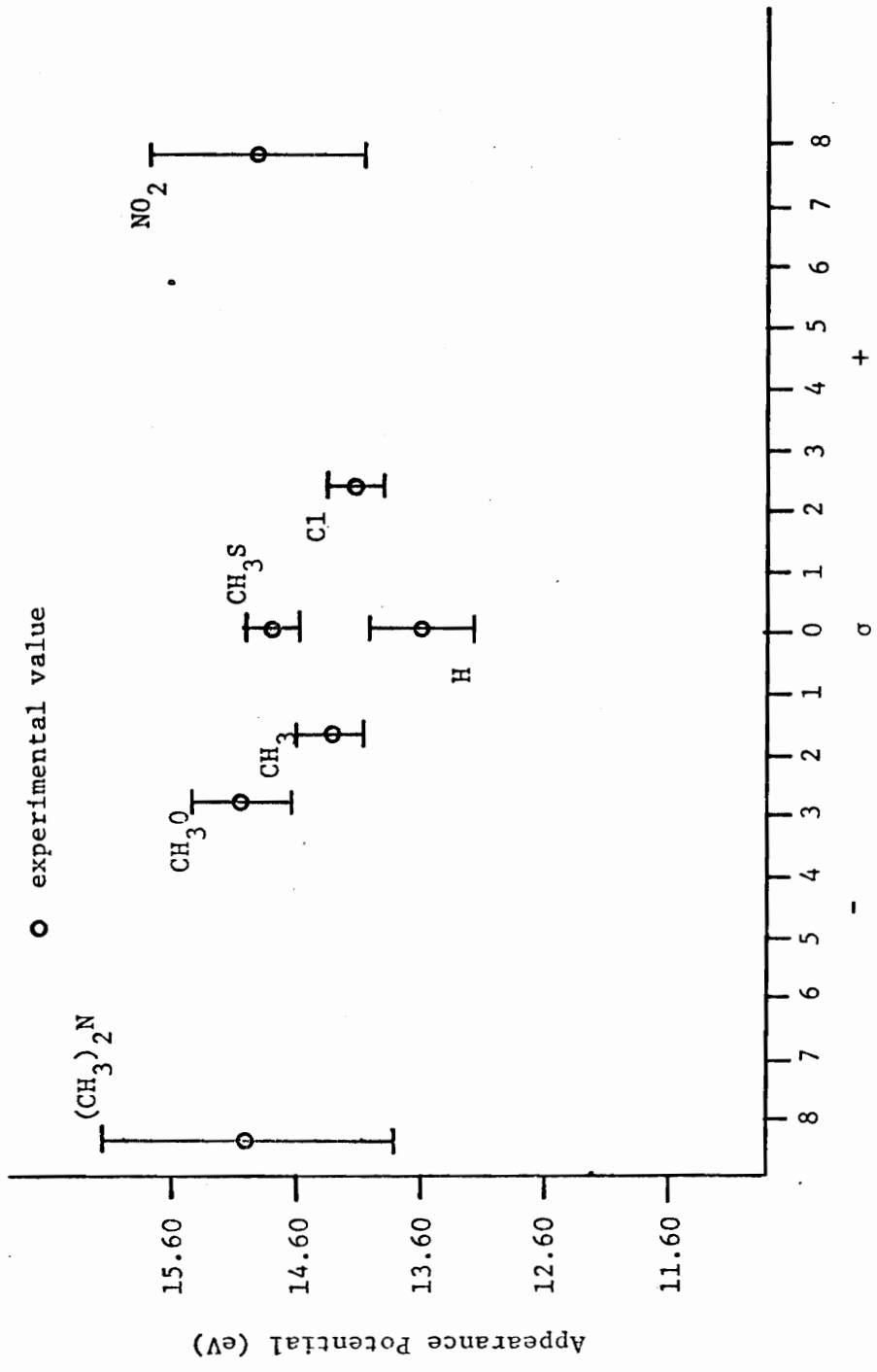

FIGURE 34. Appearance Potentials for Phenyl Ions from Monosubstituted Benzils vs. σ

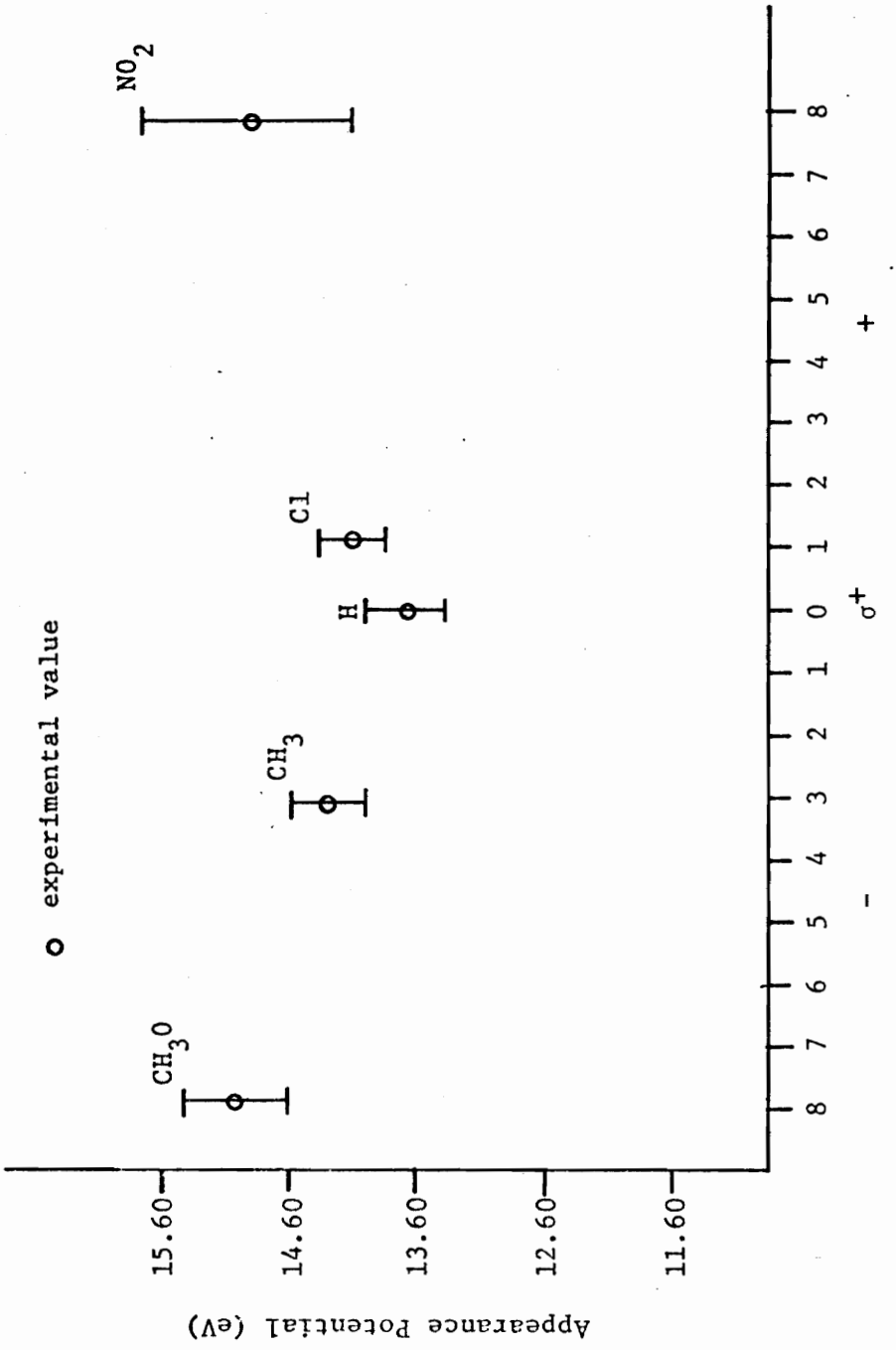

FIGURE 35. Appearance Potentials for Phenyl Ions from Monosubstituted Benzils vs. σ^+

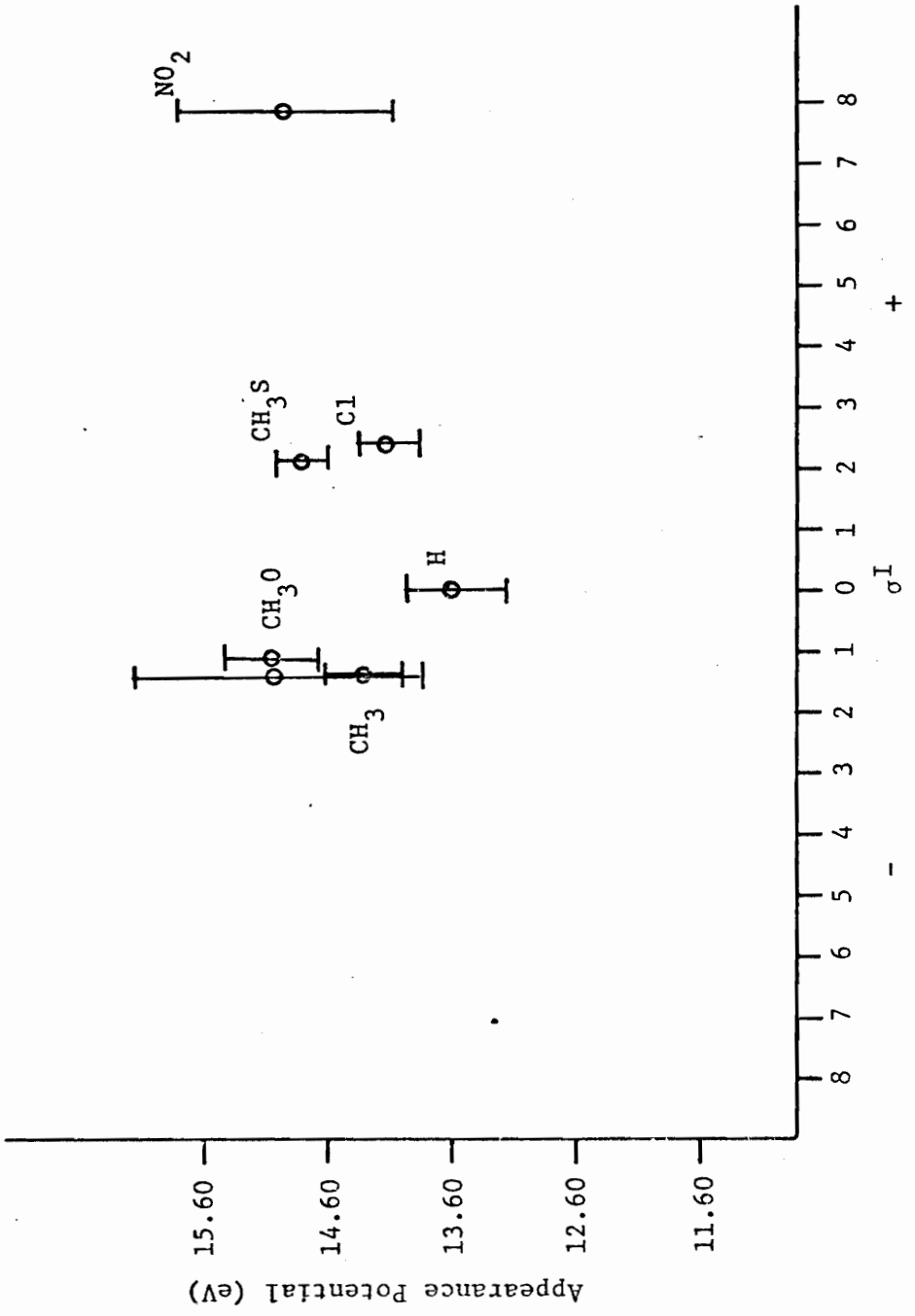

FIGURE 36. Appearance Potentials for Phenyl Ions from Monosubstituted Benzils vs. σ^I

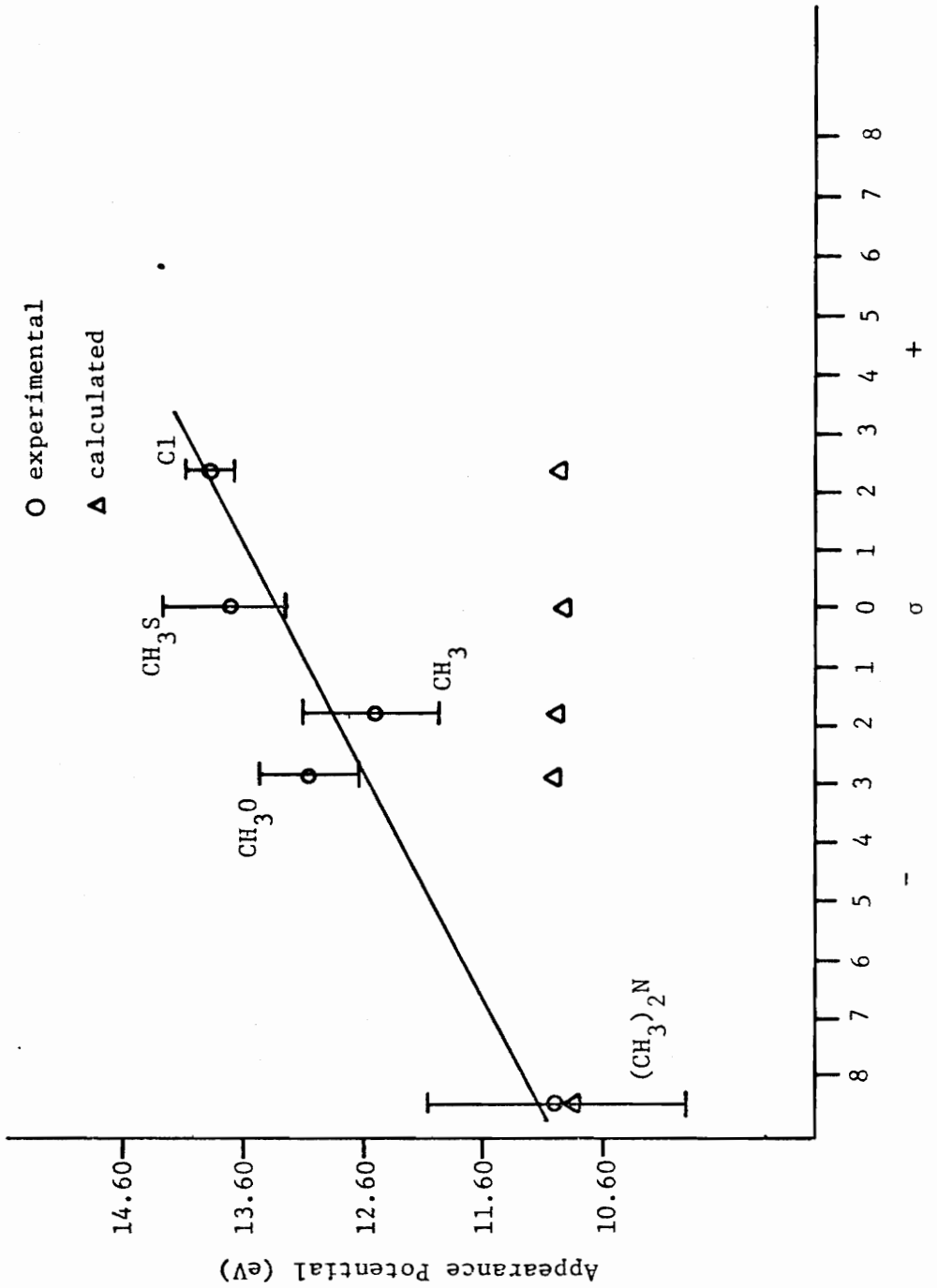

FIGURE 37. Appearance Potentials for Substituted Phenyl Ions from Monosubstituted Benzils vs. σ

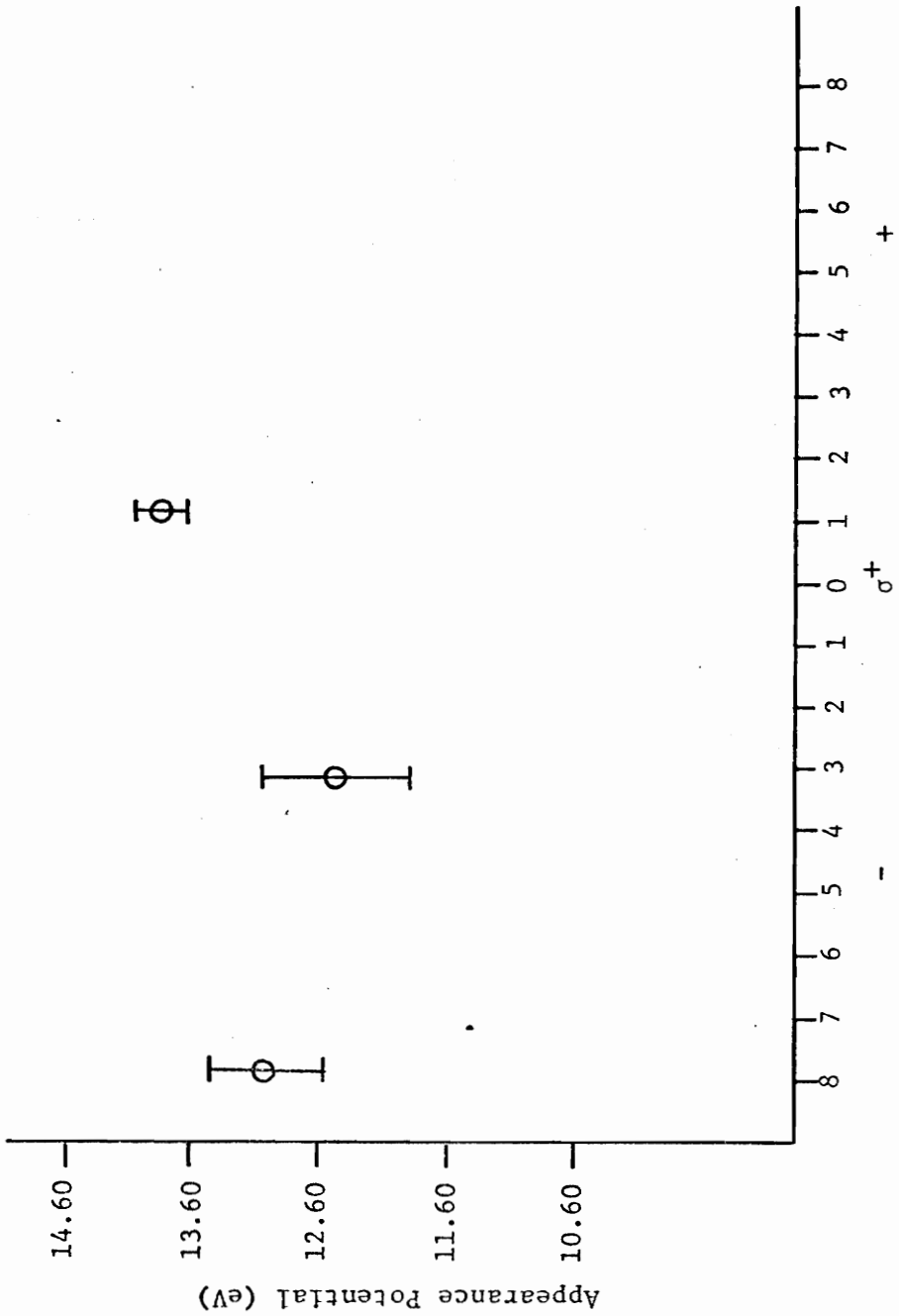

FIGURE 38. Appearance Potentials for Substituted Phenyl Ions from Monosubstituted Benzils vs. σ^+

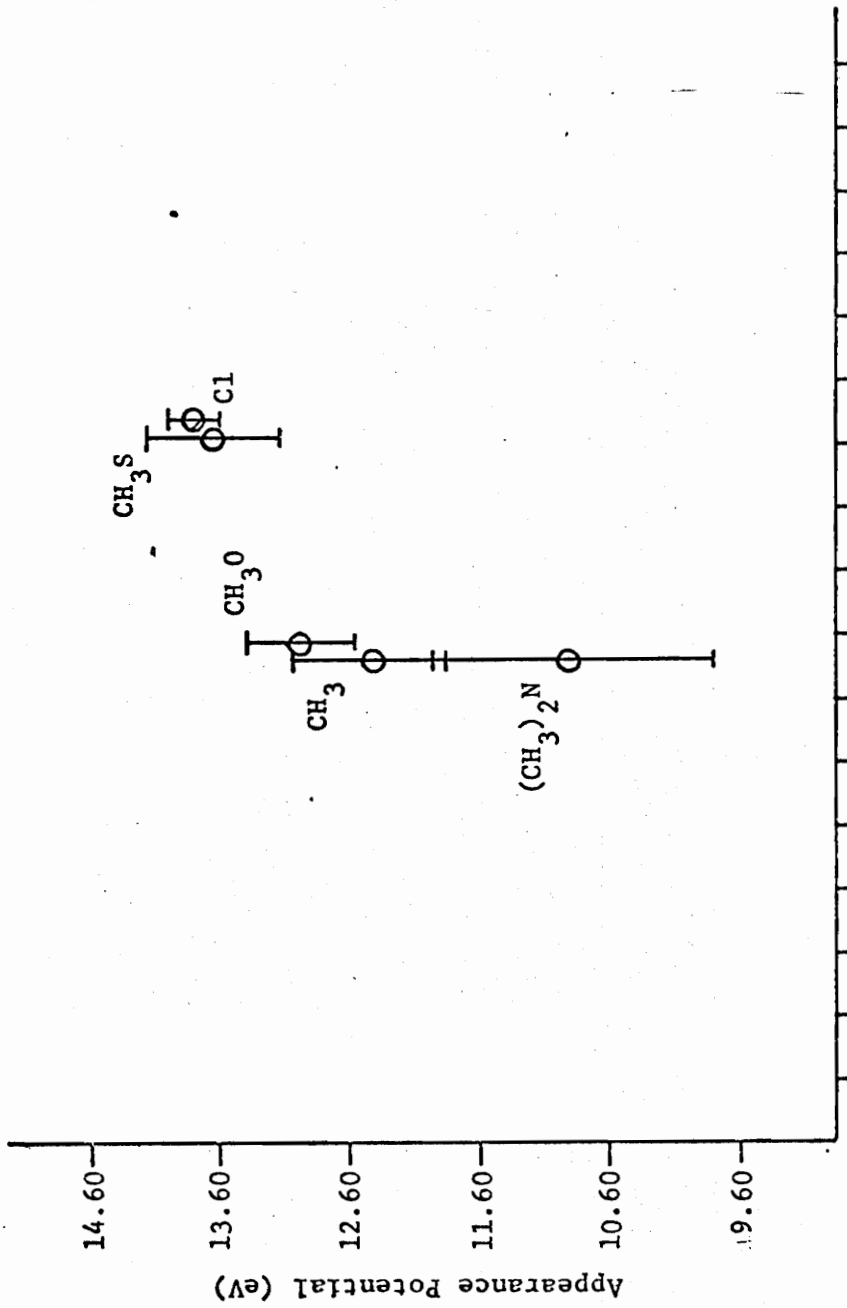

FIGURE 39. Appearance Potentials for Substituted Phenyl Ions from Monosubstituted Benzils vs. σ^I

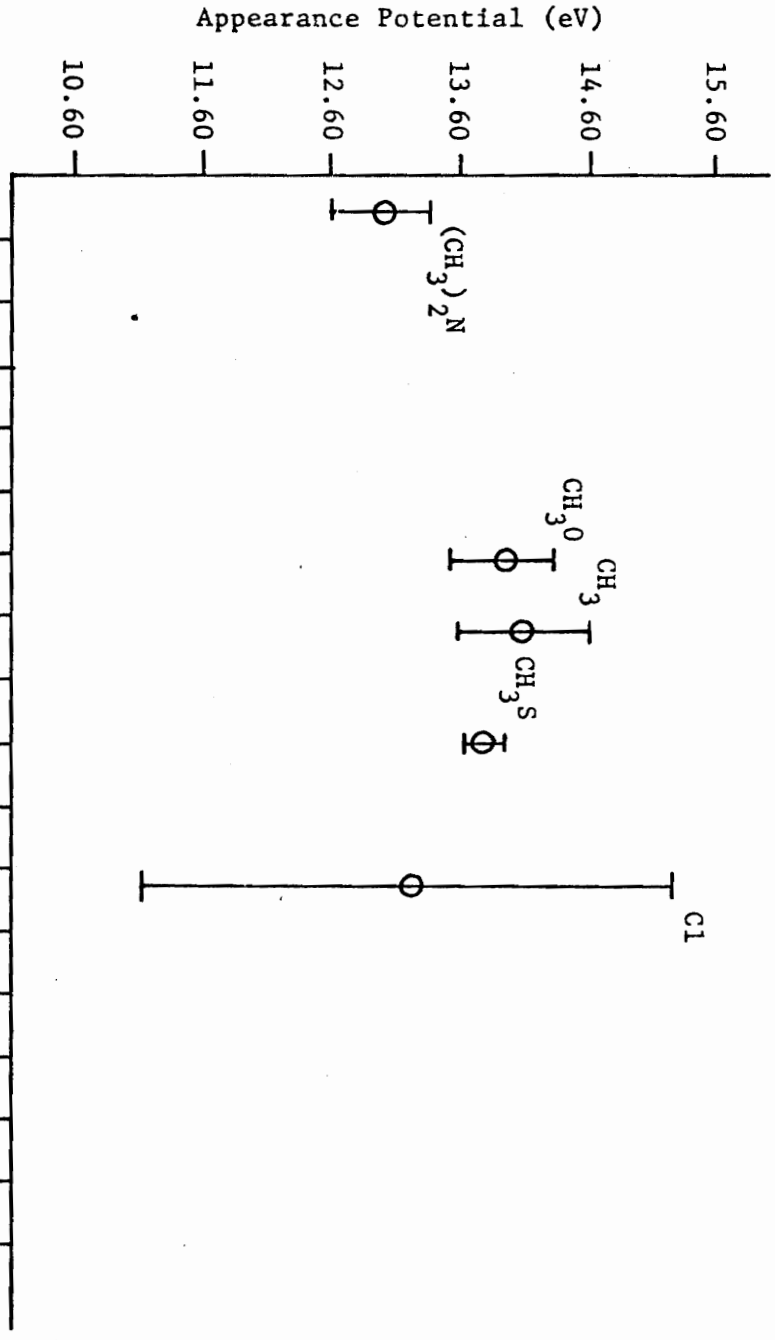

FIGURE 40. Appearance Potentials for Substituted Phenyl Ions from Disubstituted Benzils vs. σ

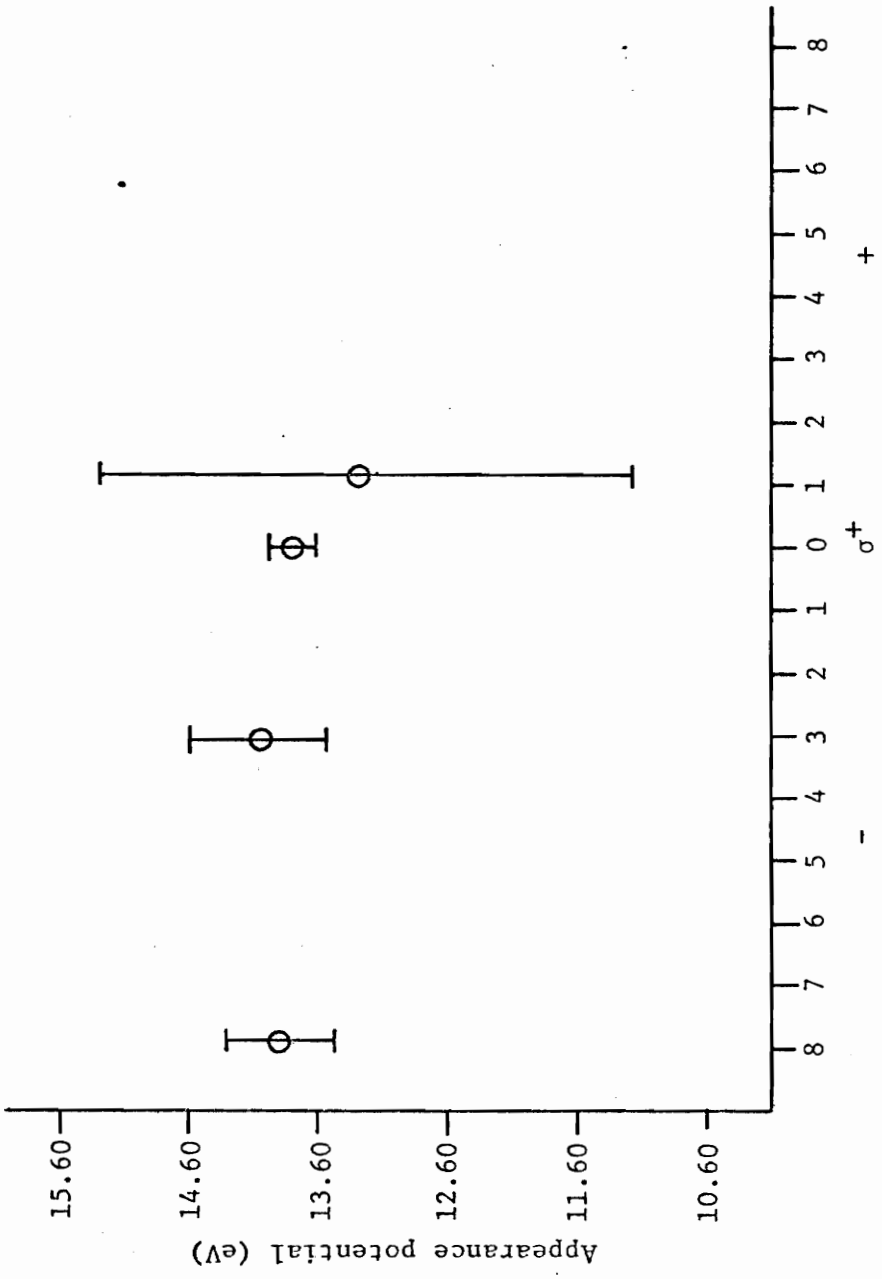

FIGURE 41. Appearance Potentials for Substituted Phenyl Ions from Disubstituted Benzils vs. σ^+

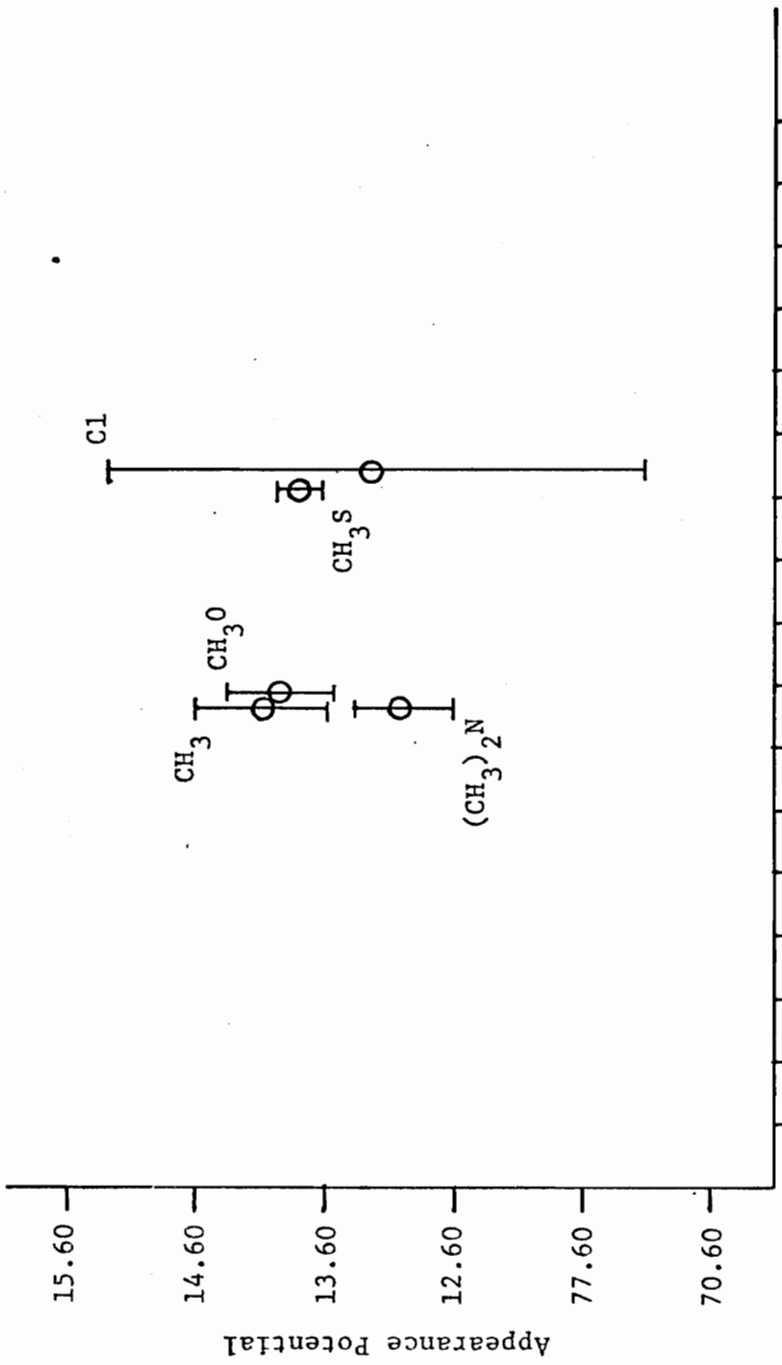

FIGURE 42. Appearance Potentials for Substituted Phenyl Ions from Disubstituted Benzils vs. σ_I

Einolf and Munson observed that "good data at low energies could be obtained only with a very clean source."[19] Variations resulting from differences in relative abundances were particularly perplexing when dealing with the 4-nitrobenzil and 4-dimethylaminobenzil. These compounds, as noted previously, demonstrate the extremes of electron withdrawing and electron donating substituents and, as a result, the ratios of substituted to unsubstituted benzoyl ions are the least and greatest, respectively. These ratios at low (15 eV) and high (50 eV) were visibly different on different occasions, and Einolf and Munson reported ratios of 0.007 and 215, respectively, for the relative abundances at 15 eV, and 0.037 and 11.6, respectively, at 70 eV. The result is that the ion with the greater electron withdrawing substituent appears in very low abundance, and the detectable lower limit of ion current is raised above the "true" appearance potential.

SECTION VI

POSITIVE ION ENERGETICS

B. DISCUSSION

A comparison of calculated, experimental, and literature values for the appearance potentials of the benzoyl and phenyl ions from benzil identifies a persistent problem in working with appearance potential data. At no time could the reported[33] values for the benzoyl and phenyl ions be reproduced. Considering the differences in source of chemicals, instrumentation, and techniques, some variation would be expected. Table 21 lists the differences between the calculated ionization potentials for the monosubstituted benzils and the calculated and experimental appearance potentials (experimental A.P. - calculated I.P.) for the benzoyls and substituted benzoyls produced. As can be seen, little discrepancy exists between these values for benzil and the data of Natalis and Franklin.[33] By any of the means used, the difference between the I.P. and A.P. of the benzoyl is near to 1 eV. Such agreement does not hold, however, for the phenyl ions. The value of Natalis and Franklin[33] is nearly a full eV higher than the calculated value which is, in turn, about 0.5 eV above the value found in these experiments. More importantly, the difference between the A.P. of the benzoyl and the A.P. of the phenyl varies greatly. From Table 22, it can be seen that the calculated difference of 3.46 eV is much lower than the reported difference of 5.42 eV.[33] In light of the differences observed with other benzils and the other reported values,[34] it appears that the reported value is too high and is the result of both the shape of the ionization efficiency curve and the detection limits of

TABLE 21

COMPARISON OF DIFFERENCES BETWEEN CALCULATED AND EXPERIMENTAL APPEARANCE POTENTIALS FOR THE PRIMARY FRAGMENT IONS FROM THE MONOSUBSTITUTED BENZILS AND THE CALCULATED IONIZATION POTENTIALS

SUBSTITUENT (R)	A.P. $C_6H_5CO^+$ - I.P. (eV)		A.P. $R\text{-}C_6H_4CO^+$ - I.P. (eV)	
	calculated	experimental	calculated	experimental
H	1.28	1.26	----	----
CH_3	1.27	2.17	1.28	1.59
Cl	1.29	1.02	1.29	1.11
NO_2	0.55	0.48	1.28	3.02
CH_3S	1.57	2.52	1.28	1.46
CH_3O	2.29 (3.51)[1]	3.03 (2.68)[1]	1.54 (1.19)[1]	2.18 (1.83)[1]
$(CH_3)_2N$	1.99	4.50	1.29	0.57

1. See Tables 14 and 15 for calculated I.P.'s.

TABLE 22

COMPARISON OF DIFFERENCES IN CALCULATED AND EXPERIMENTAL APPEARANCE POTENTIALS FOR THE SECONDARY FRAGMENTATION OF MONOSUBSTITUTED BENZILS

SUBSTITUENT (R)	A.P. ($C_6H_5CO^+$) - A.P. ($C_6H_5^+$)		A.P. ($R\text{-}C_6H_4CO^+$) - A.P. ($R\text{-}C_6H_4^+$)	
	calculated (eV)	experimental	calculated (eV)	experimental
H	4.03	3.46	----	----
CH_3	3.75 3.76	3.59	1.09	2.31
Cl	3.75 3.76	4.21	0.85	4.04
NO_2	3.75 3.83	5.12	----	----
CH_3S	3.75 4.26	3.75	1.14	3.70
CH_3O	4.11 2.94	4.47	2.03	3.44
$(CH_3)_2N$	3.77 4.17	2.41	1.54	2.37

the instrument, as will be discussed infra, p. 127.

Experimental agreement with the calculated and experimental A.P. values reported by Scheppele et al.[34] for the ions from 4-methylbenzil is actually closer than the listed values would indicate. While Scheppele[34] reported in his appendix a value of 9.98 eV for the A.P. of the benzoyl ion, this is qualified in the text by the statement that "(the SDIE curve) indicates no well-defined appearance potential..., (but) the value must be less than 10.86 eV..." Similarly, they report an SDIE curve for the phenyl ion "not inconsistent with an appearance potential of 13.95 $\pm$ 0.66 eV" and an ionization efficiency curve for the $C_7H_7^+$ ion which "starts to increase rapidly in the region 12.5 - 13 eV." No other published values for benzils are available.

Since no reliable measure of ionization potentials was possible, it is not possible to investigate directly the effect of mono- and di-substitution on the ionization potentials or to determine if ionization takes place at one site or one half of the molecule and is unaffected by substituents on the other half of the molecule. However, from the data in Tables 21 and 23, and from Figures 25 and 28, it can be seen that the appearance potentials of the benzoyl ions are apparently unaffected by the substituent on the other half of the benzil but that the substituted benzoyls: a) tend to have appearance potentials which are lower for electron donating substituents and higher for electron withdrawing substituents, b) vary little whether generated from mono- or di-substituted benzils. These conclusions are supportive of the proposition that substitution on one side of the carbonyl-carbonyl bond has little or no effect on appearance potentials for the other half of the molecule, that resonance

TABLE 23

COMPARISON OF DIFFERENCES IN CALCULATED AND EXPERIMENTAL APPEARANCE POTENTIALS FOR THE IONS FORMED IN THE PRIMARY AND SECONDARY FRAGMENTATION PROCESSES OF THE DISUBSTITUTED BENZILS

SUBSTITUENT (R)	A.P. ($R\text{-}C_6H_4CO^+$) - I.P.		A.P. ($R\text{-}C_6H_4^+$) - A.P. ($R\text{-}C_6H_4CO^+$)	
	calculated (eV)	experimental	calculated (eV)	experimental
CH_3	1.73 2.12	1.79	0.68-4.17	4.08
Cl	1.42 1.81	2.14	0.37-3.02	2.34
NO_2	2.06 2.43	1.91	----	----
CH_3S	0.58 0.98	0.50	2.03-3.33	4.50
CH_3O	0.36 1.94	0.96	0.00-5.71	4.22
$(CH_3)_2N$	2.89	2.13	0.42-3.36	4.33

forms which indicate initial ionization involving both sides of the molecule are of limited contribution, and that the ionization potential of the molecule is determined by the energy required to ionize the benzoyl half of the benzil with the more electron-donating substituent. Tables 21 and 23 which show the differences between the calculated ionization potentials and calculated and experimental appearance potentials of the substituted and unsubstituted benzoyl ions indicate that the difference between the I.P. and the lower A.P. is 2 eV or less. Extremely electron withdrawing substituents show the greatest differences between the I.P. and the A.P. of the substituted benzoyl. This is to be expected since the electron withdrawing substituent tends to destabilize the ion. The unsubstituted benzoyl ion from the same parent tends to appear at a voltage close to the parent I.P. Conversely, the electron donating substituents tend to stabilize the ion, and the A.P. of the stabilized benzoyl ion is close to the I.P. of the parent-molecule ion. Substituents which have little effect on reactivity in solution appear at the same excess energy as the unsubstituted analogues. Less predictable is the fact, apparent from Tables 21 and 23 and Figures 37 and 40, that the differences between the A.P.'s of the benzoyl ions and the A.P.'s of the phenyl ions which are their daughter ions is between 2.5 and 4 eV and not primarily dependent on the substituent. Therefore, the shape of the ionization efficiency curve for a phenyl or substituted phenyl ion observed in the spectrum of a benzil is not an a priori thermodynamic property but, rather, is dependent on the precursor ion's ionization efficiency curve. Since, as it was observed in the discussion of the relative abundances of benzoyl ions in Section V, the ratio of abundances is also a

function of the substituent, then the limit of detectability of a secondary fragment becomes the limiting factor in determinations of their appearance potentials. Slight changes in the electron energy spectrum will then have an exaggerated effect on the ratios of abundances, as was observed by Einolf and Munson,[19,22] and on the slope of the ionization efficiency curve.

The assumption in any application of the Hammett equation is that the thermodynamic product and the kinetic product should be the same. With simple systems, this is normally true as was demonstrated by McLafferty[5,13,17,20] and for the benzophenone system by Einolf and Munson.[19] The benzil system is more complicated since McLafferty-type plots do not correlate well with σ^+ as might be expected based on the benzophenones and only poorly with σ.[22] Einolf and Munson[22] ascribe this poor correlation to the hypothesis that the benzoyl ions formed from benzils have greater excess energy than those formed from systems in which the resulting benzoyl can interact with the rest of the molecule (i.e., benzophenones). This hypothesis is opposite to that of McLafferty[90] who postulated that a substituent which lowers the ionization potential will also lower the average energy of the molecular ions (the I.P.'s of benzils are ca. 0.6 eV lower than for the corresponding benzophenone). The hypothesis is supported by the low relative abundances of the parent-molecule ion, by the slow rise of the ionization efficiency curves indicating the need for excess energy for ion formation, and by the large A.P. differences between benzoyl and phenyl ions and the broad, flat-topped metastable peaks observed for their transitions. The conclusion must be that at energies greater than the A.P. of the lowest (substituted

or unsubstituted) benzoyl, the ratios of the ionic abundances are controlled by the kinetics of the competitive reactions. Scheppele et al.,[34] after an analysis of the SDIE curves, concluded that the 4-methyl substituent "exerts a dominant influence on the kinetics of competitive cleavage of the (carbonyl-carbonyl) bond in molecules possessing up to 5.0 - 5.5 eV of internal energy." However, they found that at 20 - 70 eV, the ratio of benzoyl to substituted benzoyl ions "bears no simple relationship to the effect of a methyl group on the kinetics of dissociation...." The appearance potential of a fragment, but most significantly, a secondary fragment is, therefore, difficult to measure because the number of ions formed depends not only on the energy needed to break certain bonds, but on the probability that specific bonds will break at a certain rate relative to others. The ionization efficiency curve does not rise linearly from a certain value, but irregularly as the probability of formation increases, then decreases as further fragments become thermodynamically possible and kinetically probable. The resultant slow and irregular rise observed for the secondary fragments of the benzils is in concert with Scheppele's[34] observation that the "C_7H_7 ionization efficiency curve should approach the energy axis asymptotically." At the extremes of substituent character, where the differences in A.P.'s become great, the Hammett plots begin to break down because the average energy of the parent, following McLafferty's hypothesis,[90] becomes the controlling factor. As a result, the Hammett plots of appearance potentials give good correlations only for the lower energy ions formed by primary fragmentation, and plots of the appearance potentials of secondary fragments have a slope determined by the shape of the curve of the primary fragments,

regardless of calculated values. The plots support the assertion of Bursey[13] and Natalis[33] that the benzoyl ions are formed from the ground state parent-molecule ion, but that the phenyl ions are formed from an excited benzoyl ion.

Correlations with σ do not appear to be better than those with σ^+, but no correlation with σ^I can be justified. This indicates that resonance is an important factor in determining the stability of the benzoyl ion, and the lack of an effect on the parent-molecule ion indicates that the configuration is probably skew.

Natalis and Franklin[33] indicate the following process for the formation of the phenyl ion from benzil:

$$C_6H_5COCOC_6H_5 \longrightarrow C_6H_5^+ + C_6H_5 + 2\ CO?$$

Metastable data presented supra, as well as the data of Scheppele et al.[34] and the A.P. data in all work done on the system, indicate that the phenyl ion must come from a benzoyl. Whether the radical formed in the first fragmentation step also loses CO at a later time is not evident from the data. If the conclusion of Solly and Benson[89] is correct that para substituents do not affect the stability of benzoyl radicals, the effect of the substituents would be the same in all examples, and the energy required for loss of CO by the radical would not be detectable by differences, but would be the same for all benzils. This appears to be borne out in Tables 22 and 23. No high pressure experiments were performed to determine if the possibly formed CO is involved in subsequent ion molecule reactions or if it could be reionized.

As would be expected from the spectra of the nitro-substituted benzils and from Tables 12 and 13 which list the major ions formed and

their precursors, nitro substituents cause anomalies. The primary difference between nitrobenzils and other benzils is the competition between the pathways for fragmentation seen in other benzils and the pathways involving loss of NO. A low but identifiable ion current for the ion corresponding to the loss of NO• from the parent-molecule ion is observed at less than 11 eV, which, in the absence of other effects may fragment in the normal pattern, and especially deplete the available substituted fragments in the spectrum of 4-nitrobenzil. In addition, no nitrophenyl ion is observed since the competing reaction, loss of NO is preferential to loss of CO. This is not unexpected since the nitrophenyl ion would be expected to occur at relatively high energy, ca. 16 eV, and the loss of NO is apparently a process with low energy of activation.

It is not possible to identify one factor as being the driving force in determining product ion formation or distribution, a simplification which is at the heart of any linear free energy correlation. The factors responsible for the stability of the product ion are also the factors which determine the I.P. (especially when there is no interaction across the carbonyl-carbonyl bond), but their relationship to the total excess energy and the excess energy in each fragment is less clear. As a result, McLafferty-type plots, which presume a simple relationship between substituent and ionic ratios, do not correlate well.

SECTION VII

NEGATIVE ION SPECTRA

RESULTS

The negative ion spectra of the benzils are much simpler than the positive ion spectra. All benzils studied formed a parent-molecule ion. Benzil, the methyl-substituted benzils, and the dimethylamino-substituted benzils formed only the parent-molecule ion. The methoxy- and methylthio-substituted benzils formed a second negative ion by loss of a methyl group from the parent. No CH_3^- or CH_2^- ions were detectable within the limits of the experiments indicating that if such ions are formed, they have an abundance less than 1% of the parent and are, therefore, the products of a highly unfavored process. The chlorobenzils produce Cl^- ions in addition to the parent-molecule ion but no ion corresponding to the parent less Cl. The nitro-substituted benzils are the only benzils to form more than one fragment ion. The spectrum of 4-nitrobenzil is shown in Figure 43. The ions formed by decomposition of the parent-molecule ion are an ion corresponding to the loss of NO• from the parent and NO^-, but no NO_2^-. The ion at m/e 120, which has a very low abundance relative to its positive analogue (cf. Table 12), is the only indication of a cleavage between carbonyls that was found in the negative ion spectra, and no ion at the same mass is found in the spectrum of 4,4'-dinitrobenzil. No metastables were detected in any of the negative spectra, although the high noise levels incident to high amplitude scans may be covering metastables. A complete listing of the negative ions for which appearance potentials could be determined is found in Table 24.

TABLE 24

NEGATIVE IONS AND APPEARANCE POTENTIALS FOR BENZILS

COMPOUND R_1	COMPOUND R_2	ION	A.P. (eV) i.e.c.[1]	A.P. (eV) van.	A.P. (eV) cur.[2]
H	H	$C_6H_5COCOC_6H_5^-$	0.04	0.00	
H	CH_3	$C_6H_5COCOC_6H_4\text{-}CH_3^-$	0.08	0.00	
CH_3	CH_3	$CH_3\text{-}C_6H_4COCOC_6H_4\text{-}CH_3^-$	0.09	0.00	
H	$(CH_3)_2N$	$(CH_3)_2N\text{-}C_6H_4COCOC_6H_5^-$	0.12	0.02	
$(CH_3)_2N$	$(CH_3)_2N$	$(CH_3)_2N\text{-}C_6H_4COCOC_6H_4\text{-}N(CH_3)_2^-$	0.00	0.00	
H	CH_3O	$C_6H_5COCOC_6H_4\text{-}OCH_3^-$	0.09	0.00	
		$C_6H_5COCOC_6H_4\text{-}O^-$	(3)	0.75	
CH_3O	CH_3O	$CH_3O\text{-}C_6H_4COCOC_6H_4\text{-}OCH_3^-$	0.09	0.00	
		$CH_3O\text{-}C_6H_4COCOC_6H_4\text{-}O^-$	1.08, 4.70	1.00	
H	CH_3S	$C_6H_5COCOC_6H_4\text{-}SCH_3^-$	0.03	0.03	
		$C_6H_5COCOC_6H_4\text{-}S^-$	1.30	0.93	
CH_3S	CH_3S	$CH_3S\text{-}C_6H_4COCOC_6H_4\text{-}SCH_3^-$	0.06	0.03	
		$CH_3S\text{-}C_6H_4COCOC_6H_4\text{-}S^-$	0.44	0.30	
H	Cl	$C_6H_5COCOC_6H_4\text{-}Cl^-$	0.38	0.00	
		Cl^-	4.52	2.20	(4)
Cl	Cl	$Cl\text{-}C_6H_4COCOC_6H_4\text{-}Cl^-$	1.73	0.79	
		Cl^-	4.40	2.20	(4)
H	NO_2	$C_6H_5COCOC_6H_4\text{-}NO_2^-$	0.10	0.00	
		$C_6H_5COCOC_6H_4\text{-}O^-$	2.58	1.80	
		NO^-	6.40	5.50	(4)
NO_2	NO_2	$NO_2\text{-}C_6H_4COCOC_6H_4\text{-}NO_2^-$	0.45	0.00	

TABLE 24 (continued)

COMPOUND R_1	COMPOUND R_2	ION	A.P. (eV) i.e.c.[1]	A.P. (eV) van. cur.[2]
NO_2	NO_2	$NO_2\text{-}C_6H_4COCOC_6H_4\text{-}O^-$	1.42	1.01
		NO^-	6.35	5.45

(1) Determined by comparing the center of the ionization efficiency curve with that of SF_6^-.

(2) Determined by the vanishing current method, relative to SF_6^-.

(3) No difinitive value. Peak is 4.2 eV wide at half height. See text.

(4) Approximate value. Curve rises slowly and erratically.

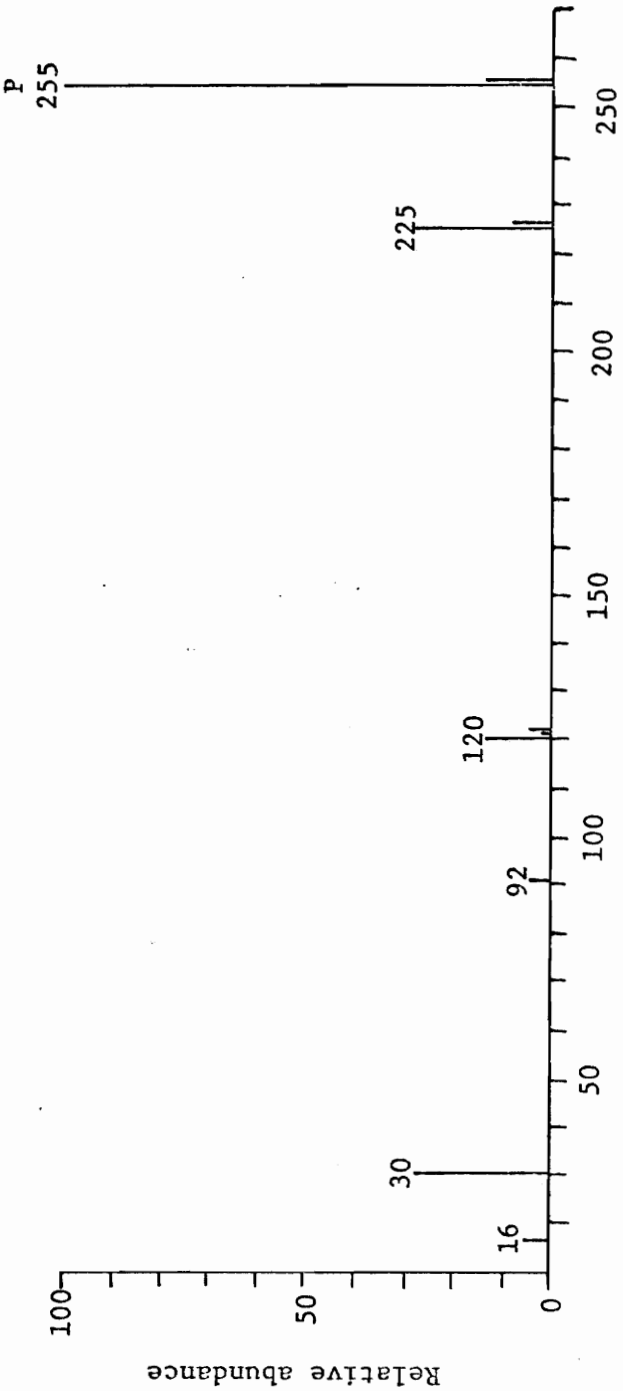

FIGURE 43. Negative Ion Mass Spectrum of 4-Nitrobenzil

SECTION VIII

NEGATIVE ION ENERGETICS

A. RESULTS

Table 24 lists the ions found and their appearance potentials as determined by measuring the voltage at maximum ion current (Column 2) and by the vanishing current method.[90] Considering the inherent errors in determining the apex of a rounded peak of relatively low intensity, the precision in determinations by the former method is no greater than 0.1 eV. The vanishing current method is slightly more accurate for ionization efficiency curves of well-defined shape, but for curves with distorted shape or erratic foot regions the reproducibility becomes a function of the operator's technique, and accuracy may be no greater than 0.5 eV. The vanishing current method is most useful in establishing onset voltages for ionization efficiency curves which are the summation of several curves corresponding to different processes or transitions.

The small differences in the appearance potentials of the parent-molecule ions are within the range of experimental error and are not of any significance, except that it should be noted that the values obtained by measuring the value at the maximum ion current are identical to those obtained by the vanishing current method for most benzils studied but higher for the chloro- and nitro-substituted benzil parent molecule ions and for all fragments. This difference represents a difference in the width of the ionization efficiency curve. The shape of the ionization efficiency curves for all parent-molecule ions except the chloro- and nitro--substituted compounds was found to be approximately Gaussian and

0.6 to 0.7 eV wide at half-height, or 0.1 to 0.2 eV wider than the SF_6^- electron capture curve. This is about 0.5 of the width reported by Christophorou et al.[50] for the benzil parent-molecule ion, and the maxima are at considerably lower voltages; cf. Figure 1. The shapes of the curves obtained by Christophorou[50] for both SF_6^- and benzil indicate conditions in their time of flight equipment analogous to those in the RMU-7 if a very high filiment current is used (i.e., a broad energy spectrum for the incident electron beam). The curves obtained for the chloro- and nitro-substituted benzils are broader than those for the other benzils' parent-molecule ions, and the result is that the maximum is offset to higher energies despite an onset at or near that of SF_6^-. The instrumental instability noted previously which occurred upon the introduction of chloro-substituted benzils was observed in the negative ion spectra as well, and accounts in part for the higher and erratic values obtained for these compounds.

The fact that the parent-molecule ion appears at both low energy and at 50 eV can be explained by the comment of Todd[36] that the appearance of parent-molecule ions in the 70 eV spectra can be accounted for "in terms of the existence of slow-moving secondary electrons produced during positive ion formation or emitted from electrode surfaces." The exact distribution of these secondary electrons is clearly a function of both the pressure in the source and the partial pressures of the various molecules in the source. No attempt has been made in this study to analyze the energy distribution in the source in terms of source pressure or to characterize the effects of other instrumental parameters, including source optics and the condition of the metal surfaces within the source, on the

energy spectrum within the source. Experimentally, it was observed that after the electron energy for resonant capture had been exceeded, there was no detectable ion current until the electron energy had been raised into the energy region corresponding to the ionization potential for the positive parent-molecule ion. This supports the hypothesis that the parent-molecule ions observed at higher energies in the benzil spectra are, indeed, the result of secondary electron capture. The logical corrolary of this hypothesis is that the ion current for any ion is less at nominal 50 eV than at the capture resonance peak, and this is the case for the benzils, with ion currents at nominal 50 eV approximately 5 to 25% of the resonance capture ion current, depending upon the extent of fragmentation.

The relative abundances of particular ions in the negative ion mass spectrum are, therefore, of little analytical utility without an analysis of the energy spectrum in the source at the time of measurement. Figure 44, which depicts the classical analysis of ion current versus electron energy for fragment ions, must be interpreted carefully since secondary electrons are capable of producing fragment ions by dissociative attachment as well as parent-molecule ions by electron capture. The electron energy, i.e. the x-axis, must be understood as the energy of the electron actually impinging upon the molecule. At energies above approximately 10 eV, ion-pair processes <u>may</u> occur in the region labeled II. The curve shown in Figure 44 is generated experimentally, albeit with a lesser intensity for that part labeled II, when one reads the x-axis as the electron energy as measured by potentiometer voltage. In such cases, the current read at higher voltages is not the result of an ion-pair process,

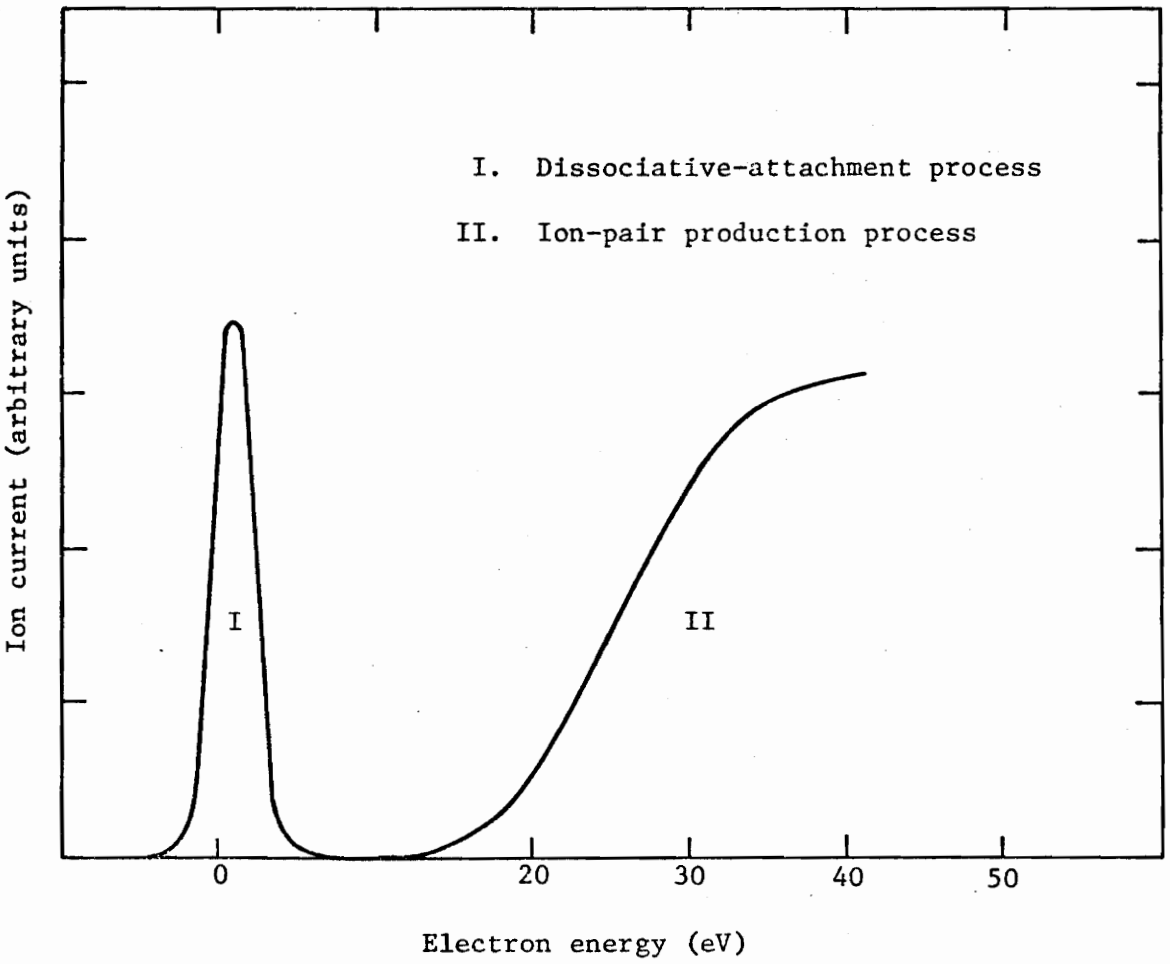

FIGURE 44. Classical Efficiency Curves for the Production of Negative Fragment Ions

but of secondary electron capture, followed by dissociation, i.e. dissociative attachment. Therefore, ion-pair processes cannot be presumed from the appearance of an ion at higher energies as measured by electron accelerating voltages. Appearance potentials for the positive and negative ions of the same m/e must be demonstrated to within ± 1 eV or closer before ion-pair processes can be presumed.

When ions other than the parent-molecule ions were present in the negative ion spectrum, several generalizations could be made. First, the ionization efficiency curve at low energies, presumably indicating a dissociative-attachment process, was found to be broader than the curve for the parent-molecule ion as indicated by the differences in appearance potential as determined by the two methods used. Second, the electron energy at which the ion appeared may serve as an indication of ionic stabilities and the number of available excited states. Third, the ions formed (and not formed) give an indication of the types of structures which are amenable to analysis by negative ion mass spectrometry. Specifically, the ions formed and the energies at which they are formed may indicate the mechanisms for rearrangement or fragmentation and why other mechanisms do not take precedence.

The breadth of the ionization efficiency curves for fragment ions cannot be explained in terms of the inhomogeniety of the electron beam. Increased breadth in the order of 0.5 eV might be so explained, but breadth at half-height of three to six times the breadth of the resonance capture peak of the parent-molecule ion can be explained only by more significant differences. The rise of the ionization efficiency curves for most fragment ions is only slightly slower than the rise for SF_6^- or for the

parent-molecule ion. Rather, the increased breadth lies in the range of voltages in which the ion current is at least 80% of the maximum current for the ion, giving a round or even flat top. The curve for the ion $C_6H_5COCOC_6H_4\text{-}O^-$ derived from 4-methoxybenzil is shown in Figure 45. The curve is 4.2 eV wide at half-height and shows no discernable peak, but rather a nearly flat top with a slight valley near the middle of a nearly 3.0 eV wide top.. The analogous ion, $CH_3O\text{-}C_6H_4COCOC_6H_4\text{-}O^-$, generated by presumably the same process from 4,4'-dimethoxybenzil, exhibits the same character, with more nearly defined maxima at 1.08 eV and 4.70 eV, as shown in Figure 46. The other fragment ions observed do not show such clear-cut divisions of their ionization efficiency curves, but all are quite broad. Fragment ions with high appearance potentials and relatively lower abundances, such as Cl^- and NO^- ions, tend to have erratic shapes in the region of the foot of the curve, as seen in Figures 47 and 48, and are less accurately measured by the vanishing current technique. The curves are, however, bell-shaped, and clear separation into two processes is not apparent.

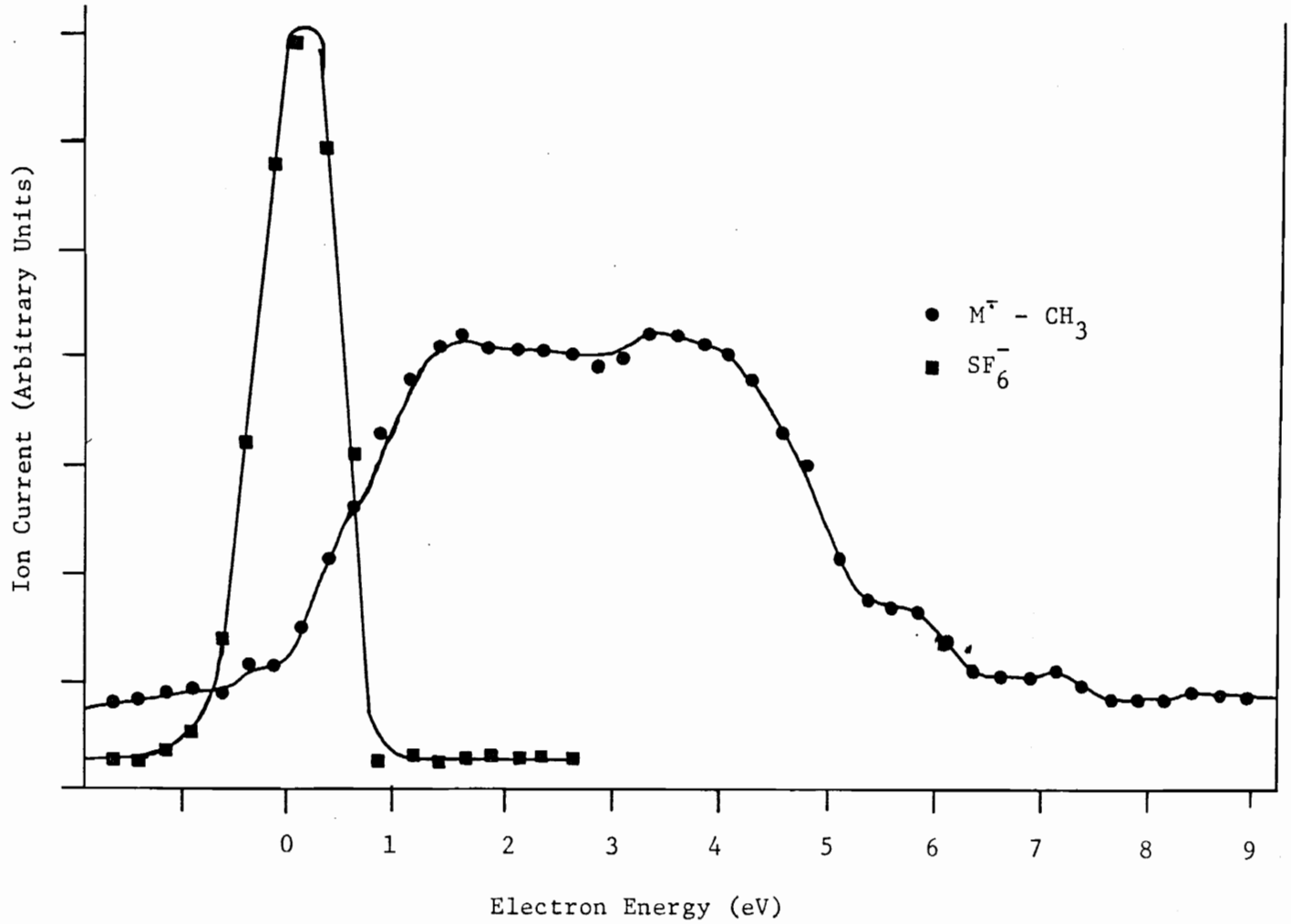

FIGURE 45. Ionization Efficiency Curve for $C_6H_5COCOC_6H_4\text{-}O^-$

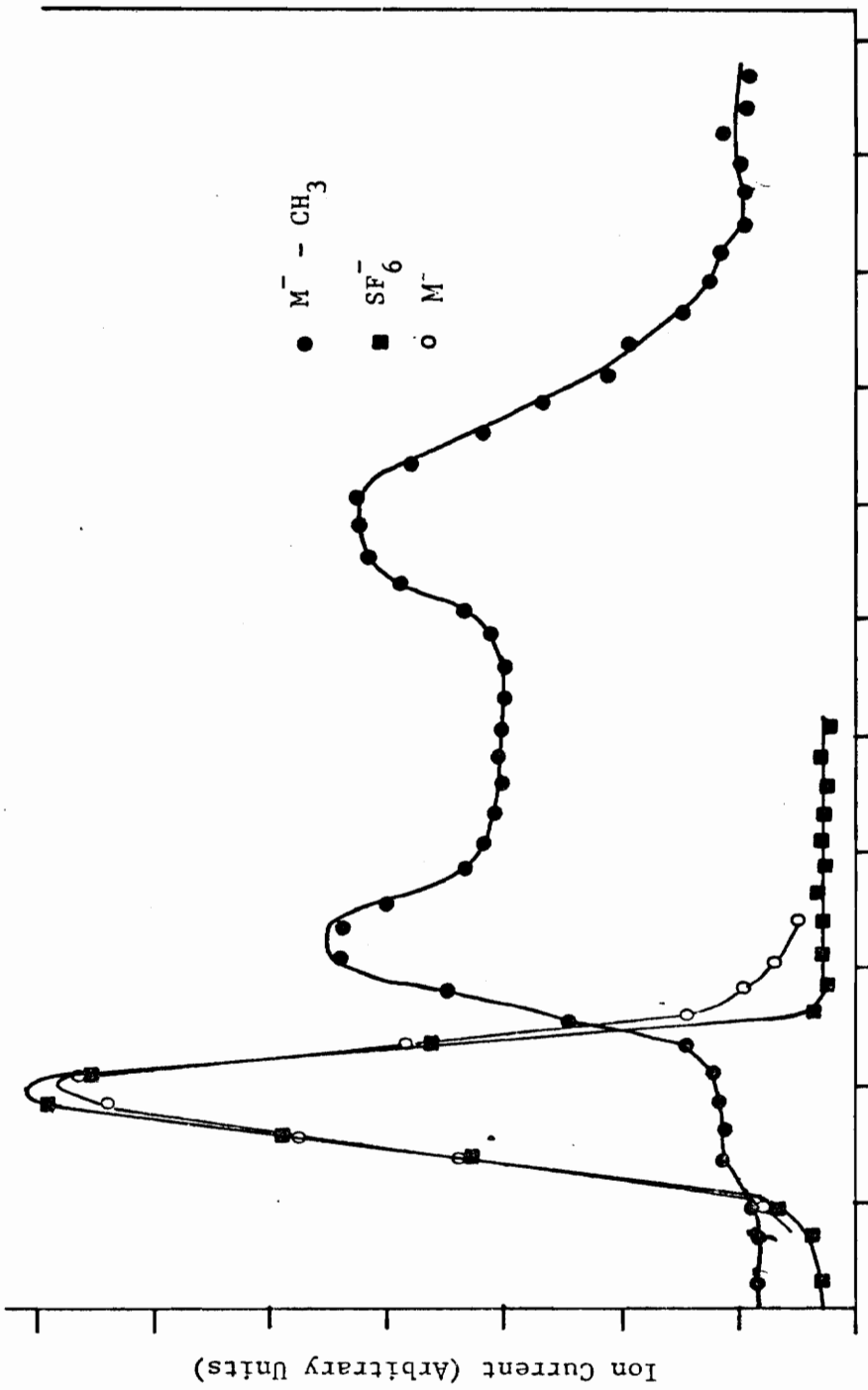

FIGURE 46. Ionization Efficiency Curve for $CH_3O\text{-}C_6H_4COCOC_6H_4\text{-}O^-$

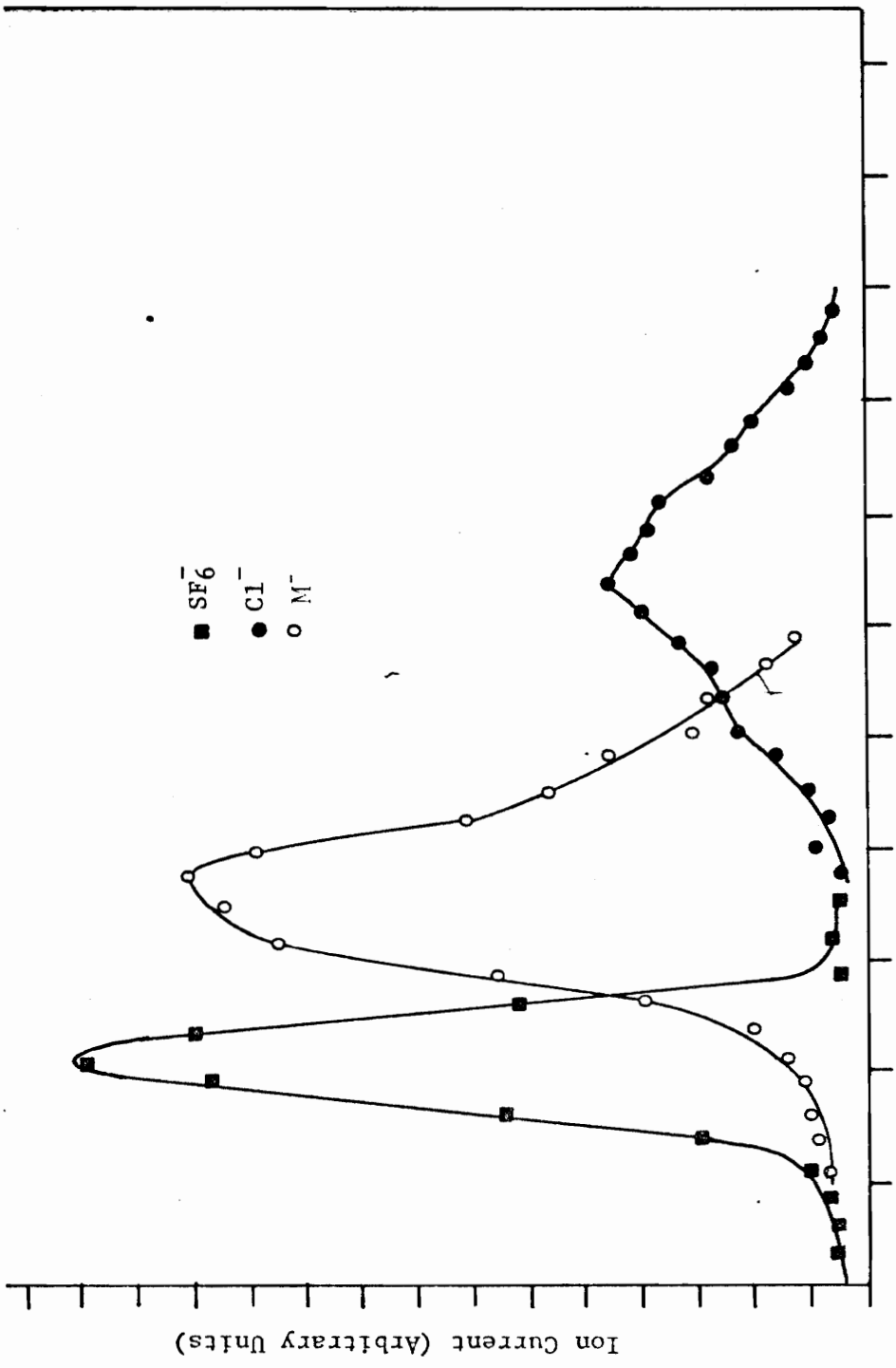

FIGURE 47. Ionization Efficiency Curve for Cl^-

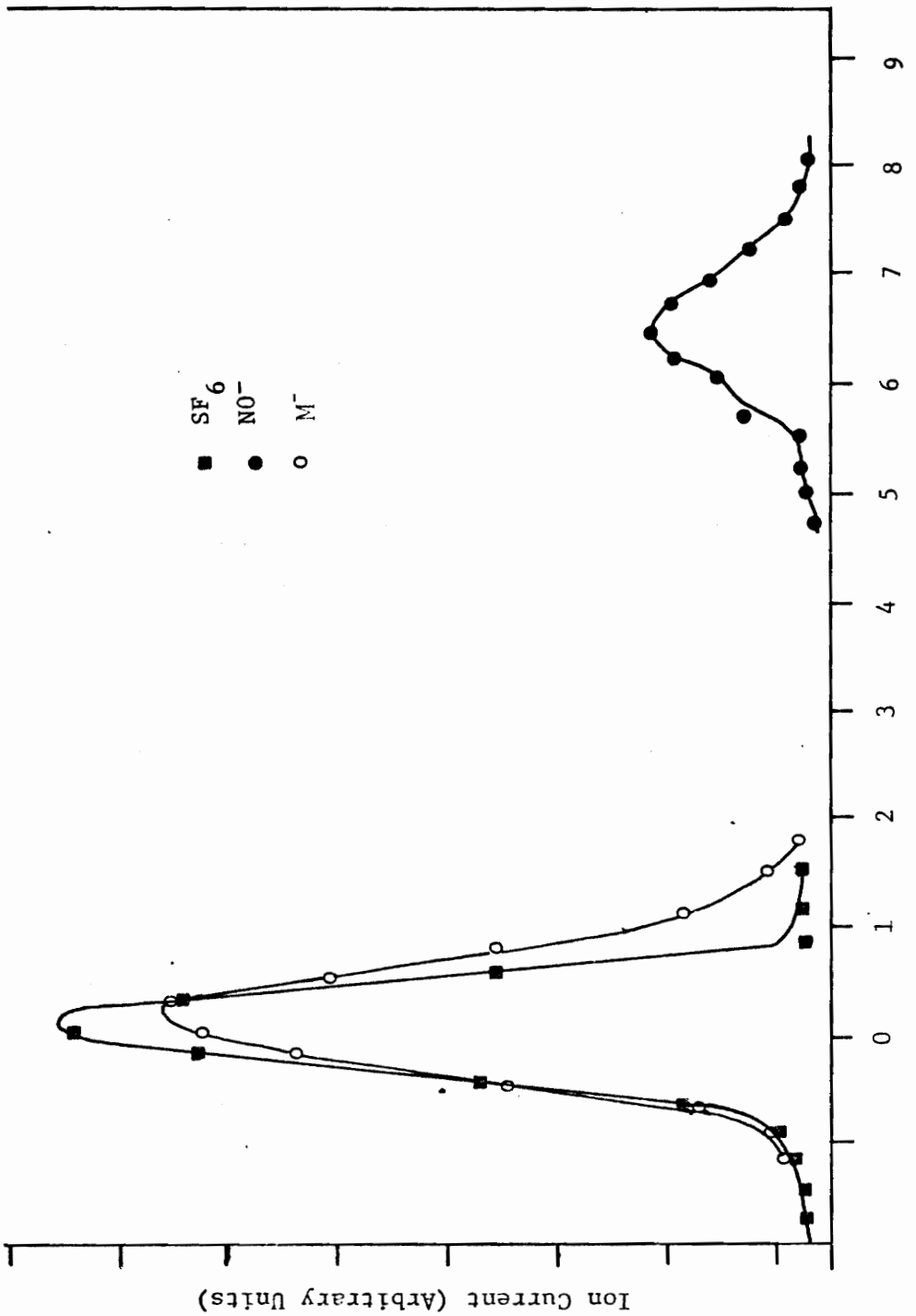

FIGURE 48. Ionization Efficiency Curve for NO^-

B. DISCUSSION

As indicated in the results section, the process for the formation of the parent-molecule ions at both low and nominally 50 eV energies is undoubtedly electron capture, presumably into an orbital which localizes the electron at the carbonyl or over the benzoyl portion of the molecule for the benzils with neutral or electron-donating substituents, since the shapes of the ionization efficiency curves and the appearance potentials are unaffected by the substituents. All fragment ions appear to be formed by dissociative-attachment.

The shapes of the ionization efficiency curves for the fragment ions indicate that the process of fragmentation must be pictured, at least formally, as being made up of two stages. It is surmised that the first step involves electron capture by the parent molecule. Since the substituent does not appear to affect the resonance capture potential, the parent-molecule ion is best depicted by a resonance form which places the odd electron at or near the carbonyl. (The benzils with electron-withdrawing substituents may be exceptions to this hypothesis). Subsequent decomposition then occurs in accordance with the rules cited by Todd.[36] Bowie and Ho[91] found that the anthraquinone esters fragment to lose the alkyl radical according to the process,

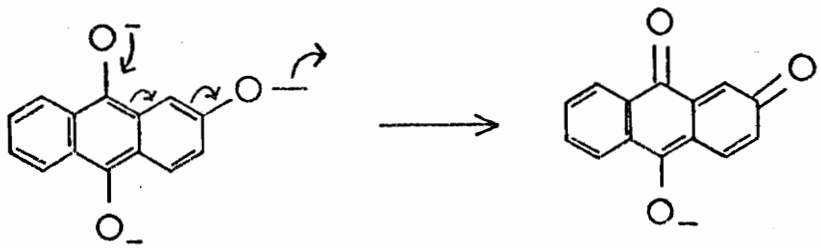

which is also formally pictured as beginning with the odd electron on a carbonyl and which leads to a structure which allows stabilization of the ion by coupling of electrons. Since the ion observed corresponds to the loss of a moiety at least a phenyl group away from the presumed locus of capture, at least one and perhaps several excited states (or M.O's) must be available for this process to occur. The availability of these excited states is reflected in the breadth of energies over which the fragment appears with significant ion current.[92] Unfortunately, no metastables were observed by which the excess energy could be verified or measured. The occurrence of structural, or at least geometric changes in the excited molecule, cannot be discounted. The curves for the methoxy-substituted benzils' fragments with two overlapping curves apparently being added together to give the observed curve could be explained either by the availability of two distinct energy levels or by the existence of two geometrically distinct excited structures. Bowie and White[93] proposed that the loss of $CH_3^{\bullet}$ from stilbenes could be explained by two mechanisms, but the systems are not directly relatable. The loss of $CH_3^{\bullet}$ by the methylthio-substituted benzils must follow a mechanism similar to that of the methoxy-substituted benzils, but the breadth of the ionization efficiency curves is notably less indicating either fewer pathways or less differentation between them. Since thiophenol is a stronger acid than phenol,[94] the sulfide anion is more easily stabilized than oxygen analogue.

The fact that the only ions observed as the result of fragmentation result from the loss, cleavage, or rearrangement of the substituent indicates that the product structure and appearance potential are

determined by the stability of the product ion, apparently with little regard for the effect of the substituent upon the stability of the parent-molecule ion. This is in direct contrast with the observations on positive ions and with McLafferty's[90] postulations on positive ions, but in accord with Solly and Benson's[89] observation that "Resonance structures in which the unpaired carbonyl electron is conjugated with a phenyl ring make no contribution to the stability of the benzoyl radical." The appearance potential of a negative fragment becomes, at least in part, a measure of the energy required to achieve coupling of the unpaired electron with some other electron in the system or, alternately, the energy required to generate another unpaired electron with which the odd electron might couple,[36] thereby satisfying Bowie's comment[46] that even-electron anions are the more stable.

The anomalous fragmentation patterns of all the nitro- and chloro-substituted benzils, and the comparatively high appearance potentials of the dinitrobenzil and dichlorobenzil parent-molecule ions, may also be explained by the assumption that for these compounds fragmentation is not consequent upon capture of an electron at the carbonyl site as is presumed for the other benzils studied. The benzils with electron-donating, neutral, or weakly inductively electron-withdrawing substituents all have the same appearance potential, and the assumption that electron capture is into an orbital overlapping the carbonyl seems justified. The higher appearance potentials for the dinitrobenzil and the dichlorobenzil parent-molecule ion and the shapes of their ionization efficiency curves may be indicative of capture at another dipolar site at or near the substituent. If this be true, then Bowie's assumption[47] that the

rearrangement on the nitro-substituted compounds begins with the odd electron situated on an oxygen of the nitro group (cf., p. 10) is more easily rationalized.

Christophorou et al.,[95] studying the negative ion lifetimes of a number of nitrophenols and nitroanilines, concluded that the "whole molecule and not only the NO_2 group participates in the capture of the [thermal] electron," based upon results of compound negative ion resonance experiments. However, in describing the stabilization of the ion, they assert that "The NO_2 group lowers the energy of the benzene ring due to charge migration from the ring to the nitro group ('inductive effect'). In non-cyclic compounds, the electrophore may be a functional group comprised of only a part of the polyatomic molecule."

The breadth of the ionization efficiency curves for the chloro- and nitro-substituted compounds may be due to the availability of two capture sites and not merely a different shape for the alternative site. The curves shown by Christophorou[95] for the nitrophenols and nitroanilines closely trace the SF_6^- curve. The other alternative may be that the odd electron is resonance stabilized. Christophorou[95] did not report the loss of NO·, only the loss of NO_2. This suggests that resonance stabilization of the product, analogous to the loss of CH_3· from methoxy-substituted benzils, is the driving force in fragmentation and, indubitably, present also in stabilization of the parent-molecule ion in spite of Solly and Benson's comments to the contrary.[89] The 4,4'-dichlorobenzil, in which the mesomeric effect is toward destabilization of the ion, is the only parent-molecule ion for which neither method of measurement affords a 0 eV appearance potential. Apparently, inductive effects of a substituent

have no effect on the stability of benzoyl radicals in the gas phase, but mesomeric effects have a pronounced effect.

The ions $C_6H_5COCOC_6H_4$-O, NO_2-$C_6H_4COCOC_6H_4$-O and NO appear in both positive and negative spectra of 4-nitrobenzil and 4,4'-dinitrobenzil, and the ion pair process,

$$C_6H_5COCOC_6H_4\text{-}NO_2 \begin{cases} \longrightarrow NO^+ + C_6H_5COCOC_6H_4\text{-}O^- \\ \longrightarrow NO^- + C_6H_4COCOC_6H_4\text{-}O^+ \end{cases}$$

could be used to explain their formation. The energies at which the negative ions are formed, however, are too low to justify an ion pair process, being at least 2 eV below the A.P. of the positive parent-molecule ion. The same conclusion was reached by Todd et al.[96] for nitro-substituted naphthalenes. This does not mean, however, that similar radical mechanisms are not involved. Figures 49 and 50 indicate two analogous mechanisms, one from a positive parent, the other from a negative parent, which would result in the generation of identically structured ions of different charge by the expulsion of NO• subsequent to a rearrangement. The formation of NO^- is probably the result of a variation in the penultimate step in the process shown and is obviously not a highly favored step. The final products of the favored steps are resonance stabilized which not only accounts for the lack of NO_2^- in the spectrum, but also for the lack of further fragmentation of the daughter ion.

The chloro-substituted parent-molecule ions, which cannot fragment to yield a stabilized derivative of the parent, can achieve electron pairing only by formation of the stable Cl^- which is the only observed fragment ion. The result is similar to that observed by Ito et al.[97] for the spectra of n-alkyl chlorides, wherein the Cl^- ion was the major fragment ion.

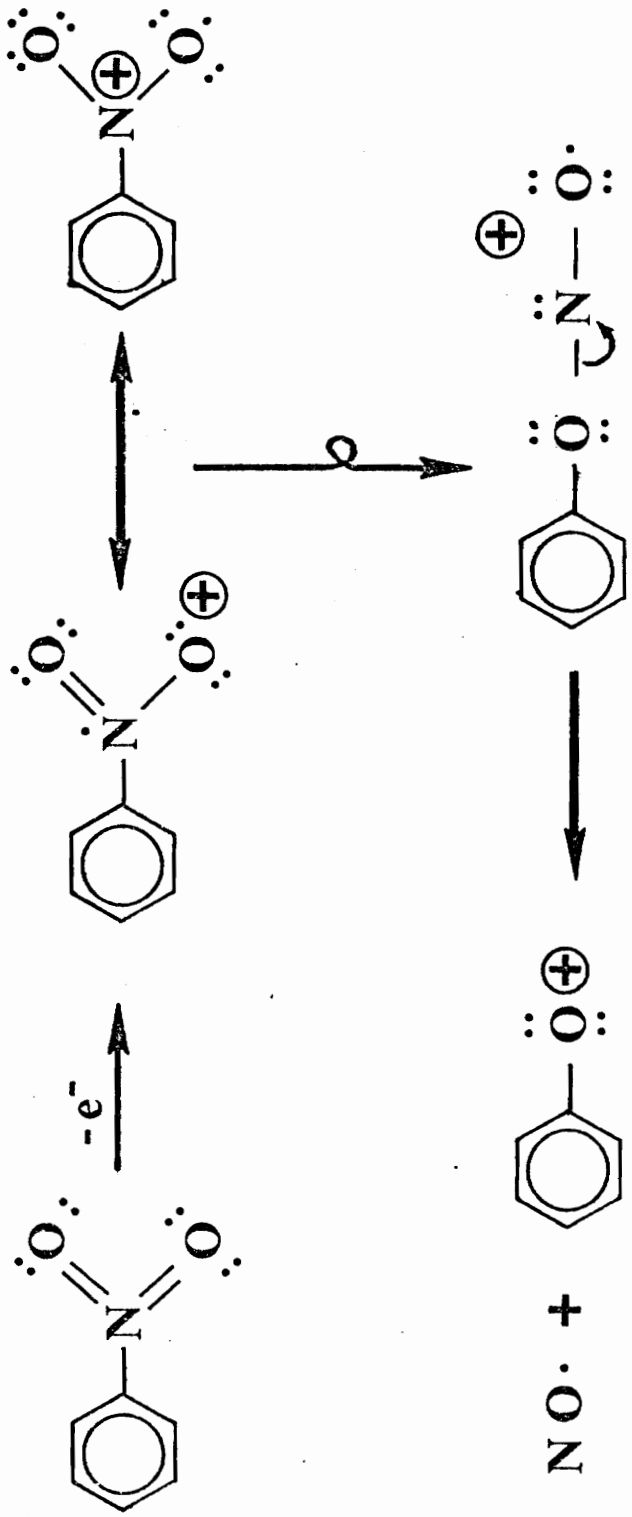

FIGURE 49. Rearrangement Mechanism for NO_2-substituted Aromatics: Positive Ions

Adapted from J. H. Bowie, Org. Mass Spectrometry, 5, 777 (1971)

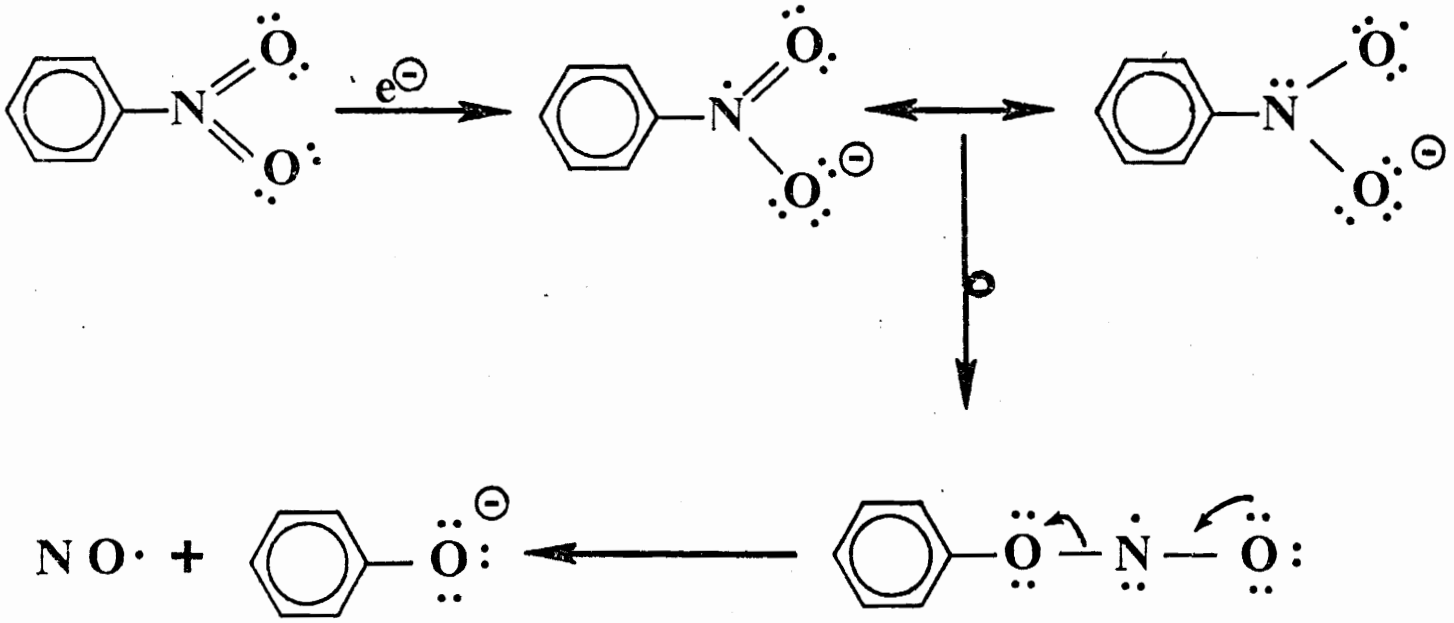

FIGURE 50. Rearrangement Mechanism for NO_2-substituted Aromatics: Negative Ions

From J. H. Bowie, Org. Mass Spectrometry, 5, 777 (1971)

Comparison of the positive and negative spectra of the other benzils provides more information about the differences in the process of ion formation than about differences in the effect of substituents. Positive parent-molecule ions have a very low abundance in the 50 eV spectra and little more at lower eV. Negative parent-molecule ions predominate in the 50 eV spectra and have the greatest ion current at the resonance capture maximum. The different fragmentation patterns for positive and negative ions are the result of the different energy requirements for the positive and negative ions. Negative ions are formed with little excess energy, and subsequent fragmentation is via mechanisms which are exothermic. Positive fragment ions are generally formed via endothermic processes and, therefore, require greater excess energy, a condition more easily achieved in positive spectra since the formation of the parent-molecule ion is a strongly endothermic process. If, according to the QET, the energy required for all fragmentations must first be in the parent, the only way that an ion formed by capture of a thermal electron will be able to fragment by a process identical to that observed for positive ions is if energy is added to the molecule in some other way. For this reason, Bowie[98] has resorted to collision-inducted spectra to "add energy" to the parent-molecule ion so that a more extensive fragmentation pattern can be obtained. Without such techniques, few ions are formed and, more importantly, very few secondary fragments are formed.

Polarography and negative ion mass spectrometry are both methods by which a single electron can be added to a molecule. They differ in the temperature of the molecule at the time that the electron is added and in the degree of solvation of the molecules and ions formed. The latter

condition is apparently of far greater consequence. Electron capture in the gas phase is not affected by most substituents, and only for the chloro-substituted benzils is additivity of substituent effects at all apparent. In solution, substituents clearly affect the half-wave potential and, as indicated by differences in the free energies, the effects of substituents are clearly additive.

In both negative ion mass spectrometry and polarography, two substituents provide anomalous effects. These are the chloro and nitro groups. Both exhibit waves at notably higher voltages than the other benzils. Both have relatively broad electron capture ionization efficiency curves for the parent-molecule ion, and both are unique in affording a small fragment negative ion from the parent, Cl^- and NO^-. Although data do not conclusively support the conclusion that the same fragments are lost by these molecules after the addition of the first electron in solution, the values for the second wave are suggestive that the observed second wave corresponds to the addition of the first electron to a slightly altered normal benzil system. This explanation accounts for both the absolute voltages observed and for the relatively small differences observed between first and second half-wave potentials.

SECTION IX

BIBLIOGRAPHY

1. J. J. Thomson, Phil. Mag., 24, 209 (1912).

2. F. W. Aston, Phil. Mag., 45, 934 (1923).

3. H. Budzikiewicz, C. Djerassi and D. H. Williams, "Interpretation of Mass Spectra of Organic Compounds," Holden-Day, San Francisco, Calif., 1964.

4. M. Vestal, A. Wahrhaftig and W. H. Johnston, J. Chem. Phys., 37, 1276 (1962).

5. F. W. McLafferty, Anal. Chem., 31, 477 (1959).

6. H. M. Rosenstock, "Absolute Rate Theory for Isolated Systems and the Mass Spectra of Polyatomic Molecules," Ph.D. Dissertation, University of Utah, Salt Lake City, 1952.

7. H. M. Rosenstock, M. B. Wallenstein, A. L. Wahrhaftig and H. Eyring, Proc. Nat'l. Acad. Sci. U. S., 667 (1952).

8. W. A. Chupka, J. Chem. Phys., 30, 191 (1959).

9. W. A. Chupka and M. Kaminsky, J. Chem. Phys., 35, 1991 (1961).

10. M. L. Vestal, "Fundamental Processes in Radiation Chemistry," P. Ausloos, Ed., Wiley-Interscience, New York, N. Y., 1968, Chapter 2.

11. H. Budzikiewicz, C. Djerassi and D. H. Williams, "Mass Spectrometry of Organic Compounds," Holden-Day, San Francisco, Calif., 1967.

12. L. P. Hammett, "Physical Organic Chemistry," McGraw-Hill, New York, N. Y., 1940.

13. M. M. Bursey and F. W. McLafferty, J. Amer. Chem. Soc., 88, 529 (1966).

14. A. Streitweiser, Jr., Prog. Phys. Org. Chem., 1, 1 (1963).

15. F. Meyer and A. G. Harrison, Can. J. Chem., 42, 1762 (1964).

16. M. S. Chin and A. G. Harrison, Org. Mass. Spectrom., 2, 1073 (1969).

17. F. W. McLafferty, T. Wachs, C. Lifshitz, G. Innorta and P. Irving, J. Amer. Chem. Soc., 92, 6867 (1970).

18. M. M. Bursey and C. E. Twine, Jr., J. Org. Chem., 35, 2012 (1970).

19. N. Einolf and B. Munson, Org. Mass Spectrom., 5, 397 (1971).

20. F. W. McLafferty, Chem. Comm., 956 (1968).

21. I. Howe, D. H. Williams and R. G. Cooks, Org. Mass Spectrom., 2, 137 (1969).

22. N. Einolf and B. Munson, Org. Mass Spectrom., 7, 155 (1973).

23. I. E. Knaggs and K. Lonsdale, Nature, 143, 1023 (1939).

24. I. Bernal, Nature, 200, 1318 (1963).

25. B. Subrahmanyan, A. Muralikrishna and N. V. Subba Roa, Curr. Sci., 33, 304 (1964).

26. P. H. Cureton, C. G. Lefevre and R.L.W. Lefevre, J. Chem. Soc., 4447 (1961).

27. N. J. Leonard, R. T. Rapala, H. L. Herzog and E. R. Blount, J. Amer. Chem. Soc., 71, 2997 (1949).

28. N. J. Leonard and E. R. Blount, J. Amer. Chem. Soc., 72, 484 (1950).

29. C.F.G.C. Geraldes and V.M.S. Gil, J. Chem. Phys., 59, 1171 (1973).

30. N. L. Bauld, J. Amer. Chem. Soc., 87, 4788 (1965).

31. T. R. Evans and P. A. Leersmakers, J. Amer. Chem. Soc., 89, 4380 (1967).

32. Y. Ogata, K. Takagi and Y. Fujii, J. Org. Chem., 37, 4026 (1972).

33. P. Natalis and J. L. Franklin, J. Phys. Chem., 69, 2943 (1965).

34. S. E. Scheppele, R. K. Mitchum, K. F. Kinneberg, G. G. Meisels and R. H. Emmel, J. Amer. Chem. Soc., 95, 5105 (1973).

35. C. E. Melton, "Mass Spectrometry of Organic Ions," F. W. McLafferty, Ed., Academic Press, New York, N. Y. and London, 1963, p. 163 ff.

36. R. G. Alexander, D. B. Bigley and J.F.L. Todd, Org. Mass Spectrom., 7, 643 (1973).

37. J. H. Freeman, W. Temple and D. Chivers, Nucl. Inst. Methods, 94, 581 (1971).

38. E. E. Muschlitz, Jr., H. D. Randolph and J. N. Ratti, Rev. Sci. Instr., 33, 445 (1962).

39. R. W. Kiser, "Introduction to Mass Spectrometry," Prentice Hall, Inc., Englewood Cliffs, N. J., 1965, p. 192.

40. C. E. Melton, "Principles of Mass Spectrometry and Negative Ions," Marcel Dekker, New York, N. Y., 1973, p. 193.

41. R. T. Alpin, H. Budzikiewica and C. Djerassi, J. Amer. Chem. Soc., 87, 80 (1965).

42. A. C. Ho, J. H. Bowie and A. Fry, J. Chem. Soc., B, 530 (1971).

43. J. H. Bowie, Org. Mass Spectrom., 5, 945 (1971).

44. J. H. Bowie, T. Blumenthal and I. Walsh, Org. Mass Spectrom., 5, 777 (1971).

45. T. Blumenthal and J. H. Bowie, Aust. J. Chem., 24, 1853 (1971).

46. J. H. Bowie, Aust. J. Chem., 24, 989 (1971).

47. J. H. Bowie, Org. Mass Spectrom., 9, 304 (1974).

48. J. H. Bowie and B. Nussey, Org. Mass Spectrom., 9, 310 (1974).

49. M. M. Bursey, Org. Mass Spectrom., 2, 907 (1969).

50. L. G. Christophorou, A. Hadjiantoniou and J. G. Carter, J. Chem. Soc., Far. Trans. II, 69, 1713 (1973).

51. R. C. Buchta and D. N. Evans, Anal. Chem., 40, 2181 (1968).

52. J. Heyrovsky, "A Polarographic Study of the Electrokinetic Phenomena of Adsorption, Electroreduction, and Overpotential Displayed at the Dropping Mercury Cathode," Actualites Scientifiques at Industrielles, No. 90, Paris, 1934.

53. J. Heyrovsky, "Polarography," Springer Verlag, Wien, Aus., 1934.

54. M. Shikata and I. Tachi, Coll. Czech. Chem. Comm., 10, 368 (1938).

55. P. Zuman, Chem. Listy, 48, 94 (1954).

56. P. Zuman, "Substituent Effects in Organic Polarography," Plenum Press, New York, N. Y., 1967.

57. L. Meites, "Polarographic Techniques," 2nd Ed., Wiley-Interscience, New York, N. Y., 1965.

58. E. Womack, N. Campbell and G. Dodds, J. Chem. Soc., 1402 (1938).

59. M. T. Clark, E. C. Hendley and O. K. Neville, J. Amer. Chem. Soc., 77, 3280 (1955).

60. T. van Es and E. Backeberg, J. Chem. Soc., 1373 (1963).

61. C.F.H. Allen and W. E. Barker, Org. Syn. Coll. Vol. II, Ed. by A. H. Blatt, John Wiley and Sons, Inc., New York, N. Y., 1943, p. 156.

62. H. H. Hatt, A. Pilgrim and W. J. Hurran, J. Chem. Soc., 93 (1936).

63. C. R. Kinney, J. Amer. Chem. Soc., 51, 1592 (1929).

64. C. D. Schackett and H. A. Smith, J. Amer. Chem. Soc., 75, 2654 (1953).

65. S. B. Coan, D. E. Trucher and E. I. Becker, J. Amer. Chem. Soc., 77, 60 (1955).

66. H. Staudinger, Chem. Ber., 46, 3530 (1913).

67. M. Weiss and M. Appel, J. Amer. Chem. Soc., 70, 3666 (1948).

68. M. Boesler, Chem. Ber., 14, 327 (1881).

69. Y. Ogata, A. Kawasaki and F. Suguira, J. Org. Chem., 34, 3981 (1969).

70. F. D. Chattaway and E. A. Coulson, J. Chem. Soc., 1361 (1928).

71. R. E. Lutz and R. S. Murphy, J. Amer. Chem. Soc., 71, 478 (1949).

72. F. J. Thaller, D. Trucher and E. I. Becker, J. Amer. Chem. Soc., 73, 228 (1951).

73. M. Gomberg and F. J. Van Natta, J. Amer. Chem. Soc., 51, 2238 (1929).

74. P. J. Montagne, Rec. Trav. Chim., 21, 6 (1902).

75. R. Stierlin, Chem. Ber., 22, 380 (1889).

76. H. B. Wisbert, J. Chem. Soc., 3121 (1928).

77. N. P. Buu-Hoi and N. G. Hoan, J. Org. Chem., 17, 350 (1952).

78. N. P. Buu-Hoi, N. D. Xuang, M. Sy, G. Lefeune and N. B. Tien, Bull. Soc. Chim. Fr., 1594 (1955).

79. L. Ettinger and P. Friedlaender, Chem. Ber., 45, 2081 (1912).

80. C. Tuzun, M. A. Ogliaruso and E. I. Becker, Org. Syn., 41, 1 (1961).

81. A.J.C. Nicholson, J. Chem. Phys., 29, 1312 (1958).

82. J. L. Franklin, J. G. Dillard, H. M. Rosenstock, J. T. Herron, K. Draxl and F. H. Field, Nat'l. Stand. Ref. Data Serv., Nat'l. Bur. Stand., No. 26 (1969).

83. J. W. Warren, Nature, 165, 810 (1950).

84. R. W. Kiser, "Introduction to Mass Spectrometry," Prentice Hall, Inc., Englewood Cliffs, N. J., 1965, p. 124 ff.

85. R. S. Gohlke and L. H. Thompson, Anal. Chem., 40, 1004 (1968).

86. J. M. Saveant and L. Nadjo, J. Electroanal. Chem. Interfacial Electrochem., 30, 41 (1971).

87. J. L. Franklin, J. Chem. Phys., 21, 2029 (1953).

88. H. D. Springall and T.R.J. White, J. Chem. Soc., 2764 (1954).

89. R. K. Solly and S. W. Benson, J. Amer. Chem. Soc., 93, 1592 (1971).

90. F. W. McLafferty, "Topics in Organic Mass Spectrometry," A. L. Burlingame, Ed., Wiley-Interscience, New York, N. Y., 1970, p. 235.

91. J. H. Bowie and A. C. Ho, Aust. J. Chem., 24, 1093 (1971).

92. C. L. Brown and W. P. Weber, J. Amer. Chem. Soc., 92, 5775 (1970).

93. J. H. Bowie and P. Y. White, Org. Mass Spectrom., 6, 135 (1972).

94. J. March, "Advanced Organic Chemistry," McGraw-Hill, New York, N. Y., 1968, p. 224.

95. A. Hadjiantoniou, L. G. Christophorou and J. G. Carter, J. Chem. Soc., Faraday Trans. II, 1691 (1973).

96. J.F.J. Todd, R. B. Turner, B. C. Webb and C.H.J. Wells, J. Chem. Soc., Perkin Trans., (2), 1167 (1973).

97. A. Ito, K. Matsumoto and T. Takeuchi, Org. Mass Spectrom., 6, 1045 (1972).

98. J. H. Bowie, J. Amer. Chem. Soc., 95, 5795 (1973).

SECTION X

APPENDIX 1

PARA-SUBSTITUTED BENZILS

R_1-$C_6H_4COCOC_6H_4$-R_2

R_1	R_2	Reference
H	CH_3	10,16,34,64,71,88
H	C_2H_5	10
H	n-C_3H_7	10,109
H	i-C_3H_7	10
H	n-C_4H_9	10
H	i-C_4H_9	10
H	t-C_4H_9	109
H	n-C_5H_{11}	10
H	i-C_5H_{11}	10
H	n-C_6H_{13}	10
H	n-C_7H_{15}	10
H	n-C_8H_{17}	10
H	n-$C_{10}H_{21}$	10
H	n-$C_{11}H_{23}$	102
H	C_6H_5	31,34,67,74
H	p-$C_{11}H_{23}C_6H_5$	102
H	$BrCH_2$	50
H	NH_3	4,69,107
H	$(CH_3)_2N$	39,54,60,69,73,75,83,109
H	NO_2	9,14,34,25,62,85,97

APPENDIX 1 (continued)

R_1	R_2	Reference
H	OH	28,32,82
H	CHO	50
H	CH_3O	16,20,28,32,36,47,54, 61,63,64,69,78,88,106,108
H	C_2H_5O	28,88
H	n-C_3H_7O	28
H	n-C_4H_9O	28
H	n-$C_5H_{11}O$	28
H	n-$C_6H_{13}O$	28
H	n-$C_7H_{15}O$	28
H	n-$C_8H_{17}O$	28
H	n-$C_9H_{19}O$	28
H	n-$C_{10}H_{21}O$	28
H	n-$C_{11}H_{23}O$	28
H	C_6H_5O	18
H	C_6H_5CO	33
H	CO_2H	25,50
H	CH_3CO_2	25
H	p-$NO_2C_6H_4CO$	33
H	p-ClC_6H_4CO	33
H	p-BrC_6H_4CO	33
H	CH_3S	17
H	C_6H_5S	18

APPENDIX 1 (continued)

R_1	R_2	Reference
H	CH_3SO_2	17
H	F	53
H	Cl	16,25,34,56,69, 88,106,109
NH_3	NO_2	25
NH_3	Br	25
$(CH_3)_2N$	$(CH_3)_2N$	23,24,90
$(CH_3)_2N$	CH_3O	12
$(CH_3)_2N$	Cl	20,40,109
OH	OH	30,80,82,96
NO_2	NO_2	8,15,25,30,44
NO_2	Cl	25
NO_2	Br	25
NO_2	CH_3	64
NO_2	CH_3O	43,54,57
NO_2	C_2H_5O	45
NO_2	$\underline{n}$-C_3H_7O	45
NO_2	$\underline{n}$-C_4H_9O	45
NO_2	CO_2H	25
NO_2	CH_3CO_2	25
CHO	CHO	51
CH_3O	CH_3O	11,13,17,19,20,26,30,36, 38,47,48,49,61,62,64, 65,68,70,72,76,78,80,81, 82,84,85,87,95,101,109

APPENDIX 1 (continued)

R_1	R_2	Reference
CH_3O	Cl	12,41,109
CH_3O	Br	67
C_2H_5O	C_2H_5O	13,20,80,93
CH_2CHO	CH_2CHO	99
C_6H_5O	C_6H_5O	3,18,20,79,80,100
p-$CH_3C_6H_4O$	p-$CH_3C_6H_4O$	3
CO_2H	CO_2H	25
CO_2H	SO_2NH_2	25
H	Br	25,34,58,88
H	CN	25
H	SO_2NH_2	25
CH_3	CH_3	11,17,47,48,56,64,65,68, 78,79,84,87,93,105,109
C_2H_5	C_2H_5	87,100
i-C_3H_7	i-C_3H_7	20,78
s-C_4H_9	s-C_4H_9	97
t-C_4H_9	t-C_4H_9	109
C_6H_{11}	C_6H_{11}	77
C_6H_5	C_6H_5	20,22,31,48,94
C_6H_5	p-$CH_3C_6H_4$	94
C_6H_5	p-$CH_3OC_6H_4$	94
C_6H_5	p-ClC_6H_4	94
C_6H_5	o-ClC_6H_4	94

APPENDIX 1 (continued)

R_1	R_2	Reference
C_6H_5CHCH	C_6H_5CHCH	21
2-(9-anthryl)vinyl	2-(9-anthryl)vinyl	51
p-C_6H_5-C_6H_4CHCH	p-C_6H_5-C_6H_4CHCH	51
CN	CN	25
CN	SO_2NH_2	25
CN	NO_2	25
C_6H_5NCH	C_6H_5NCH	51
NH_3	CH_3	43
NH_3	NH_3	29,52,104
NH_3	OH	43
NH_3	C_2H_5O	43
NH_3	n-C_3H_7O	43
NH_3	n-C_4H_9O	43
CO_2CH_3	CO_2CH_3	25
CO_2CH_3	SO_2NH_2	25
CH_3OCH_2O	CH_3OCH_2O	53
$C_6H_5OC_6H_4O$	$C_6H_5OC_6H_4O$	2
F	F	42,92
F	CF_3	55
C_6H_5S	C_6H_5S	18,20
SO_2NH_2	SO_2NH_2	25
SO_2NH_2	Cl	25
SO_2NH_2	Br	25

APPENDIX 1 (continued)

R_1	R_2	Reference
Cl	Cl	5,6,25,27,31,35,37, 42,68,89,91
Cl	Br	25,108
Br	Br	1,7,17,20,25,103
CH_2Br	CH_2Br	51
I	I	25
$CH=\overset{O}{\overset{\uparrow}{N}}C_6H_4-N(CH_3)_2$	$CH=\overset{O}{\overset{\uparrow}{N}}C_6H_4-N(CH_3)_2$	51
$-CH_2-Pyr]^+Br^-$	$-CH_2-Pyr]^+Br^-$	51
$-CH_2-P(C_6H_5)_3]^+Br^-$	$-CH_2-P(C_6H_5)_3]^+Br^-$	51

1. C.F.H. Allen and J. A. van Allan, J. Amer. Chem. Soc., 66, 7 (1944).

2. B. A. Arbuzon and D. A. Akhmed-Zade, J. Gen. Chem. (U.S.S.R.), 12, 212 (1942); C.A., 37:2732.

3. Y. Asahina and Y. Tanase, Proc. Imp. Acad. (Tokoyo), 16, 297 (1940).

4. J. M. Augl and J. V. Duffy, Annu. Conf., S. P. I. Reinf. Plast./ Compos. Div., Proc., 26th, 1971, 19-D (1971).

5. G. T. Barry and R. Boyer, Can. J. Research, 26B, 518 (1948).

6. N. L. Bauld, Tetrahedron Lett., 1841 (1963).

7. H. Biltz, Chem. Ber., 41, 1761 (1908).

8. H. Biltz, Ann., 368, 262 (1909).

9. M. L. Black and H. A. Smith, J. Org. Chem., 17, 1315 (1952).

10. E. R. Bockstagler and D. L. Wright, J. Amer. Chem. Soc., 71, 3760 (1949).

11. M. Boesler, Chem. Ber., 14, 327 (1881).

APPENDIX 1 (continued)

12. J. S. Buck and W. S. Ide, J. Amer. Chem. Soc., 52, 4107 (1930).

13. E. Catterlain and P. Charbrier, Bull. soc. chim. France, 1103 (1947).

14. F. D. Chattaway and E. A. Coulson, J. Chem. Soc., 1080 (1928).

15. F. D. Chattaway and E. A. Coulson, J. Chem. Soc., 1361 (1928).

16. M. T. Clark, E. C. Hendley and O. K. Neville, J. Amer. Chem. Soc., 77, 3280 (1955).

17. S. B. Coan, D. E. Trucher and E. I. Becker, J. Amer. Chem. Soc., 77, 60 (1955).

18. V. F. D'Agostino, M. J. Dunn, A. E. Erhlich and E. I. Becker, J. Org. Chem., 23, 1539 (1958).

19. C. V. Deliwala and S. Rajagopalan, Proc. Indian Acad. Sci., 31A, 107 (1950); C.A., 45:6177.

20. W. Dilthey, O. Trosken, K. Plum and W. Schommer, J. prakt. Chem., 141, 331 (1934).

21. G. Drefahl and W. Hartrodt, J. prakt. Chem., 4, 99 (1956).

22. G. Drefahl and G. Ploetner, Chem. Ber., 95, 2782 (1962).

23. C. Dufraisse, A. Etienne and J. Aubry, Compt. rend., 239, 1170 (1954).

24. C. Dufraisse, A. Etienne and J. Aubry, Bull. soc. chim., 21, 1201 (1954).

25. T. van Es and E. Backeberg, J. Chem. Soc., 1373 (1963).

26. H. Fiesselman and J. Ribka, Chem. Ber., 89, 27 (1956).

27. E. E. Fleck, J. Org. Chem., 12, 708 (1947).

28. A. Friedman, W. Gugig, L. Mehr and E. I. Becker, J. Org. Chem., 24, 516 (1959).

29. H. L. Gee and J. Herley-Mason, J. Chem. Soc., 251 (1947).

30. H. Gilman and H. S. Broadbent, J. Amer. Chem. Soc., 70, 2619 (1948).

31. M. Gomberg and F. J. Van Natta, J. Amer. Chem. Soc., 51, 2238 (1929).

32. J. G. Garvin, Nature, 161, 208 (1948).

APPENDIX 1 (continued)

33. H. Greenberg, T. van Es and O. G. Backeberg, J. Org. Chem., 32, 2964 (1967).

34. H. H. Hatt, A. Pilgrim and W. J. Hurran, J. Chem. Soc., 93 (1936).

35. H. H. Hodgson and W. Rosenburg, J. Chem. Soc., 14 (1930).

36. B. Holden and W. Rigby, J. Chem. Soc., 1924 (1951).

37. L. Horner and W. Naumann, Ann., 587, 93 (1954).

38. R. Jaunin and G. Sechaud, Helv. Chim. Acta., 39, 1257 (1956).

39. S. S. Jenkins, J. S. Buck and L. A. Bigelow, J. Amer. Chem. Soc., 52, 4495 (1930).

40. S. S. Jenkins, J. Amer. Chem. Soc., 53, 3115 (1931).

41. S. S. Jenkins, J. Amer. Chem. Soc., 56, 1137 (1934).

42. A. Kalusayner, J. Org. Chem., 24, 995 (1959).

43. S. Kanno, J. Pharm. Soc. Japan, 72, 1193 (1952).

44. S. Kanno, J. Pharm. Soc. Japan, 73, 118 (1953).

45. S. Kanno and S. Suzuki, J. Pharm. Soc. Japan, 71, 1247 (1951).

46. C. R. Kinney, J. Amer. Chem. Soc., 51, 1592 (1929).

47. B. Klein, J. Amer. Chem. Soc., 63, 1474 (1941).

48. J. Klosa, Arch. Pharm., 288, 465 (1955).

49. A. Kreutzberger, J. Org. Chem., 27, 886 (1962).

50. B. Krieg and G. Maneche, Chem. Ber., 101, 1480 (1968).

51. B. Krieg, Chem. Ber., 102, 371 (1969).

52. R. Kuhn, E. F. Moller and G. Wendt, Chem. Ber., 76B, 405 (1943).

53. H. Kunimoto, Nippon Kagaku Zasshi, 83, 1282 (1962); C.A. 59:11309.

54. H. Kwart and M. M. Baevsky, J. Amer. Chem. Soc., 80, 580 (1958).

55. I. Lelezari, M. Hatefi, M. Khoyi, N. Guiti and F. Abtahi, J. Med. Chem., 14, 1138 (1971).

APPENDIX 1 (continued)

56. K. Lempert, Chem. Ber., 95, 2885 (1962).

57. K. Lempert and A. Wolfner, Periodica Polytech., 8, 237 (1964); C.A. 63:6992.

58. N. J. Leonard, R. T. Rapala, H. L. Herzog and E. R. Blount, J. Amer. Chem. Soc., 71, 2997 (1947).

59. A. Lespagnol, J. Turlur and L. Lespagnol, Bull. sci. pharmacol., 46, 305 (1939); C.A. 33:8182.

60. K. Matsumura, J. Amer. Chem. Soc., 57, 955 (1935).

61. L. P. McHatton and M. J. Soulal, J. Chem. Soc., 2771 (1952).

62. L. P. McHatton and M. J. Soulal, J. Chem. Soc., 4095 (1953).

63. A. McKenzie, E. M. Luis, M. Tiffeneau and P. Weill, Bull. soc. chim., 45, 414 (1929).

64. A. McKillop, O. H. Oldenziel, B. P. Swann, E. C. Taylor and R. L. Robey, J. Amer. Chem. Soc., 93, 733 (1971).

65. A. McKenzie, O. H. Oldenziel, B. P. Swann, E. C. Taylor and R. L. Robey, J. Amer. Chem. Soc., 95, 1296 (1973).

66. A. McKillop, B. P. Swann, M. E. Ford and E. C. Taylor, J. Amer. Chem. Soc., 95, 3641 (1973).

67. A. Mee, A. Robertson and W. B. Whalley, J. Chem. Soc., 3093 (1957).

68. L. Mehr, E. I. Becker and P. E. Sproerri, J. Amer. Chem. Soc., 77, 984 (1955).

69. K. W. Merz and D. Plauth, Chem. Ber., 90, 1744 (1957).

70. S. K. Myeong, Y. Sawa, M. Ryang and S. Tsutsumi, Bull. Chem. Soc. Japan, 38, 330 (1964).

71. T. Nagano, J. Amer. Chem. Soc., 77, 6680 (1955).

72. F. Nerdel, J. Buddrus and K. Hoeher, Chem. Ber., 97, 124 (1964).

73. Y. Ogata, A. Kawasaki and F. Suguira, J. Org. Chem., 34, 3981 (1969).

74. Y. Ogata, K. Takagi and Y. Fujii, J. Org. Chem., 37, 4026 (1972).

APPENDIX 1 (continued)

75. A. Renee and C-W Cheng, Rec. Fac. Farm. Bioquim. Univ. Nac. Mayor San Marcos (Lima), 30, 9 (1968); C.A. 71:49456h.

76. W. Rigby, J. Chem. Soc., 793 (1951).

77. H. Schubert, G. Jaenecke and H. Taubert, J. prakt. Chem., 15, 86 (1961).

78. C. D. Shacklett and H. A. Smith, J. Amer. Chem. Soc., 75, 2654 (1953).

79. N. Shapiro, Chem. Ber., 66B, 1103 (1933).

80. A. Shonberg and O. Kraemer, Chem. Ber., 55, 1174 (1922).

81. P. P. Shoruigin, V. I. Isagulyantz and A. R. Guseva, J. Gen. Chem. (U.S.S.R.), 4, 683 (1934); C.A. 29:3671.

82. I. N. Somin and S. G. Kuznetsov, Khim. Nauk. i Prom., 4, 801 (1959); C.A. 54:10950.

83. H. Staudinger, Chem. Ber., 46, 3530 (1913).

84. R. Stierlin, Chem. Ber., 22, 376 (1889).

85. M. Sugii and R. Nakai, J. Org. Chem., 22, 288 (1957).

86. W. Tadros and L. Ekladius, Nature, 166, 525 (1950).

87. W. Tadros, A. B. Sakla, A.A.A. Helmy and M. K. Khalal, J. Chem. Soc., 3994 (1965).

88. B. S. Tanaseichuk and S. V. Yartseva, Uch. Zap. Mord. Univ., 90 (1971); C.A. 75:110236.

89. F. J. Thaller, D. Trucher and E. I. Becker, J. Amer. Chem. Soc., 73, 228 (1951).

90. C. Tuzun, M. A. Ogliaruso and E. I. Becker, Org. Syn., 41, 1 (1961).

91. W. Voegtli, H. Muhr and P. Lauger, Helv. Chim. Acta., 37, 1627 (1954).

92. W. Voegtli, H. Muhr and P. Lauger, Helv. Chim. Acta., 38, 46 (1955).

93. D. Vorlander, Chem. Ber., 44, 2455 (1911).

94. J. S. Walia, J. Singh, M. S. Chatta and M. Satayanarayana, Tetrahedron Lett., 195 (1969).

APPENDIX 1 (continued)

95. M. Weiss and M. Appel, J. Amer. Chem. Soc., 70, 3666 (1948).

96. F. V. Wesseley, A. Bauer and E. Kerschbaum, Naturwissenshaften, 31, 417 (1943).

97. P. Weyerstahl, R. Zielke and F. Nerdel, Justus Lieblings Ann. Chem., 731 (1970).

98. E. B. Womack, N. Campbell and G. B. Dobbs, J. Chem. Soc., 1402 (1938).

99. Ger. Pat. #892,288 to Cassella Farbwerke Mainkurt Akt-Ges., for Walter Persch and A. Schmidt; C.A. 52:P13802.

100. Ger. Pat. #913,891 to Badische Anilin und Soda Fabrik Akt-Ges., for W. Braun; C.A. 52:P14691.

101. Ger. Offen. #2,231,677 to M. Virgnau (Roussel-UCLAF); C.A. 78:83449n.

102. Neth. Pat. Appl. #6,400,338 to Ciba Ltd.; C.A. 62:4147f.

103. Ger. Offen. #2,133,897 to A. Sieber, H. Kny and W. Oliver (Ciba-Geigy, A. G. and Agripat, S. A.); C.A. 112900u.

104. U. S. Pat. #2,359,280 to G. W. Anderson (American Cyanimide); C.A. 39:P785.

105. U. S. Pat. #3,033,894 to W. L. Fierce and W. J. Sander (Pure Oil Co.); C.A. 57:P12387.

106. U. S. Pat. #3,592,922 to P. Manos (E. I. duPont de Nemours Co.); C.A. 75:P88322.

107. U. S. Pat. #3,642,700 to J. M. Augl (U. S. Dept. of the Navy); C.A. 76:154384j.

108. S. African Pat. #68 03 146 to K. Gubler; C.A. 74:P126187.

109. J. S. Luloff, M.S. Thesis, Univ. of Del., June, 1953.

APPENDIX 2

HAMMETT SUBSTITUENT CONSTANTS

SUBSTITUENT	σ [1]	σ^+ [1]	σ_I [2]
NO_2	0.78	0.79	0.79
Cl	0.23	0.11	0.24
CH_3S	0.00 $(0.22)^2$	----	0.22
H	0.00	0.00	0.003
CH_3O	-0.27	-0.78	-0.11
CH_3	-0.17	-0.31	-0.13
$(CH_3)_2N$	-0.83	----	-0.13

1. Values of N. Einolf and B. Munson, Org. Mass. Spec., 7, 155 (1973).
2. Values of P. J. Wells, Chem. Rev., 63, 171 (1963).

SECTION XI

VITA

Joseph Herbert O'Toole was born March 23, 1945, in Baltimore, Maryland. He attended Mt. Washington Country School, Baltimore and graduated from Loyola High School, Towson, Maryland, in June, 1963. He received a Bachelor of Science degree from Loyola College, Baltimore, in June, 1963.

The author enrolled in the Graduate School at Virginia Polytechnic Institute in September of 1967 and was a National Defence Education Act Fellow from September, 1968 to August, 1970. He enrolled in the University of Maryland, School of Law, in September, 1971 and received the Juris Doctor degree from that institution May 30, 1974. While at the University, he worked with Dr. Nasir Bashirelahi of the University Dental School under a grant from the American Cancer Society.

PUBLICATIONS:

1. J. H. O'Toole, A. Tsafiri, E. G. Armstrong, J. D. Young and N. Bashirelahi, The Journal of Steroid Biochemistry, 5, 333 (1974).

Joseph Herbert O'Toole

SECTION XII

MASS SPECTROMETRY OF SUBSTITUTED BENZILS

Joseph Herbert O'Toole

ABSTRACT

The positive and negative ion mass spectra and appearance potentials were determined for the following compounds: benzil, 4-methylbenzil, 4-methoxybenzil, 4-methylmercaptobenzil, 4-dimethylaminobenzil, 4-chlorobenzil, 4-nitrobenzil, 4,4'-dimethylbenzil, 4,4'-dimethoxybenzil, 4,4'-bis(methylmercapto)benzil, 4,4'-bis(dimethylamino)benzil, 4,4'-dichlorobenzil, and 4,4'-dinitrobenzil. Metastable data were used to establish that the fragmentation mechanism for positive ions involves cleavage between the carbonyls followed by loss of CO. Calculated appearance potentials are compared with those generated experimentally. The appearance potentials of the substituted benzoyl ions exhibit substituent effects correlatable with the Hammett σ, but no substituent effect is demonstrated for the unsubstituted benzoyl. Loss of CO by the benzoyl ion does not appear to involve substituent effects but required 2.5-4.0 eV excess energy above that required to form the precursor. The nitro-substituted benzils fragment by two competing mechanisms, that described supra and the loss of NO• following rearrangement of the substituent.

The base peak in all negative ion spectra at 50 eV was the parent-molecule ion. Benzil, the methyl-substituted benzils, and the dimethylamino-substituted benzils form no daughter ions. The methoxy-substituted benzils and the methylmercapto-substituted benzils formed a daughter ion by loss of CH_3• from the parent. The chloro-substituted benzils fragment

to produce Cl^-. The nitro-substituted benzils lose NO•, apparently following a rearrangement similar to that observed for positive ions, and also fragment to lose NO^- in low abundance.

Appearance potential data indicate that all parent-molecule ions are formed by electron capture, and all fragments by dissociative-attachment. The electron-withdrawing substituents cause a broadening of the ionization efficiency curve for the parent-molecule ion; all other substituents have no effect on the curves' shape. Daughter ion ionization efficiency curves are broader than the parent-molecule i.e. curves, and the i.e. curves for the daughter ions from the methoxy-substituted benzils appear to be composits of at least two curves. NO^- and Cl^- are of low abuncance, with onset at 2.2 eV and 5.5 eV respectively above SF_6^-.

The most abundant negative daughter ions are resonance stabilized; Cl^- and NO^- are formed by electron pairing at an electronegative site. Negative ions are not formed with sufficient excess energy to fragment by the same mechanism as positive ions, with the exception of the anomalous nitro-substituted mechanism.

Polarographic half-wave potentials were compared to negative ion mass spectrometric data. Benzils with electron-donating substituents fit a plot of $E_{1/2}$ vs. σ. Substituent effects for these benzils are additive, as indicated by comparison of ΔG for one and two substituents to that for benzil. Chloro-substituted and nitro-substituted benzils have second waves at only 0.3 to 0.4 v more negative than the first wave, in contrast to 0.6 to 0.8 v differences for the other benzils. Loss of a substituent, as observed in the negative ion mass spectra, is suggested as an explanation

$E_{3/4} - E_{1/4}$ values were calculated and indicate that waves in the region 1.0 to 1.4 v are probably reversible.